Mechanisms of Regulation of the Spindle Position Checkpoint Kinase, Kin4

Leon Y. Chan

B.A. English, Mathematics, Physics
University of California, Berkeley
College of Letters and Science 2000

Submitted to the Department of Biology in partial fulfillment
of the requirements for the degree of

Doctor of Philosophy in Biology
Massachusetts Institute of Technology
June 2010

Signature of the Author: _____
Department of Biology
10 May 2010

Certified by: _____
Angelika Amon
Professor of Biology
Thesis Supervisor

Accepted by: _____
Stephen P. Bell
Professor of Biology
Chair, Committee for Graduate Students

Mechanisms of Regulation of the Spindle Position Checkpoint Kinase, Kin4

Leon Y. Chan

Submitted to the Department of Biology on May 10, 2010 in partial fulfillment of the requirements for the Degree of Doctor of Philosophy in Biology

Abstract

Most cells are polarized in that they are aware of spatial cues and can respond to these cues accordingly. One major aspect of cell function that is often responsive to these polarization cues is cell division. Cell division, the process of making two cells from one progenitor, requires equal distribution of the genetic material to the two progeny cells. When polarized cells divide, an additional constraint on the segregation of the genetic material is imposed, namely, cells must divide the genetic material along axes defined by polarization cues. In eukaryotes, this problem is generally solved by the positioning of the mitotic spindle according to these spatial cues. Defects in spindle positioning can lead to the generation of cells with incorrect organelle, genetic and molecular contents, fate and/or, spatial orientation. Cells have evolved feedback mechanisms that monitor defects in spindle positioning and delay the cell cycle in response to such defects. These mechanisms are best elucidated in the budding yeast, *Saccharomyces cerevisiae*. The protein kinase Kin4 inhibits the Mitotic Exit Network when the spindle is mis-positioned. How Kin4 is itself regulated and whether or how Kin4 responds to spindle mis-position is not known. The work presented in this thesis elucidates the regulation of Kin4. We identify a novel spindle position checkpoint component, PP2A-Rts1, and show that it promotes checkpoint function by enabling proper Kin4 localization. We also identify domains and sequence determinants within Kin4 that control localization and function. We present a model of how the spindle position checkpoint senses spindle position and test this model for Kin4 function. We find that the generation of positive and negative mitotic exit regulatory zones allows the cell to sense and translate the spatial information of spindle position into a chemical cell cycle signal.

Acknowledgements

As much as science is an individual pursuit, no good science is done alone. I first have to thank Angelika for mentoring me and creating a place where we as lab mates can interact and learn from one another. I'm not going to list the litany of what I've learned from you but no doubt your open and enthusiastic personality is the reason our lab is what it is.

To my past baymate Gloria, thank you for putting up with me and cheering me up with pictures of cute animals. I have to admit, they were effective. To Rami, thank you for the opportunity to rotate with you and teaching me so much about the basics of yeast research and the field of mitotic exit. To Andreas, thank you for helping me settle down and focus on one project. To Bret and Chi, thank you for all the help with stuff I had no clue about. To Ly-sha, thanks for the support to the lab and the crossword puzzles. To Fernando, you were my sole accomplice in mitotic exit for quite some time and without our exchanges, I would have never made progress on my project. To Katie, thank you for letting me squat on your bench when I joined and teaching me the tricks to Kin4 – as we both know, there are quite a few of them. To Monica, I always enjoyed our exchanges about each other's projects. Science is grind for the truth and your example really showed me that.

To Matt, Michelle, Jeremy, Thomas, Folket, Elcin and Alexi – I have had some of the most spontaneous and exciting scientific discussions with you and your willingness to talk about my science or anyone else's has been the reason I love working in this lab. Our exchanges have made me a better scientist. To Matt, thanks for rotating with me and really pushing me to think hard about Kin4 and how it might work. To Jeremy, thanks for being the second rotation student, I was completely under-prepared and I appreciate your ability to adapt to the haphazard experimental plan. You became my go-to person for mitotic exit and I appreciate you putting up with the random questions. To Michelle, our exchanges have made me think harder about mitotic exit and I value our discussions about how we teach science. To Elcin, I have learned so much from you on so many levels. I will always remember when we would both wonder about a question and set off on independent PubMed searches to figure it out. To Alexi, our discussions have led me to think about some fascinating questions I would have never otherwise thought about. Moreover, I will always value your view of the world as it is and how it should be.

To my committee members, Frank, Steve, Terry, Thomas and Fred – your input was always insightful and always appreciated.

I would not be here were it not for Drew and his lab. He gave me an chance when he really had no reason to. To Sri and Heather, I learned so much from the both of you in Drew's lab and I will always value our time working on T7 together.

To my parents and sister, I would not be the person I am without you.

And to my partner and best friend Sarah, you are my one constant and I cannot imagine having done this without you.

Table of Contents

Chapter I: Introduction

Summary

During polarized cell division, the mitotic spindle must be positioned along the predetermined axis of division. Feedback mechanisms that delay cell cycle progression in response to defects in this process have been described in a number of organisms and are best understood in budding yeast. The work in this thesis concerns the control of the checkpoint kinase Kin4 and how this control gives rise to a spindle position sensing mechanism that feeds back on the cell cycle. The introduction will discuss the general problem of polarized cell division with specific examples of how polarity is established and how this polarity is linked to the spindle positioning machinery. The actual machinery that positions the spindle in budding yeast is then discussed followed by a brief summary of cell cycle control in budding yeast. Lastly, checkpoint mechanisms that delay the cell cycle in response to defects in mitosis will be discussed with emphasis on the spindle position checkpoint, our current knowledge of it, proposed mechanisms of checkpoint function and the outstanding questions that remain.

Polarized cells: case studies

Cell polarization is key to cell motility, growth and division. Discussed below are a number of case studies in polarized cell division and the important features they highlight. Two key commonalities are shared across these examples:

(i) The generation of cell polarity by a core complex that involves the GTPase Cdc42.

(ii) Coordination of cell polarity with spindle position by recruitment of microtubule associated proteins to sites of polarization.

The first three case studies are examples of asymmetric cell division, which are perhaps the most dramatic examples of polarized cell division.

Stem cell division: the generation of cells with differing fates

Stem cells can divide by two different modes. They can give rise to two identical stem cells or they can give rise to a stem cell and a progeny cell with decreased potency. In the second mode, cell division is inherently asymmetric. One of the best studied stem cell

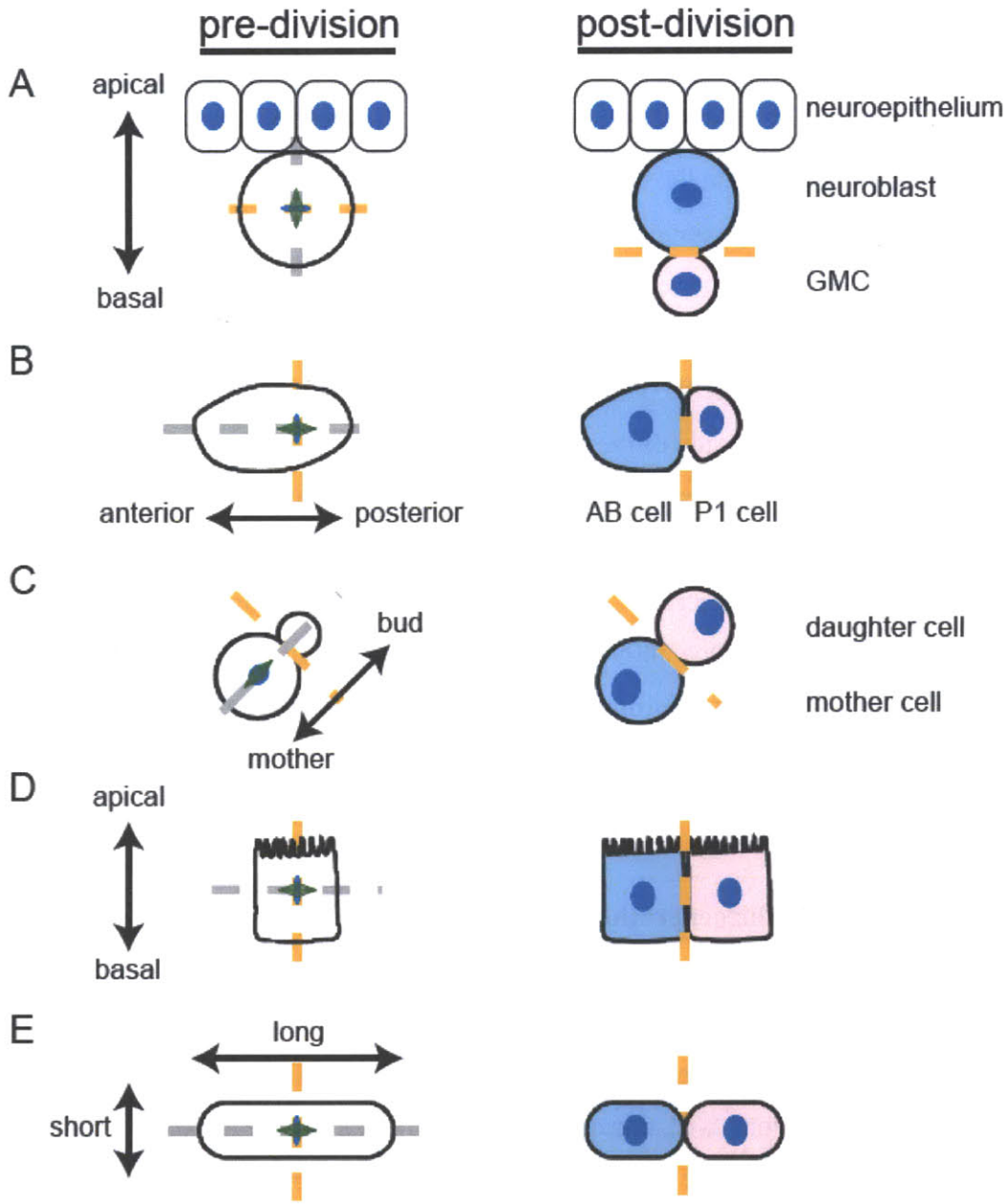

Figure 1: Examples of polarized cell division

In all diagrams, the yellow dashed line is the axis of cytokinesis, the gray dashed line is the axis or plane of division and the spindle is in green. The double headed arrows depict the major axes of polarization and the cues that define them. The differential coloration of the progeny cells highlights the polarized nature of the cell division.

(A) Division of the fly neuroblast to give rise to another neuroblast and a GMC.
(B) The first embryonic division of the worm to give rise to the AB and P1 cells.
(C) Division of budding yeast to give rise to a mother cell and a daughter cell.
(D) Division of an epithelial cell to give rise to two cells in the epithelial plane.
(E) Division of the fission yeast along the long axis to give rise to two progeny cells.

divisions is the division of the *Drosophila melanogaster* neuroblast. The fly neuroblast can divide asymmetrically to produce another neuroblast and a ganglion mother cell (GMC) (Figure 1A). Polarity is initially generated from external cues in an unknown fashion. However, it is clear that the neuroblast, which resides on the basal lamina of the neuroepithelium, localizes the core polarization complex consisting of the structural proteins Par-3 (Bazooka) and Par-6; the GTPase, Cdc42; and the kinase, aPKC to the apical side of the dividing neuroblast (reviewed in (Knoblich 2008)). These master regulators of cell polarity dictate the polarization of cell fate determinants such as Numb, Prospero and Brat to the basal side of the dividing neuroblast. The polarization complex also appears to govern spindle position to align along the apical-basal axis. Par-3 ultimately recruits NuMA (Mud), a microtubule (MT) and dynein binding protein, to the apical side of the cell and thus recruits (by an unknown mechanism) one of the spindle poles (reviewed in (Siller and Doe 2009)). In most eukaryotes, cytokinesis is defined by the spindle midzone and thus by coordinating the segregation of cell fate determinants with the position of the spindle through the same core polarization machinery, the fly neuroblast is able to generate two progeny cells with different fates.

Embryonic cell division: the generation of the body plan

Asymmetric cell division is also a major mode of organismal development. The first embryonic cell division of the worm *Caenorhabditis elegans* is highly asymmetric. The asymmetry is initially generated by the site of entry of the fertilizing sperm, which defines the anterior-posterior (A-P) axis of the cell and ultimately, the organism (Goldstein and Hird 1996) (Figure 1B). The same core polarization complex consisting of Par-3, Par-6, Cdc42 and aPKC is then localized to the anterior cortex of the cell (reviewed in (Schneider and Bowerman 2003)). The mitotic spindle is positioned in two phases that depend on cell polarity. The first phase involves rotation of the centrosomes prior to mitosis to align along the A-P axis and the second phase involves linear translation of the anaphase spindle off the central axis (perpendicular to the A-P axis) to produce an off axis cytokinesis and thus progeny cells with differing sizes and fates. As in flies, both of these spindle movements are governerned by the recruitment of NuMA (Lin-5) (reviewed in (Siller and Doe 2009)). The role of NuMA is better understood in

worms; NuMA binds Lis1-Dynein and generates MT pulling forces. During prophase centrosome rotation, NuMA is recruited to the anterior cortex by the core polarization complex to exert greater pulling forces on one of the centrosomes thus resulting in spindle rotation. In anaphase, NuMA is localized to the posterior cortex through opposite polarity factors and pulls the anaphase spindle off center axis towards the posterior cortex resulting in a small posterior and large anterior progeny cells.

Budding yeast cell division: asymmetric cell division in the absence of external cues

Asymmetric cell division is also observed in single cell organisms. The budding yeasts, including *Saccharomyces cerevisiae*, divide in an asymmetric manner and give rise to a daughter cell that is smaller in size, opposite in sex and longer lived than the mother cell (Figure 1C). The budding yeast also defines cell polarization using the GTPase, Cdc42. Cdc42 directs actin polymerization through the formin proteins and thus allows vectorial transport and the construction of a daughter cell (reviewed in (Chant 1999)). In haploid cells, proteins recruited to the previous site of cytokinesis, likely through septins, in turn recruit Cdc42, which determines the site of bud formation and the overall polarization of the cell (reviewed in (Casamayor and Snyder 2002)). This determination occurs in G1 and thus the site of bud growth, which is necessarily the site of future cytokinesis, is determined prior to mitosis. This necessitates positioning of the spindle along the mother-bud axis to partition the genetic material equally. Here too, the polarization machinery plays a key role in regulating spindle position. Astral MTs emanating from the spindle pole body (SPB, yeast centrosome) destined for the bud are transported to the bud tip by Kar9-Bim1 and anchored there (reviewed in (Pearson and Bloom 2004)). The transport requires a polarized actin cytoskeleton and the anchorage is mediated by the polarity factor, Bud6. Both of these processes require the core polarization factor, Cdc42. The positioning of the mitotic spindle in budding yeast is reviewed in detail later on. Proper position of the mitotic spindle ensures that chromosome segregation occurs on the mother-bud axis resulting in two euploid but asymmetric progeny cells.

Epithelial cell division: division constrained to a plane

While asymmetric cell divisions are necessarily polarized, there are also many cells that divide symmetrically but in a polarized fashion. These polarization cues can be derived from both intracellular and extracellular cues. A prime example of such a cell division is that of epithelial cells. Epithelial cells, the cells that make up the thin covering of internal surfaces in the body, often grow in a layer that is only one cell thick. This planar cell monolayer constrains cell division to axes that lie in the plane (perpendicular to the apical-basal axis) (Figure 1D). In mammalian epithelial cells, the core polarization complex proteins, Par-3, Par-6, and aPKC, are localized to the apical side of the cells (Jaffe et al. 2008, Mizuno et al. 2003). Cdc42 both promotes the localization of the core polarity complex and promotes the proper positioning of the spindle perpendicular to the apical-basal axis (Chen et al. 2006, Jaffe et al. 2008). How Cdc42 promotes the positioning of the spindle is not fully understood but it is clear that dynein, astral microtubules and the Adenomatosis Polyposis Coli (APC) protein (the homolog of Kar9) are involved (Beamish et al. 2009, O'Connell and Wang 2000). Proper positioning of the spindle parallel to the epithelial plane ensures that the two progeny cells also lie in the epithelium.

Fission yeast cell division: division according to the geometric axes of the cell

Fission yeast cells are cylindrical in shape and thus have short and long axes. Cell growth occurs at the tips of the cylinder and cell division occurs at the midpoint resulting in two cylindrical progeny cells (Figure 1E). Polarization along the long axis of the cell is accomplished by the Tea1p, Tea4p, Tip1p protein complex, which localizes to the growing tips of the cell (reviewed in (Martin 2009)). This complex ultimately recruits the GTPase, Cdc42, which is required for apical growth at cell tips (Miller and Johnson 1994). The Tea1, Tea4, Tip1 complex also allows capture of astral MT plus ends at the cell tips, possibly through the MT binding protein, Mal3p (EB1 in mammals) (Busch and Brunner 2004). Generation of equal microtubule pushing forces moves the SPBs and the nucleus into the middle of the cell in interphase (Tran et al. 2001). Simultaneously, the Mid1 protein is also localized to the middle of the cell by counteracting signals from the cell tips by the polarity factor, Pom1 (Martin and Berthelot-Grosjean 2009, Moseley et al.

2009). At the middle of the cell, Mid1 and signals from the nucleus collaborate to form the medial cortex zone (Daga and Chang 2005). This medial cortex nucleates an actin network that interacts with astral MTs and likely exerts forces on the astral MTs to position the spindle parallel to the long axis (Gachet et al. 2006). While more indirect, here too, spindle position is coordinated by the same machinery that determines cell polarity.

Mechanisms that position the budding yeast spindle

Positioning of the mitotic spindle is a stepwise process that involves many players. The spindle is typically positioned after SPB duplication through metaphase although it is important to note that the anaphase spindle can be positioned as defects in spindle position can be corrected after spindle elongation has occurred. Two main, partially redundant pathways position the spindle. The first involves the protein Kar9 and the actin cytoskeleton (Figure 2). The second pathway relies on the MT motor dynein and the cortical anchor Num1 (Figure 2). Also discussed is a much less well understood pathway that promotes interactions between astral MTs and the bud neck (Figure 2).

The Kar9 pathway

The function of Kar9 (APC in mammals) is intimately tied to SPB asymmetry. Kar9 initially localizes to only one SPB in prophase and this SPB is ultimately destined to segregate to the daughter cell (Liakopoulos et al. 2003, Maekawa and Schiebel 2004, Maekawa et al. 2003). How this initial asymmetry is generated is not well understood but Clb4-CDK co-localizes with Kar9 and is required for this asymmetry (Maekawa and Schiebel 2004). As an aside, it is interesting to note that the analog of Clb4 in mammals, Cyclin A, appears to also regulate APC function and mutations in either Cyclin A or APC lead to spindle position defects in cultured cells (Beamish et al. 2009). Kar9 is complexed with the MT end binding protein, Bim1 (EB1 in mammals) (Korinek et al. 2000, Lee et al. 2000, Miller, Cheng and Rose 2000). This complex along with Clb4-CDK are transported by the action of the kinesin, Kip2, to the plus ends of astral MTs that emanate from the daughter bound SPB (Maekawa et al. 2003). Kar9 also binds the class V myosin, Myo2, and through the action of Myo2, astral MTs are transported along the bud

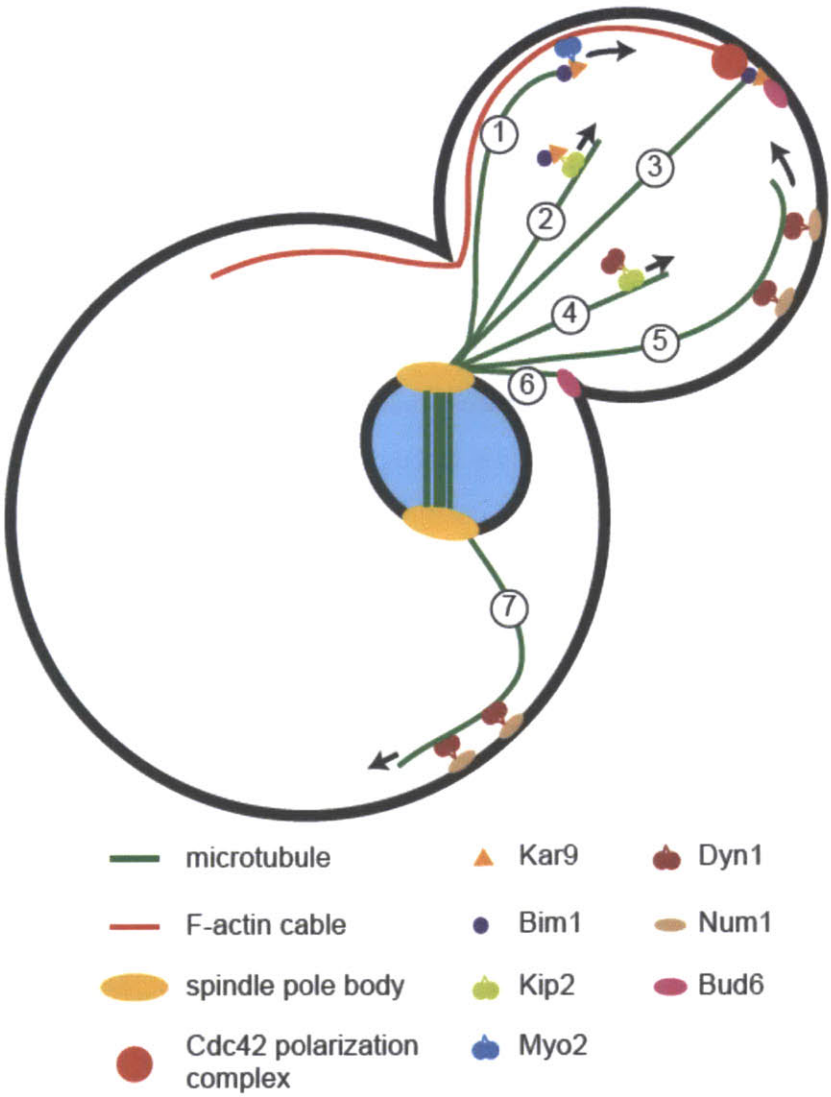

Figure 2: Multiple pathways position the mitotic spindle of budding yeast

(1-3) Kar9-Bim1 is transported to plus ends of microtubules (MTs) by the kinesin, Kip2. At MT plus ends, Kar9-Bim1 interacts with the myosin, Myo2, to transport MTs to the bud tip along F-actin cables. At the bud tip, MT are anchored by the combined action of Kar9-Bim1 and Bud6.

(4-5) The minus end directed MT motor, dynein, is transported to plus ends of MTs by Kip2. At the plus end of growing MTs, dynein can be captured by the cortical anchor, Num1. Once anchored, dynein can exert minus end direct forces on the MT to slide the MT to the bud tip where it can be anchored by Bud6.

(6) Astral MTs can interact with the bud neck via Bud6.

(7) Astral MTs in the mother cell can be transported along the cell cortex by the same mechanism as in (4-5).

cortex along actin cables to the bud tip (Hwang et al. 2003, Yin et al. 2000). Once these astral MTs arrive at the bud tip, they are anchored there through the action of Kar9-Bim1 and the polarity factor, Bud6 (Segal, Bloom and Reed 2000). The generation of forces on these MTs is not fully understood but may proceed by MT plus end depolymerization by the kinesin Kip3 while still maintaining anchorage to the bud tip (Gupta et al. 2006). Additionally, the minus end directed kinesin, Kar3, might also mediate MT shortening at the SPBs to generate forces although evidence for this role has been elusive. However these forces are generated, they ultimately result in the spindle being pulled from one end into the bud neck.

The dynein pathway

Dynein along with its regulatory complex, dynactin, is transported to the plus ends of astral MTs through the action of Kip2 (Carvalho et al. 2004, Lee, Oberle and Cooper 2003). While this transport occurs on astral MTs that emanate from both SPBs, there does appear to be a stronger concentration of dynein on the SPB destined for the daughter and the MTs it polyermizes (Lee et al. 2003). Dynein localized to the plus ends of MTs is then captured by the cortical dynein anchor, Num1. Num1 is localized to static patches on the cortex and can bind dynein (Farkasovsky and Kuntzel 2001, Heil-Chapdelaine, Oberle and Cooper 2000). A model has been proposed that while transported by Kip2 to MT plus ends, dynein is inactive, but once bound by Num1, dynein is activated for its minus end directed motor activity. These motor forces would thus allow astral MTs to slide along the cortex to opposite poles of the cell, thus aligning the spindle. Due to the higher concentration of dynein to the daughter astral MTs, asymmetric forces may be generated that promote spindle rotation to the mother-bud axis. An interesting additional asymmetry to note is that Num1 initially localizes only to the mother cell cortex and only in late G2 does it localize to both the mother and bud cortices (Farkasovsky and Kuntzel 1995, Heil-Chapdelaine et al. 2000). This asymmetry may also regulate differential force generation on the poles of the spindle.

The bud neck pathway

The polarity factor Bud6 also localizes to the bud neck where it mediates capture of astral MTs (Segal et al. 2000). The factors involved in astral MT-bud neck connections are unknown. However, generation of pulling forces on these MTs would also contribute to positioning of the spindle to the bud neck but the nature of these pulling forces is also unknown.

Cell cycle control in budding yeast

Control of the cell cycle in budding yeast, as in other eukaryotes, is mediated by cyclin dependent kinases (CDKs). The single CDK in budding yeast is encoded by the *CDC28* gene, and associates with various cyclin subunit proteins that activate and regulate CDK levels during the cell cycle (Figure 3). Cyclin-CDK complexes are primarily regulated in budding yeast through directly binding inhibitor proteins (CKIs) and cyclin degradation by ubiquitin mediated proteolysis by the proteosome. The major CKI in yeast, Sic1, inhibits the activity of mitotic cyclin-CDK complexes. The major E3-ubiquitin ligases involved in cell cycle control are the SCF (Skp1/cullin/F-box) and the APC/C (anaphase promoting complex/cyclosome). The roles of CDKs and their inhibitors in cell cycle progression are summarized below.

G1 cyclins and the control of cell cycle entry

Entry into the cell cycle is controlled by the Cln family of cyclins, Cln1, Cln2 and Cln3. Cln3 gene expression is sensitive to nutrient conditions but this relationship is not well understood (Polymenis and Schmidt 1997). Cln3-CDK phosphorylates Whi5, an inhibitor of the transcription factor Swi4/6 that controls Cln1/2 expression, which results in its inactivation via nuclear export (Costanzo et al. 2004, de Bruin et al. 2004). Expression of Cln1/2 promotes the transition from G1 into S phase by targeting the Clb-CDK inhibitor, Sic1, for degradation, and also promotes bud formation through activation of Cdc42 and initiates SPB duplication (Schneider, Yang and Futcher 1996, Gulli et al. 2000, Cvrckova and Nasmyth 1993, Benton et al. 1993, Haase, Winey and Reed 2001). The SCF targets Sic1 and the G1 cyclins for destruction through the specificity F-box subunits, Cdc4 and

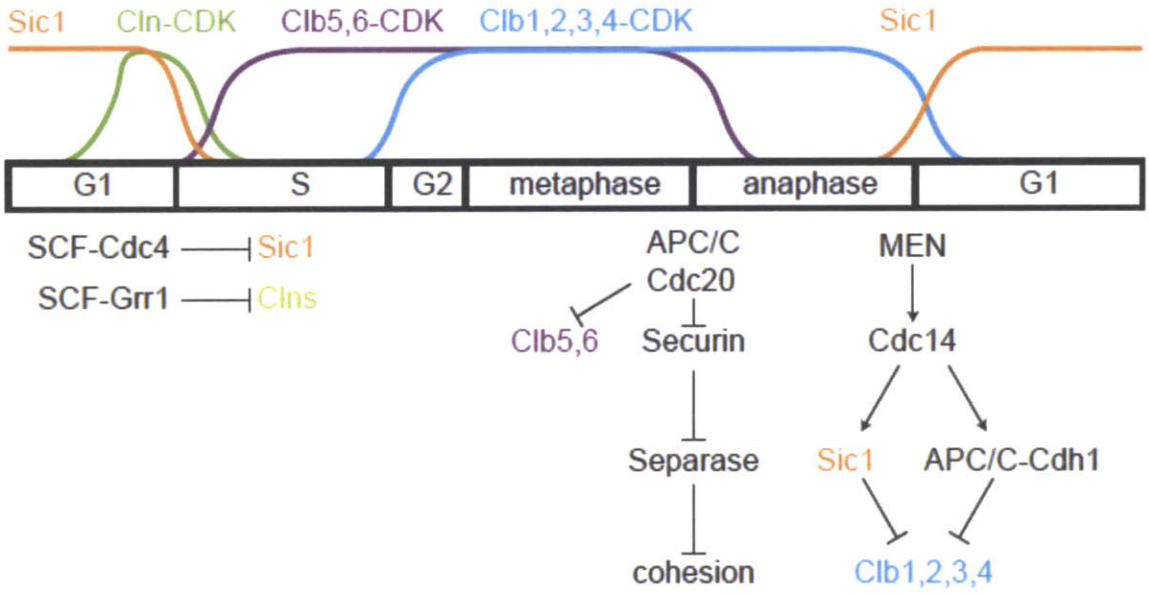

Figure 3: Control of the cell cycle by cyclin-CDK complexes

In early G1 phase, there is no cyclin-CDK activity and levels of the CKI, Sic1 and the APC/C activating subunit, Cdh1, are high thus inhibiting any Clb-CDK activity. Upon meeting nutrient requirements, Cln3-CDK begins to accumulate thus activating the synthesis of Cln1,2. Cln1,2-CDK phosphorylates Sic1 to target it for destruction by SCF-Cdc4, promotes the synthesis of S-phase cyclins, Clb5,6 and is thought to auto-phosphorylate thus targeting themselves for destruction by SCF-Grr1. At the metaphase-anaphase transition, APC/C in complex with Cdc20 targets Securin for destruction thus leading to the removal of cohesion from chromosomes by Separase and thus allows spindle elongation and anaphase entry. At mitotic exit, the MEN is activated and results in the sustained release and activation of Cdc14 which inhibits Clb-CDK activity by upregulating Sic1 and activating APC/C-Cdh1 mediated destruction of the mitotic cyclins.

Grr1 respectively (Feldman et al. 1997, Skowyra et al. 1997, Barral, Jentsch and Mann 1995).

S phase cyclins and the initiation of DNA replication

Pre-replicative complexes (preRCs) comprised of the ORC complex, the MCM helicase complex, Cdc6 and Cdt1 are loaded onto origins of DNA replication in G1 (reviewed in (Tabancay and Forsburg 2006)). The S-phase cyclin-CDKs along with the Dbf4 dependent kinase (DDK) phosphorylate components of the preRC and activate origin

firing. Origins can only fire once due to the inhibition of preRC reassembly on replication origins by the S-phase kinases, Clb5/6-CDK.

Mitotic cyclins and the segregation of chromosomes

Expression of the remaining Clb cylcins (Clb1-4) promotes the events required for proper chromosome segregation. During pro-metaphase and metaphase, assembly of a bipolar spindle and coordination of proper spindle dynamics requires mitotic CDK activity (reviewed in (Nigg 2001)). Positioning of the pro-metaphase/metaphase spindle, through asymmetric SPB determination, generation of motor forces and spindle dynamics, is also regulated by mitotic CDKs. At the metaphase-anaphase transition, the E3-ubiquitin ligase, Anaphase Promoting Complex/Cyclosome (APC/C) in complex with the specificity factor Cdc20 degrades the Separase inhibitor, Securin (reviewed in (Peters 2006)). Activated Separase cleaves cohesin complexes, the protein rings that hold sister chromatids together thus allowing chromosome separation and spindle elongation. Here too, CDKs appear to play a critical role. The APC/C is likely activated by mitotic CDK activity and spindle elongation also requires mitotic CDK activity, possibly by regulating MT motor activity (Rahal and Amon 2008, Rudner and Murray 2000).

Exit from the cell cycle and the destruction of mitotic cyclins

Cells exit mitosis and reenter the G1 phase of the cell cycle after the completion of anaphase. This involves disassembly of the spindle, decondensation of the chromosomes and cytokinesis. This is achieved through inactivation of mitotic cyclin-CDK complexes and in budding yeast, is mediated by the phosphatase, Cdc14 (reviewed in (Stegmeier and Amon 2004)). Cdc14 activation is controlled by two signaling pathways, the FEAR network and the MEN and are discussed in detail below. Active Cdc14 dephosphorylates the key substrates, Cdh1, Swi5 and Sic1 (Jaspersen, Charles and Morgan 1999, Visintin et al. 1998, Zachariae et al. 1998). Cdh1 is a specificity factor for the APC/C. Dephosphorylation of Cdh1 leads to its activation thus allowing APC/C-Cdh1 to target mitotic cyclins for destruction. Dephosphorylation of Sic1 leads to its stabilization and thus promotes its CKI function. Lastly, Sic1 levels are also upregulated by the dephosphorylation of the Swi5 transcription factor thus allowing its nuclear import and

transcriptional activation of Sic1. While these three substrates are key players in mitotic exit, it is thought that Cdc14 reverses most CDK dependent phosphorylations thus fully returning the cell to G1.

Control of Mitotic Exit by the FEAR network and the MEN

Mitotic exit is controlled by two pathways that govern activation of Cdc14. Cdc14 resides in the nucleolus until early anaphase, when it is transiently released from its inhibitor, Cfi1/Net1 by the Cdc14 Early Anaphase Release (FEAR) network (Shou et al. 1999, Stegmeier, Visintin and Amon 2002, Visintin, Hwang and Amon 1999). Later on in anaphase, Cdc14 is released in a sustained manner by the Mitotic Exit Network (MEN).

FEAR network mediated release of Cdc14 is not essential for cell viability but does contribute to the proper stabilization of the spindle, the segregation of the rDNA and many other events during anaphase (reviewed in (Rock and Amon 2009)). How the FEAR network functions is not understood at a molecular level but it appears that Separase activated at the metaphase-anaphase transition along with the kinetochore protein, Slk19 promote the downregulation of PP2A-Cdc55 phosphatase, likely through the Zds1/2 proteins (Queralt et al. 2006, Queralt and Uhlmann 2008). Downregulation of PP2A-Cdc55 allows CDK to phosphorylate Cdc14's nucelolar inhibitor, Cfi1/Net1 and results in the release of Cdc14 (Azzam et al. 2004). CDK also appears to phosphorylate Spo12, which is important for FEAR network function, but this is not subject to PP2A-Cdc55 regulation (Stegmeier et al. 2004, Tomson et al. 2009). The polo like kinase, Cdc5, appears to act in parallel to promote early anaphase release of Cdc14 (Yoshida and Toh-e 2002, Shou et al. 2002).

The sustained release of Cdc14 by the MEN is essential for cell viability (Figure 4). The MEN is controlled by the small GTPase switch, Tem1 (Shirayama, Matsui and Toh 1994b). In the active (likely GTP bound) form, Tem1 activates and recruits to the SPB, the kinases Cdc15 and Dbf2-Mob1 (Visintin and Amon 2001). Dbf2-Mob1 is required to release Cdc14 from Cfi1 (Visintin et al. 1999, Mohl et al. 2009). Tem1 is positively

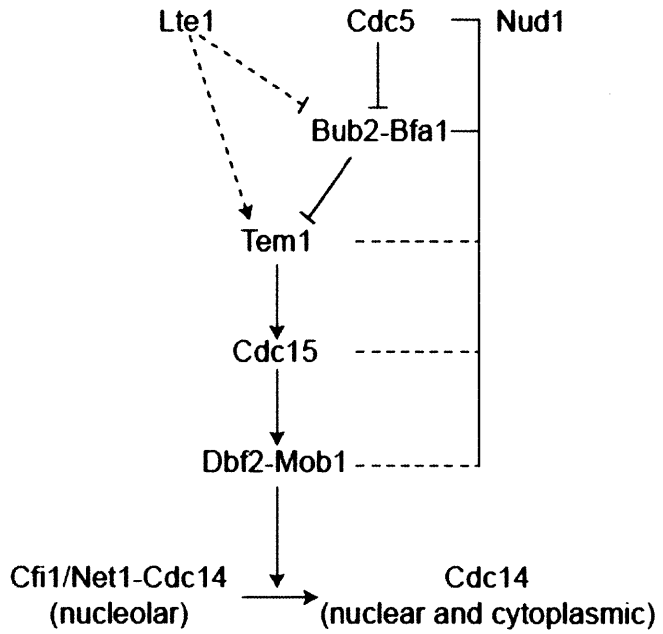

Figure 4: The mitotic exit network

The mitotic exit network is controlled by the GTPase, Tem1. Tem1 signals through the kinases Cdc15 and Dbf2-Mob1 to release and activate Cdc14. Tem1 is controlled positively by Lte1 and negatively by the two-component GAP complex, Bub2-Bfa1. Nud1 anchors Bub2-Bfa1 and Cdc5 to the SPB and is thought to act as a scaffold for Tem1, Cdc15 and Dbf2-Mob1. Dashed lines indicate hypothetical interations.

regulated by the bud associated protein, Lte1 and negatively by the two component GTPase activating protein (GAP) complex, Bub2-Bfa1 (Bardin, Visintin and Amon 2000, Bloecher, Venturi and Tatchell 2000, Geymonat et al. 2002, Lee et al. 1999, Li 1999, Pereira et al. 2000, Shirayama et al. 1994a). Cdc5 promotes the function of the MEN at multiple levels. Cdc5 phosphorylates and inactivates the GAP complex allowing Tem1 to signal (Geymonat et al. 2003, Hu et al. 2001). Cdc5 also likely plays a role very downstream at the level of Cdc14-Cfi1 interaction to promote Cdc14 release (Shou et al. 2002, Visintin et al. 2008, Yoshida and Toh-e 2002). All of the components of the MEN with the exception of Lte1 localize to the SPB and this localization is thought to be critical for signaling (Bardin et al. 2000, Fraschini et al. 1999, Lee et al. 1999, Li 1999, Molk et al. 2004, Pereira et al. 2000, Cenamor et al. 1999, Song et al. 2000, Frenz et al. 2000). Nud1, a component of the SPB outer plaque, is required for MEN function but it

has only been shown to physically interact with the GAP complex and Cdc5 (Gruneberg et al. 2000, Ho et al. 2002).

Mitotic checkpoint control of the yeast cell cycle

The cell employs various feedback mechanisms to delay cell cycle progression in response to defects in key cell division processes. Discussed below are the two mitotic checkpoints that delay the cell cycle in response to spindle defects, the spindle assembly checkpoint and the spindle position checkpoint. Special attention will be paid to the mechanisms that communicate with the cell cycle machinery.

The spindle assembly checkpoint

Sister chromatids must be segregated to opposite poles of the spindle to ensure equal genome partitioning. This is accomplished by sister kinetochores being attached to opposite spindle poles through MTs. This MT-kinetochore attachment configuration is referred to as bi-orientation and all pairs of sister kinetochores must be bi-oriented for proper genome partitioning. When sister kinetochores are bi-oriented, they have equal MT pulling forces exerted on them and are said to be under tension.

The spindle assembly checkpoint (SAC) responds to defects in MT-kinetochore attachment and tension. The likely triggering event for the checkpoint is the existence of an unattached kinetochore. A current model of how unattachment is sensed and relayed to the cell cycle machinery is as follows (reviewed in (Musacchio and Salmon 2007)). The APC/C, the master regulator of the metaphase-anaphase transition, is inhibited by the mitotic checkpoint complex (MCC), which consists of the APC/C specificity subunit, Cdc20 and the SAC proteins, Mad2, Mad3 and Bub3. Assembly of the MCC is not entirely understood but Mad2 appears to exist in "open" and "closed" conformational states and is in the closed state when in the MCC. Generation of closed-Mad2 appears to occur via a "self-templating" process where closed-Mad2 can interact with open-Mad2 and convert it to the closed state. Closed-Mad2 is first generated at unattached kinetochores in concert with Mad1, which localizes to kinetochores in pro-metaphase. This pool of closed-Mad2 self-templates and converts the cytosolic pool of Mad2 to the

closed state which binds and inhibits APC/C-Cdc20. This model helps to explain how a single unattached kinetochore and thus a very small pool of closed-Mad2 is still sufficient to mediate a strong cell-cycle arrest. Once all kinetochores are attached, Mad1-Mad2 is transported away from kinetochores by dynein along the newly attached microtubule. Other mechanisms also promote checkpoint silencing which may reset the cytosolic pool of closed-Mad2-Cdc20 such as $p31^{comet}$ and the ubiqutylation (not for degradation) of Cdc20.

The tension sensing aspect of the SAC does not seem to communicate directly with the cell cycle machinery, rather lack of tension results in the generation of an unattached kinetochore which triggers the SAC response. The kinase Ipl1 (Aurora B in other systems) resides at centromeres and phsophorylates the KMN network of proteins, the major MT binding activity at kinetochores (DeLuca et al. 2006, Cheeseman et al. 2006, Tanaka et al. 2002). Phosphorylation of the KMN network destabilizes MT-kinetochore interactions. When kinetochores are not under tension, they reside at the centromere where Ipl1 can destabilize MT-kinetochore interactions. Generation of an unattached kinetochore is then sensed by the MCC resulting in cell cycle arrest. When kinetochores are properly under tension, they are pulled away from the centromere and Ipl1 cannot destabilize kinetochore-MT interactions, thus effectively promoting bi-orientation (Liu et al. 2009, Tanaka et al. 2002).

The Spindle Position Checkpoint

As highlighted above, the spindle must be positioned along pre-determined axes to ensure accurate genome partitioning during polarized cell division. Evidence for a checkpoint mechanism that delays cell cycle progression in response to defects in spindle positioning has been presented in cultured rat kidney cells, fly germline stem cells and budding yeast.

Evidence from mammalian cells

O'Connell et al. perturbed the position of the mitotic spindle relative to the dividing kidney cell by mechanically deforming the cell with a glass needle (O'Connell and Wang 2000). They found that upon deformation, the spindle would rotate or linearly translate

back to the center of the deformed cell. They found that these corrective movements were dependent on MTs (likely astral) and dynein. Interestingly, they also observed a delay in anaphase onset while cells repositioned their spindles, suggestive of a checkpoint mechanism.

Evidence from *Drosophila* stem cells

Drosophila male germline stem cells undergo asymmetric cell divisions, giving rise to one stem cell and one gonialblast. Similar mechanisms that define cell axes and coordinate spindle position act during this cell division as they do in fly neuroblasts described above. Cheng et al. found that during mitotic prophase of germline stem cells derived from old flies, the centrosomes were often mispositioned with respect to the polarity axis (Cheng et al. 2008). Consistent with a checkpoint mechanism, they also found that anaphase initiation was delayed until the centrosomes were re-oriented to the correct axis. Moreover, old stem cells with mispositioned centrosomes were observed to not enter mitosis as frequently as cells that correctly positioned their centrosomes. Taken together, these two observations suggest a mechanism that delays mitotic onset until the centrosomes are correctly positioned.

Evidence from budding yeast

In budding yeast, Yeh et al. found that in the absence of dynein, cells have difficulty positioning the spindle along the mother-bud axis and thus anaphase spindle elongation often times occurred entirely in the mother (Yeh et al. 1995). When the spindle did elongate in the mother, they observed that the cell did not undergo cytokinesis until the spindle had been repositioned along the correct axis. Furthermore, they observed a very consistent time interval between the spindle entering the bud and cytokinesis, suggesting that mitotic exit is triggered by spindle entry into the bud. They proposed the existence of a spindle position checkpoint (SPOC) mechanism that delays mitotic exit in the presence of spindle misposition and found examples of cells that could delay this cell cycle transition for over three hours, suggesting that such a checkpoint mechanism could be quite potent.

Molecular characterization of the SPOC: Bub2, Bfa1 and Lte1

A number of groups identified the first factor involved in this checkpoint. In the absence of *BUB2*, a subunit of the Tem1 GAP, cells with mispositioned spindles were observed to inappropriately exit mitosis and thus produce progeny cells with no nuclei and two nuclei (Bardin et al. 2000, Bloecher et al. 2000, Pereira et al. 2000). Absence of *BFA1* was found to have the same effect. Interestingly, the Tem1 activator, Lte1, was found to have the opposite effect. Cells overexpressing Lte1 also prematurely exited mitosis, suggesting that Lte1 antagonizes this checkpoint (Bardin et al. 2000). However, Bub2, Bfa1 and Lte1 have roles in regulating mitotic exit outside the context of the SPOC.

Identification and studies of the first SPOC factor, Kin4

The protein kinase, Kin4, was identified in a screen for antagonizers of mitotic exit and found to be a SPOC specific factor (D'Aquino et al. 2005, Pereira and Schiebel 2005). Initial work demonstrated that Kin4 is a potent inhibitor of mitotic exit. Cells terminally arrest and cannot exit mitosis when Kin4 is overexpressed (D'Aquino et al. 2005). Cells that normally delay exit from mitosis in response to spindle misposition fail to do so in the absence of Kin4 (D'Aquino et al. 2005, Pereira and Schiebel 2005). Genetic experiments showed that Kin4 inhibits mitotic exit through inhibition of the MEN and various epistasis-type experiments placed Kin4 upstream of or parallel to the GAP complex, Bub2-Bfa1 (D'Aquino et al. 2005, Pereira and Schiebel 2005). Interestingly, Kin4 inhibition of the MEN correlated very well with exclusion of Tem1 loading to SPBs. In cells that overexpress Kin4, Tem1 fails to load on to SPBs (D'Aquino et al. 2005). In cells that misposition their spindles, Tem1 is excluded from both SPBs but in the absence of *KIN4*, cells fail to exclude Tem1 (D'Aquino et al. 2005). Taken together, these data suggested that Kin4's ultimate function in inhibiting the MEN was to exclude Tem1 from loading to SPBs, a localization that highly correlates with MEN activation. Kin4 also displayed a very unusual localization pattern. Kin4 was observed to asymmetrically localize to the mother cell cortex during the cell cycle (D'Aquino et al. 2005, Pereira and Schiebel 2005). Additionally, Kin4 was also observed to load onto the mother bound SPB during anaphase and onto both SPBs during anaphase when the spindle was mispositioned (Pereira and Schiebel 2005). Very few proteins to date have

been described to have mother cell cortex restricted localization and no proteins have been described to asymmetrically localize to the mother bound SPB.

Subsequent studies elucidated the mechanism of how Kin4 inhibits the MEN. Bub2-Bfa1 are phosphorylated and inhibited by the polo-like kinase, Cdc5 (Geymonat et al. 2003, Hu et al. 2001). It was observed under conditions where Cdc5 dependent phosphorylation of Bfa1 was normally low, that in the absence of Kin4, this phosphorylation was greatly increased (Pereira and Schiebel 2005). This suggested a mechanism whereby Kin4's role in inhibiting the MEN was to antagonize the phosphorylation of Bfa1 by Cdc5. Indeed, Kin4 was found to phosphorylate Bfa1 on two serine residues and when these residues were mutated to alanine, Bfa1 was found to be checkpoint incompetent (Maekawa et al. 2007). Additionally, Bfa1 phosphorylation and inhibition by Cdc5 became unregulated in the double serine mutant (Maekawa et al. 2007). This study also provided key evidence that the site of MEN inhibition by Kin4 is at the SPBs. Alleles of *KIN4* that could not localize to SPBs could not mediate MEN inhibition during SPOC activation (Maekawa et al. 2007). Conversely, alleles that were constitutively targeted to SPBs caused a mild anaphase delay that required the presence of the GAP complex, even in the absence of spindle misposition (Maekawa et al. 2007).

Models of the Spindle Position Checkpoint

How spindle misposition is sensed and how that information is relayed to the cell cycle machinery is not well understood. Three main models of how spindle position defects are sensed and translated into MEN inhibitory signals have been proposed. They are discussed below.

Models of the SPOC I: GAP disappearance from the mother bound SPB triggers the MEN

Bfa1, a component of the GAP complex, localizes symmetrically to both SPBs in metaphase but becomes strongly concentrated on the daughter bound SPB during

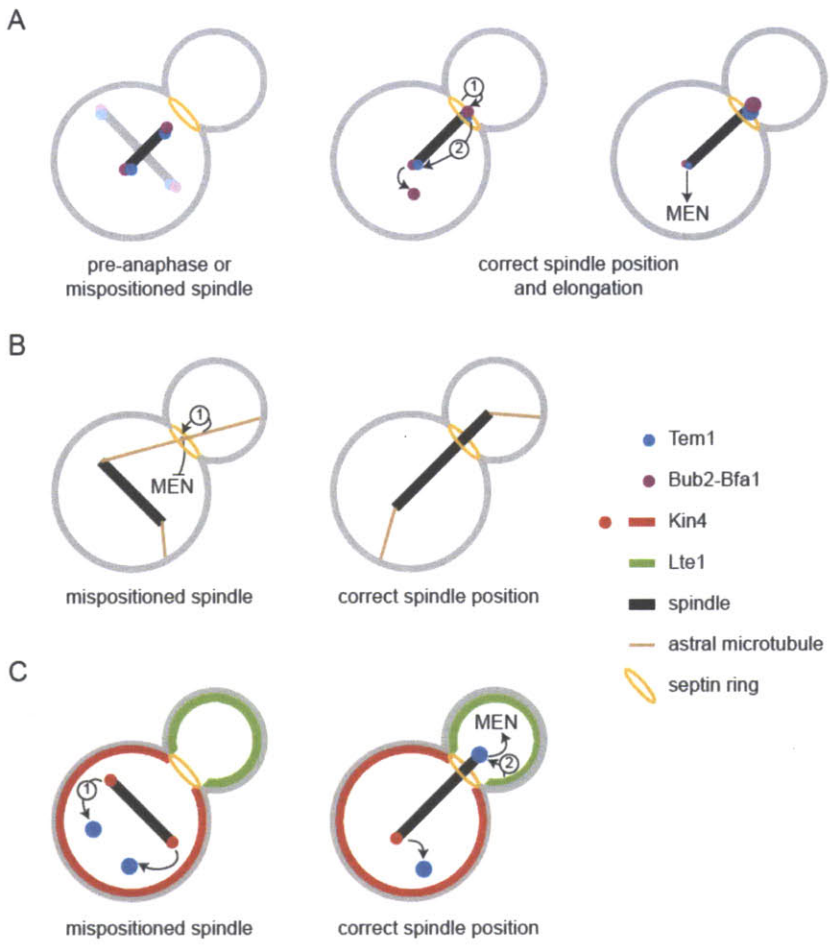

Figure 5: Models of SPOC function

(A) The mother pole activates MEN model:
During metaphase or when the spindle is mispositioned, the SPBs are not in contact with the bud neck. When the spindle elongates, interactions between the daughter SPB and the bud neck (1) generate a signal that is (2) transduced to the mother SPB for Bub2-Bfa1 disappearance. Disappearance of Bub2-Bfa1 activates Tem1 on the mother SPB to trigger MEN signaling.

(B) Bud neck-astral MT interaction model:
During metaphase or when the spindle is mispositioned, astral MTs pass through the bud neck. Interactions between these astral MTs and the bud neck (1) generate MEN inhibitory signals.

(C) The zone model:
When SPBs are in the mother cell during anapahse, Kin4 can load onto these SPBs and antagonize Tem1 loading (1). When the spindle elongates along the correct axis, one SPB escapes the zone of MEN inhibition or the mother cell where Kin4 resides and enters the zone of MEN activation or the daughter cell where Lte1 resides. Upon entry into the daughter cell, the Tem1 bearing SPB can be activated for MEN signaling by Lte1 (2).

anaphase. This asymmetric localization in anaphase is mirrored by Tem1 and correlates very strongly with MEN activation. However, considering that the Bub2-Bfa1 GAP complex is a negative regulator of the MEN, it poses a seeming contradiction: why co-localize Tem1 with its inhibitor during the phase of the cell cycle where Tem1 should be active and mitotic exit should be promoted? Fraschini et al. have proposed a model of MEN activation and SPOC function that attempts to reconcile this discrepancy. They propose a model where passage of the daughter bound SPB through the bud neck transmits a signal for the GAP complex to off-load from the mother bound SPB thus allowing the Tem1 that remains there to signal and trigger mitotic exit (Fraschini et al. 2006) (Figure 5A). Cells that mispositioned their spindles never pass a SPB through the neck and thus Bfa1 remains loaded on both SPBs and the MEN remains inhibited (D'Aquino et al. 2005). Again, the high correlation between Bfa1 asymmetry and MEN activation supports this model. Additionally, Fraschini et al. isolated an allele of Bub2 that localizes the GAP symmetrically to both SPBs (Bub2-9Myc) and it was found that this allele of Bub2 was hyperactive for MEN inhibition (Fraschini et al. 2006). The authors also found that consistent with the passage of the daughter bound SPB through the bud neck triggering a signal to the mother SPB for GAP disappearance, bud neck mutants failed to asymmetrically localize the GAP complex (Fraschini et al. 2006).

This model does not offer a mechanistic basis for the signal the daughter SPB receives upon passage through the bud neck nor does it propose how the daughter SPB communicates with the mother SPB. Additionally, this model does not account for Lte1 or Kin4 in MEN regulation or SPOC function and is inconsistent with the localization pattern of Kin4. If the mother SPB is the SPB from which MEN signaling is initiated, why does Kin4 localize there? Subsequent studies have challenged the two key findings that the model is based on: (1) symmetric GAP localization promotes MEN inhibition and (2) passage through the bud neck promotes GAP asymmetry. Caydasi et al. constructed two symmetric GAP fusion proteins, Bfa1-Cnm67 and Bub2-Cnm67, which constitutively load to both SPBs in all phases of the cell cycle. In contrast to the Bub2-9myc fusion, both of these constructs failed to inhibit the MEN during spindle misposition (Caydasi and Pereira 2009). It is important to note that all three constructs

are competent to inhibit the MEN in the presence of spindle assembly defects suggesting that these protein fusions are all functional at some level (Caydasi and Pereira 2009, Fraschini et al. 2006). Also, when examined by both live cell and fixed cell microscopy, two independent groups failed to reproduce the defects in GAP asymmetry in bud neck mutants (Monje-Casas and Amon 2009) (Gislene Pereira personal communication). The source of this discrepancy is unclear.

Models of the SPOC II: astral MT-bud neck interactions inhibit mitotic exit

When the spindle is not elongated into the bud, often times, there are astral MTs that extend through the bud neck and attach to the bud cortex. This situation occurs prior to anaphase before spindle elongation but also during anaphase when the spindle is mispositioned. Based on time lapse observations that noted a high correlation between loss of astral MTs from the bud neck and mitotic exit, Adames et al. proposed a model where interaction between astral MTs and the bud neck inhibit mitotic exit (Adames, Oberle and Cooper 2001) (Figure 5B). Consistent with this model, mutants that lack astral MTs were observed to bypass the SPOC (Adames et al. 2001). Subsequent studies showed that laser ablation of astral MTs that interacted with the bud neck also triggered mitotic exit (Moore et al. 2009). However, it is important to note that the bypass of the SPOC in mutants lacking astral MTs only occurred in ~ 20% of cells that mispositioned their spindles whereas the *bub2*Δ mutant bypassed the SPOC in ~ 100% of cells (Adames et al. 2001). Thus, astral MT-bud neck interactions cannot account for the majority of SPOC activity. The molecular roles of Bub2, Bfa1, Lte1, Kin4 and Tem1 are not well accounted for in this model but it has been proposed that unidentified SPOC regulating factors could load from the bud neck to the SPB via an interacting astral MT and that once the spindle is repositioned and thus astral MT-bud neck interactions are lost, these factors no longer load thus silencing the SPOC (Moore et al. 2009).

Models of the SPOC III: spatial restriction of Lte1 and Kin4 couple spindle position to mitotic exit

Lte1 is targeted to the bud cortex during all phases of the cell cycle. As noted above, Tem1 is initially symmetrically loaded on SPBs in metaphase but becomes concentrated

on the daughter bound SPB in anaphase. Based on these localization patterns, Bardin et al. proposed a model based on the spatial restriction of the Tem1 activator, Lte1. The model states that in order for the MEN to activate, a Tem1 bearing SPB must enter the bud where Lte1 resides thus coupling proper spindle elongation to MEN activation (Bardin et al. 2000) (Figure 5C). In accordance with this model, experiments that targeted Lte1 to both daughter and mother cell compartments bypassed the SPOC. Bardin et al. first showed this by overexpression of Lte1 (Bardin et al. 2000). Castillon et al. showed this without having to overexpress Lte1 by disabling the spetin ring diffusion barrier between the mother and daughter cells thus allowing Lte1 to leak into the mother cell (Castillon et al. 2003). Most recently, Geymonat et al. have isolated an allele of Lte1 that localizes to both the mother and daughter cell cortices (Geymonat et al. 2009). Here too, cells that misposition their spindles fail to downregulate the MEN and prematurely exit mitosis .

These experiments underscored the importance of maintaining Lte1 in the bud but many have noted that this mechanism cannot account for the entirety of MEN activation and SPOC function. Lte1 is only required for mitotic exit at temperatures below 18°C and only promotes timely mitotic exit at higher temperatures (Adames et al. 2001, Shirayama et al. 1994a). The missing piece was proposed to be Kin4 based on its localization being asymmetric in the mother cell (D'Aquino et al. 2005). The model was extended to state that in order for the MEN to signal, the daughter SPB had to first escape the zone of MEN inhibition or the mother cell where Kin4 resides and then enter the daughter cell or the zone of MEN activation where Lte1 resides (Figure 5C).

This model has not been tested for Kin4's proposed function. Furthermore, this model does not mechanistically account for how Lte1 and Kin4 communicate with Tem1 and the role of the Bub2-Bfa1 GAP complex in this process.

Outstanding questions remaining in SPOC and Tem1 regulation

The molecular details of how the SPOC functions and how Tem1 is regulated are only partially understood. Biochemical studies of Tem1, Bub2-Bfa1 and Lte1 have unveiled

additional questions. Tem1 was found to be an unusual GTPase. Most small G-proteins are very inefficient at both GTP hydrolysis and GDP disassociation and only catalyze either reaction in the presence of the appropriate GAPs or guanine nucleotide exchange factors (GEFs) (reviewed in (Paduch, Jelen and Otlewski 2001)). Tem1 was found to be quite proficient for both GTP hydrolysis and for GDP exchange (Geymonat et al. 2002). Addition of Bfa1 alone to the Tem1 reaction showed that Bfa1 acts as a disassociation inhibitor (GDI) for both Tem1-GDP and unusually, Tem1-GTP (Fraschini et al. 2006, Geymonat et al. 2009, Geymonat et al. 2002). Further addition of Bub2 to the reaction restored the GTPase activity of Tem1 but only back to the basal hydrolysis rate of Tem1 alone (Fraschini et al. 2006, Geymonat et al. 2002). These findings challenge the notion that Bub2-Bfa1 acts as a GAP at all.

How Lte1 promotes Tem1 activation is also unclear. Lte1 contains putative GEF domains and has been proposed to act as a GEF for Tem1 (Bardin et al. 2000, Shirayama et al. 1994a). However, no *in vitro* GEF activity could be detected for Lte1 (Geymonat et al. 2009). It has been proposed that Lte1 may promote Bub2-Bfa1 asymmetry but the functional importance of Bub2-Bfa1 localization remains unclear.

Many outstanding questions also remain for Kin4. Kin4 promotes the sustained activation of the GAP complex by protecting it from Cdc5 mediated inhibition. How does this sustained activation translate to Tem1 exclusion from the SPBs? How is Kin4 regulated and how is its localization controlled? Does Kin4 respond to spindle misposition, and if so, how does it sense such a spatial defect?

Findings of the work presented in this thesis dissertation

This thesis presents three main findings. First, we identify a new SPOC component, PP2A-Rts1 and show that this phosphatase controls both Kin4 phosphorylation and localization. Second, we identify domains and sequence determinants of Kin4 that control MEN inhibition, cortical localization and asymmetric mother cell restriction. Lastly, we show that Kin4 does not respond to spindle mis-position but that spindle mis-position is

sensed by the spatial restriction of Kin4 to the mother cell indicating that a key event in triggering MEN signaling is the escape of an SPB from the zone of Kin4 activity.

References

Adames, N. R., J. R. Oberle & J. A. Cooper (2001) The surveillance mechanism of the spindle position checkpoint in yeast. *J Cell Biol,* 153, 159-68.

Azzam, R., S. L. Chen, W. Shou, A. S. Mah, G. Alexandru, K. Nasmyth, R. S. Annan, S. A. Carr & R. J. Deshaies (2004) Phosphorylation by cyclin B-Cdk underlies release of mitotic exit activator Cdc14 from the nucleolus. *Science,* 305, 516-9.

Bardin, A. J., R. Visintin & A. Amon (2000) A mechanism for coupling exit from mitosis to partitioning of the nucleus. *Cell,* 102, 21-31.

Barral, Y., S. Jentsch & C. Mann (1995) G1 cyclin turnover and nutrient uptake are controlled by a common pathway in yeast. *Genes Dev,* 9, 399-409.

Beamish, H., L. de Boer, N. Giles, F. Stevens, V. Oakes & B. Gabrielli (2009) Cyclin A/cdk2 regulates adenomatous polyposis coli-dependent mitotic spindle anchoring. *J Biol Chem,* 284, 29015-23.

Benton, B. K., A. H. Tinkelenberg, D. Jean, S. D. Plump & F. R. Cross (1993) Genetic analysis of Cln/Cdc28 regulation of cell morphogenesis in budding yeast. *EMBO J,* 12, 5267-75.

Bloecher, A., G. M. Venturi & K. Tatchell (2000) Anaphase spindle position is monitored by the BUB2 checkpoint. *Nat Cell Biol,* 2, 556-8.

Busch, K. E. & D. Brunner (2004) The microtubule plus end-tracking proteins mal3p and tip1p cooperate for cell-end targeting of interphase microtubules. *Curr Biol,* 14, 548-59.

Carvalho, P., M. L. Gupta, Jr., M. A. Hoyt & D. Pellman (2004) Cell cycle control of kinesin-mediated transport of Bik1 (CLIP-170) regulates microtubule stability and dynein activation. *Dev Cell,* 6, 815-29.

Casamayor, A. & M. Snyder (2002) Bud-site selection and cell polarity in budding yeast. *Curr Opin Microbiol,* 5, 179-86.

Castillon, G. A., N. R. Adames, C. H. Rosello, H. S. Seidel, M. S. Longtine, J. A. Cooper & R. A. Heil-Chapdelaine (2003) Septins have a dual role in controlling mitotic exit in budding yeast. *Curr Biol,* 13, 654-8.

Caydasi, A. K. & G. Pereira (2009) Spindle alignment regulates the dynamic association of checkpoint proteins with yeast spindle pole bodies. *Dev Cell,* 16, 146-56.

Cenamor, R., J. Jimenez, V. J. Cid, C. Nombela & M. Sanchez (1999) The budding yeast Cdc15 localizes to the spindle pole body in a cell-cycle-dependent manner. *Mol Cell Biol Res Commun,* 2, 178-84.

Chant, J. (1999) Cell polarity in yeast. *Annu Rev Cell Dev Biol,* 15, 365-91.

Cheeseman, I. M., J. S. Chappie, E. M. Wilson-Kubalek & A. Desai (2006) The conserved KMN network constitutes the core microtubule-binding site of the kinetochore. *Cell,* 127, 983-97.

Chen, L., G. Liao, L. Yang, K. Campbell, M. Nakafuku, C. Y. Kuan & Y. Zheng (2006) Cdc42 deficiency causes Sonic hedgehog-independent holoprosencephaly. *Proc Natl Acad Sci U S A,* 103, 16520-5.

Cheng, J., N. Turkel, N. Hemati, M. T. Fuller, A. J. Hunt & Y. M. Yamashita (2008) Centrosome misorientation reduces stem cell division during ageing. *Nature,* 456, 599-604.

Costanzo, M., J. L. Nishikawa, X. Tang, J. S. Millman, O. Schub, K. Breitkreuz, D. Dewar, I. Rupes, B. Andrews & M. Tyers (2004) CDK activity antagonizes Whi5, an inhibitor of G1/S transcription in yeast. *Cell,* 117, 899-913.

Cvrckova, F. & K. Nasmyth (1993) Yeast G1 cyclins CLN1 and CLN2 and a GAP-like protein have a role in bud formation. *EMBO J,* 12, 5277-86.

D'Aquino, K. E., F. Monje-Casas, J. Paulson, V. Reiser, G. M. Charles, L. Lai, K. M. Shokat & A. Amon (2005) The protein kinase Kin4 inhibits exit from mitosis in response to spindle position defects. *Mol Cell,* 19, 223-34.

Daga, R. R. & F. Chang (2005) Dynamic positioning of the fission yeast cell division plane. *Proc Natl Acad Sci U S A,* 102, 8228-32.

de Bruin, R. A., W. H. McDonald, T. I. Kalashnikova, J. Yates, 3rd & C. Wittenberg (2004) Cln3 activates G1-specific transcription via phosphorylation of the SBF bound repressor Whi5. *Cell,* 117, 887-98.

DeLuca, J. G., W. E. Gall, C. Ciferri, D. Cimini, A. Musacchio & E. D. Salmon (2006) Kinetochore microtubule dynamics and attachment stability are regulated by Hec1. *Cell,* 127, 969-82.

Farkasovsky, M. & H. Kuntzel (1995) Yeast Num1p associates with the mother cell cortex during S/G2 phase and affects microtubular functions. *J Cell Biol,* 131, 1003-14.

--- (2001) Cortical Num1p interacts with the dynein intermediate chain Pac11p and cytoplasmic microtubules in budding yeast. *J Cell Biol,* 152, 251-62.

Feldman, R. M., C. C. Correll, K. B. Kaplan & R. J. Deshaies (1997) A complex of Cdc4p, Skp1p, and Cdc53p/cullin catalyzes ubiquitination of the phosphorylated CDK inhibitor Sic1p. *Cell,* 91, 221-30.

Fraschini, R., C. D'Ambrosio, M. Venturetti, G. Lucchini & S. Piatti (2006) Disappearance of the budding yeast Bub2-Bfa1 complex from the mother-bound spindle pole contributes to mitotic exit. *J Cell Biol,* 172, 335-46.

Fraschini, R., E. Formenti, G. Lucchini & S. Piatti (1999) Budding yeast Bub2 is localized at spindle pole bodies and activates the mitotic checkpoint via a different pathway from Mad2. *J Cell Biol,* 145, 979-91.

Frenz, L. M., S. E. Lee, D. Fesquet & L. H. Johnston (2000) The budding yeast Dbf2 protein kinase localises to the centrosome and moves to the bud neck in late mitosis. *J Cell Sci,* 113 Pt 19, 3399-408.

Gachet, Y., C. Reyes, S. Goldstone & S. Tournier (2006) The fission yeast spindle orientation checkpoint: a model that generates tension? *Yeast,* 23, 1015-29.

Geymonat, M., A. Spanos, G. de Bettignies & S. G. Sedgwick (2009) Lte1 contributes to Bfa1 localization rather than stimulating nucleotide exchange by Tem1. *J Cell Biol,* 187, 497-511.

Geymonat, M., A. Spanos, S. J. Smith, E. Wheatley, K. Rittinger, L. H. Johnston & S. G. Sedgwick (2002) Control of mitotic exit in budding yeast. In vitro regulation of Tem1 GTPase by Bub2 and Bfa1. *J Biol Chem,* 277, 28439-45.

Geymonat, M., A. Spanos, P. A. Walker, L. H. Johnston & S. G. Sedgwick (2003) In vitro regulation of budding yeast Bfa1/Bub2 GAP activity by Cdc5. *J Biol Chem,* 278, 14591-4.

Goldstein, B. & S. N. Hird (1996) Specification of the anteroposterior axis in Caenorhabditis elegans. *Development,* 122, 1467-74.

Gruneberg, U., K. Campbell, C. Simpson, J. Grindlay & E. Schiebel (2000) Nud1p links astral microtubule organization and the control of exit from mitosis. *EMBO J,* 19, 6475-88.

Gulli, M. P., M. Jaquenoud, Y. Shimada, G. Niederhauser, P. Wiget & M. Peter (2000) Phosphorylation of the Cdc42 exchange factor Cdc24 by the PAK-like kinase Cla4 may regulate polarized growth in yeast. *Mol Cell,* 6, 1155-67.

Gupta, M. L., Jr., P. Carvalho, D. M. Roof & D. Pellman (2006) Plus end-specific depolymerase activity of Kip3, a kinesin-8 protein, explains its role in positioning the yeast mitotic spindle. *Nat Cell Biol,* 8, 913-23.

Haase, S. B., M. Winey & S. I. Reed (2001) Multi-step control of spindle pole body duplication by cyclin-dependent kinase. *Nat Cell Biol,* 3, 38-42.

Heil-Chapdelaine, R. A., J. R. Oberle & J. A. Cooper (2000) The cortical protein Num1p is essential for dynein-dependent interactions of microtubules with the cortex. *J Cell Biol,* 151, 1337-44.

Ho, Y., A. Gruhler, A. Heilbut, G. D. Bader, L. Moore, S. L. Adams, A. Millar, P. Taylor, K. Bennett, K. Boutilier, L. Yang, C. Wolting, I. Donaldson, S. Schandorff, J. Shewnarane, M. Vo, J. Taggart, M. Goudreault, B. Muskat, C. Alfarano, D. Dewar, Z. Lin, K. Michalickova, A. R. Willems, H. Sassi, P. A. Nielsen, K. J. Rasmussen, J. R. Andersen, L. E. Johansen, L. H. Hansen, H. Jespersen, A. Podtelejnikov, E. Nielsen, J. Crawford, V. Poulsen, B. D. Sorensen, J. Matthiesen, R. C. Hendrickson, F. Gleeson, T. Pawson, M. F. Moran, D. Durocher, M. Mann, C. W. Hogue, D. Figeys & M. Tyers (2002) Systematic identification of protein complexes in Saccharomyces cerevisiae by mass spectrometry. *Nature,* 415, 180-3.

Hu, F., Y. Wang, D. Liu, Y. Li, J. Qin & S. J. Elledge (2001) Regulation of the Bub2/Bfa1 GAP complex by Cdc5 and cell cycle checkpoints. *Cell,* 107, 655-65.

Hwang, E., J. Kusch, Y. Barral & T. C. Huffaker (2003) Spindle orientation in Saccharomyces cerevisiae depends on the transport of microtubule ends along polarized actin cables. *J Cell Biol,* 161, 483-8.

Jaffe, A. B., N. Kaji, J. Durgan & A. Hall (2008) Cdc42 controls spindle orientation to position the apical surface during epithelial morphogenesis. *J Cell Biol,* 183, 625-33.

Jaspersen, S. L., J. F. Charles & D. O. Morgan (1999) Inhibitory phosphorylation of the APC regulator Hct1 is controlled by the kinase Cdc28 and the phosphatase Cdc14. *Curr Biol,* 9, 227-36.

Knoblich, J. A. (2008) Mechanisms of asymmetric stem cell division. *Cell,* 132, 583-97.

Korinek, W. S., M. J. Copeland, A. Chaudhuri & J. Chant (2000) Molecular linkage underlying microtubule orientation toward cortical sites in yeast. *Science,* 287, 2257-9.

Lee, J., H. S. Hwang, J. Kim & K. Song (1999) Ibd1p, a possible spindle pole body associated protein, regulates nuclear division and bud separation in Saccharomyces cerevisiae. *Biochim Biophys Acta,* 1449, 239-53.

Lee, L., J. S. Tirnauer, J. Li, S. C. Schuyler, J. Y. Liu & D. Pellman (2000) Positioning of the mitotic spindle by a cortical-microtubule capture mechanism. *Science,* 287, 2260-2.

Lee, W. L., J. R. Oberle & J. A. Cooper (2003) The role of the lissencephaly protein Pac1 during nuclear migration in budding yeast. *J Cell Biol,* 160, 355-64.

Li, R. (1999) Bifurcation of the mitotic checkpoint pathway in budding yeast. *Proc Natl Acad Sci U S A,* 96, 4989-94.

Liakopoulos, D., J. Kusch, S. Grava, J. Vogel & Y. Barral (2003) Asymmetric loading of Kar9 onto spindle poles and microtubules ensures proper spindle alignment. *Cell,* 112, 561-74.

Liu, D., G. Vader, M. J. Vromans, M. A. Lampson & S. M. Lens (2009) Sensing chromosome bi-orientation by spatial separation of aurora B kinase from kinetochore substrates. *Science,* 323, 1350-3.

Maekawa, H., C. Priest, J. Lechner, G. Pereira & E. Schiebel (2007) The yeast centrosome translates the positional information of the anaphase spindle into a cell cycle signal. *J Cell Biol,* 179, 423-36.

Maekawa, H. & E. Schiebel (2004) Cdk1-Clb4 controls the interaction of astral microtubule plus ends with subdomains of the daughter cell cortex. *Genes Dev,* 18, 1709-24.

Maekawa, H., T. Usui, M. Knop & E. Schiebel (2003) Yeast Cdk1 translocates to the plus end of cytoplasmic microtubules to regulate bud cortex interactions. *EMBO J,* 22, 438-49.

Martin, S. G. (2009) Microtubule-dependent cell morphogenesis in the fission yeast. *Trends Cell Biol,* 19, 447-54.

Martin, S. G. & M. Berthelot-Grosjean (2009) Polar gradients of the DYRK-family kinase Pom1 couple cell length with the cell cycle. *Nature,* 459, 852-6.

Miller, P. J. & D. I. Johnson (1994) Cdc42p GTPase is involved in controlling polarized cell growth in Schizosaccharomyces pombe. *Mol Cell Biol,* 14, 1075-83.

Miller, R. K., S. C. Cheng & M. D. Rose (2000) Bim1p/Yeb1p mediates the Kar9p-dependent cortical attachment of cytoplasmic microtubules. *Mol Biol Cell,* 11, 2949-59.

Mizuno, K., A. Suzuki, T. Hirose, K. Kitamura, K. Kutsuzawa, M. Futaki, Y. Amano & S. Ohno (2003) Self-association of PAR-3-mediated by the conserved N-terminal domain contributes to the development of epithelial tight junctions. *J Biol Chem,* 278, 31240-50.

Mohl, D. A., M. J. Huddleston, T. S. Collingwood, R. S. Annan & R. J. Deshaies (2009) Dbf2-Mob1 drives relocalization of protein phosphatase Cdc14 to the cytoplasm during exit from mitosis. *J Cell Biol,* 184, 527-39.

Molk, J. N., S. C. Schuyler, J. Y. Liu, J. G. Evans, E. D. Salmon, D. Pellman & K. Bloom (2004) The differential roles of budding yeast Tem1p, Cdc15p, and Bub2p protein dynamics in mitotic exit. *Mol Biol Cell,* 15, 1519-32.

Monje-Casas, F. & A. Amon (2009) Cell polarity determinants establish asymmetry in MEN signaling. *Dev Cell,* 16, 132-45.

Moore, J. K., V. Magidson, A. Khodjakov & J. A. Cooper (2009) The spindle position checkpoint requires positional feedback from cytoplasmic microtubules. *Curr Biol,* 19, 2026-30.

Moseley, J. B., A. Mayeux, A. Paoletti & P. Nurse (2009) A spatial gradient coordinates cell size and mitotic entry in fission yeast. *Nature,* 459, 857-60.

Musacchio, A. & E. D. Salmon (2007) The spindle-assembly checkpoint in space and time. *Nat Rev Mol Cell Biol,* 8, 379-93.
Nigg, E. A. (2001) Mitotic kinases as regulators of cell division and its checkpoints. *Nat Rev Mol Cell Biol,* 2, 21-32.
O'Connell, C. B. & Y. L. Wang (2000) Mammalian spindle orientation and position respond to changes in cell shape in a dynein-dependent fashion. *Mol Biol Cell,* 11, 1765-74.
Paduch, M., F. Jelen & J. Otlewski (2001) Structure of small G proteins and their regulators. *Acta Biochim Pol,* 48, 829-50.
Pearson, C. G. & K. Bloom (2004) Dynamic microtubules lead the way for spindle positioning. *Nat Rev Mol Cell Biol,* 5, 481-92.
Pereira, G., T. Hofken, J. Grindlay, C. Manson & E. Schiebel (2000) The Bub2p spindle checkpoint links nuclear migration with mitotic exit. *Mol Cell,* 6, 1-10.
Pereira, G. & E. Schiebel (2005) Kin4 kinase delays mitotic exit in response to spindle alignment defects. *Mol Cell,* 19, 209-21.
Peters, J. M. (2006) The anaphase promoting complex/cyclosome: a machine designed to destroy. *Nat Rev Mol Cell Biol,* 7, 644-56.
Polymenis, M. & E. V. Schmidt (1997) Coupling of cell division to cell growth by translational control of the G1 cyclin CLN3 in yeast. *Genes Dev,* 11, 2522-31.
Queralt, E., C. Lehane, B. Novak & F. Uhlmann (2006) Downregulation of PP2A(Cdc55) phosphatase by separase initiates mitotic exit in budding yeast. *Cell,* 125, 719-32.
Queralt, E. & F. Uhlmann (2008) Separase cooperates with Zds1 and Zds2 to activate Cdc14 phosphatase in early anaphase. *J Cell Biol,* 182, 873-83.
Rahal, R. & A. Amon (2008) Mitotic CDKs control the metaphase-anaphase transition and trigger spindle elongation. *Genes Dev,* 22, 1534-48.
Rock, J. M. & A. Amon (2009) The FEAR network. *Curr Biol,* 19, R1063-8.
Rudner, A. D. & A. W. Murray (2000) Phosphorylation by Cdc28 activates the Cdc20-dependent activity of the anaphase-promoting complex. *J Cell Biol,* 149, 1377-90.
Schneider, B. L., Q. H. Yang & A. B. Futcher (1996) Linkage of replication to start by the Cdk inhibitor Sic1. *Science,* 272, 560-2.
Schneider, S. Q. & B. Bowerman (2003) Cell polarity and the cytoskeleton in the Caenorhabditis elegans zygote. *Annu Rev Genet,* 37, 221-49.
Segal, M., K. Bloom & S. I. Reed (2000) Bud6 directs sequential microtubule interactions with the bud tip and bud neck during spindle morphogenesis in Saccharomyces cerevisiae. *Mol Biol Cell,* 11, 3689-702.
Shirayama, M., Y. Matsui, K. Tanaka & A. Toh-e (1994a) Isolation of a CDC25 family gene, MSI2/LTE1, as a multicopy suppressor of ira1. *Yeast,* 10, 451-61.
Shirayama, M., Y. Matsui & E. A. Toh (1994b) The yeast TEM1 gene, which encodes a GTP-binding protein, is involved in termination of M phase. *Mol Cell Biol,* 14, 7476-82.
Shou, W., R. Azzam, S. L. Chen, M. J. Huddleston, C. Baskerville, H. Charbonneau, R. S. Annan, S. A. Carr & R. J. Deshaies (2002) Cdc5 influences phosphorylation of Net1 and disassembly of the RENT complex. *BMC Mol Biol,* 3, 3.
Shou, W., J. H. Seol, A. Shevchenko, C. Baskerville, D. Moazed, Z. W. Chen, J. Jang, A. Shevchenko, H. Charbonneau & R. J. Deshaies (1999) Exit from mitosis is

triggered by Tem1-dependent release of the protein phosphatase Cdc14 from nucleolar RENT complex. *Cell,* 97, 233-44.
Siller, K. H. & C. Q. Doe (2009) Spindle orientation during asymmetric cell division. *Nat Cell Biol,* 11, 365-74.
Skowyra, D., K. L. Craig, M. Tyers, S. J. Elledge & J. W. Harper (1997) F-box proteins are receptors that recruit phosphorylated substrates to the SCF ubiquitin-ligase complex. *Cell,* 91, 209-19.
Song, S., T. Z. Grenfell, S. Garfield, R. L. Erikson & K. S. Lee (2000) Essential function of the polo box of Cdc5 in subcellular localization and induction of cytokinetic structures. *Mol Cell Biol,* 20, 286-98.
Stegmeier, F. & A. Amon (2004) Closing mitosis: the functions of the Cdc14 phosphatase and its regulation. *Annu Rev Genet,* 38, 203-32.
Stegmeier, F., J. Huang, R. Rahal, J. Zmolik, D. Moazed & A. Amon (2004) The replication fork block protein Fob1 functions as a negative regulator of the FEAR network. *Curr Biol,* 14, 467-80.
Stegmeier, F., R. Visintin & A. Amon (2002) Separase, polo kinase, the kinetochore protein Slk19, and Spo12 function in a network that controls Cdc14 localization during early anaphase. *Cell,* 108, 207-20.
Tabancay, A. P., Jr. & S. L. Forsburg (2006) Eukaryotic DNA replication in a chromatin context. *Curr Top Dev Biol,* 76, 129-84.
Tanaka, T. U., N. Rachidi, C. Janke, G. Pereira, M. Galova, E. Schiebel, M. J. Stark & K. Nasmyth (2002) Evidence that the Ipl1-Sli15 (Aurora kinase-INCENP) complex promotes chromosome bi-orientation by altering kinetochore-spindle pole connections. *Cell,* 108, 317-29.
Tomson, B. N., R. Rahal, V. Reiser, F. Monje-Casas, K. Mekhail, D. Moazed & A. Amon (2009) Regulation of Spo12 phosphorylation and its essential role in the FEAR network. *Curr Biol,* 19, 449-60.
Tran, P. T., L. Marsh, V. Doye, S. Inoue & F. Chang (2001) A mechanism for nuclear positioning in fission yeast based on microtubule pushing. *J Cell Biol,* 153, 397-411.
Visintin, C., B. N. Tomson, R. Rahal, J. Paulson, M. Cohen, J. Taunton, A. Amon & R. Visintin (2008) APC/C-Cdh1-mediated degradation of the Polo kinase Cdc5 promotes the return of Cdc14 into the nucleolus. *Genes Dev,* 22, 79-90.
Visintin, R. & A. Amon (2001) Regulation of the mitotic exit protein kinases Cdc15 and Dbf2. *Mol Biol Cell,* 12, 2961-74.
Visintin, R., K. Craig, E. S. Hwang, S. Prinz, M. Tyers & A. Amon (1998) The phosphatase Cdc14 triggers mitotic exit by reversal of Cdk-dependent phosphorylation. *Mol Cell,* 2, 709-18.
Visintin, R., E. S. Hwang & A. Amon (1999) Cfi1 prevents premature exit from mitosis by anchoring Cdc14 phosphatase in the nucleolus. *Nature,* 398, 818-23.
Yeh, E., R. V. Skibbens, J. W. Cheng, E. D. Salmon & K. Bloom (1995) Spindle dynamics and cell cycle regulation of dynein in the budding yeast, Saccharomyces cerevisiae. *J Cell Biol,* 130, 687-700.
Yin, H., D. Pruyne, T. C. Huffaker & A. Bretscher (2000) Myosin V orientates the mitotic spindle in yeast. *Nature,* 406, 1013-5.

Yoshida, S. & A. Toh-e (2002) Budding yeast Cdc5 phosphorylates Net1 and assists Cdc14 release from the nucleolus. *Biochem Biophys Res Commun,* 294**,** 687-91.
Zachariae, W., M. Schwab, K. Nasmyth & W. Seufert (1998) Control of cyclin ubiquitination by CDK-regulated binding of Hct1 to the anaphase promoting complex. *Science,* 282**,** 1721-4.

Chapter II: The Protein Phosphatase 2A functions in the spindle position checkpoint by regulating the checkpoint kinase Kin4

Reprinted from Cold Spring Harbor Press:

Chan, L. Y., Amon, A. The Protein Phosphatase 2A functions in the spindle position checkpoint by regulating the checkpoint kinase Kin4. *Genes Dev.* **23**, 1639-49.

Summary

In budding yeast, a surveillance mechanism known as the spindle position checkpoint (SPOC) ensures accurate genome partitioning. In the event of spindle mis-position the checkpoint delays exit from mitosis by restraining the activity of the mitotic exit network (MEN). To date, the only component of the checkpoint to be identified is the protein kinase Kin4. Furthermore, how the kinase is regulated by spindle position is not known. Here, we identify the protein phosphatase PP2A in complex with the regulatory subunit, Rts1, as a component of the SPOC. Loss of PP2A-Rts1 function abrogates the spindle position checkpoint but not other mitotic checkpoints. We further show that the protein phosphatase functions upstream of Kin4, regulating the kinase's phosphorylation and localization during an unperturbed cell cycle and during spindle position checkpoint activation thus defining the phosphatase as a key regulator of SPOC function.

Introduction

Many cell divisions are polarized, with intrinsic and/or extrinsic cues dictating the directionality of cell division. To ensure that the genetic material is segregated accurately during polarized division, the mitotic spindle must be positioned according to these polarization cues. There is mounting evidence to suggest that this process of spindle positioning is coupled to the cell cycle. In cultured rat kidney cells, a delay in anaphase onset occurs when the metaphase spindle is mis-positioned (O'Connell and Wang 2000). In Drosophila male germline stem cells, cell cycle progression also appears delayed when the spindle is mis-positioned (Cheng et al. 2008). Such coupling is suggestive of a feedback mechanism that delays the cell cycle in response to defects in spindle position.

A surveillance mechanism that delays the cell cycle in response to defects in spindle position has been described in the budding yeast, *Saccharomyces cerevisiae*, and is termed the spindle position checkpoint (SPOC) (Yeh et al. 1995). Each cell division of budding yeast is asymmetric and thus inherently polarized. Budding yeast cells divide by forming a bud and hence determine the site of cytokinesis during entry into the cell cycle long before the mitotic spindle is formed. This manner of dividing requires the active positioning of the mitotic spindle along this predetermined division axis, which is known in yeast as the mother-bud axis. The spindle position checkpoint ensures proper spindle position and thus chromosome segregation by delaying exit from mitosis, specifically anaphase spindle disassembly and cytokinesis, until the spindle is correctly positioned along the mother-bud axis (Yeh et al. 1995). The function of the SPOC is most apparent in cells deficient in cytoplasmic microtubule dynamics, guidance and capture. Such cells fail to position the mitotic spindle along the division axis resulting in anaphase spindle elongation in the mother cell(Yeh et al. 1995). Failure of this checkpoint results in the formation of anucleated and multi-nucleated cells.

The spindle position checkpoint delays exit from mitosis by inhibiting the mitotic exit network (MEN). The MEN is a signal transduction pathway whose activity is controlled by the small GTPase, Tem1(Shirayama, Matsui and Toh 1994b). Tem1 regulates a kinase cascade, whose activation ultimately leads to a sustained release of the phosphatase

Cdc14 from its nucleolar inhibitor Cfi1/Net1(Bardin, Visintin and Amon 2000, Lee et al. 2001, Luca et al. 2001, Mah, Jang and Deshaies 2001, Shirayama et al. 1994b, Shou et al. 1999, Visintin, Hwang and Amon 1999). Once released, Cdc14 dephosphorylates key substrates to bring about exit from mitosis(Jaspersen, Charles and Morgan 1999, Visintin et al. 1998, Zachariae et al. 1998, Bardin et al. 2000).

Several proteins have been identified that regulate Tem1 during the cell cycle and in response to spindle position defects. Tem1 is controlled positively by the bud cortex restricted protein, Lte1 (which resembles a guanine nucleotide exchange factor; GEF) and negatively by the two-component GTPase activating protein (GAP), Bub2-Bfa1(Bardin et al. 2000, Bloecher, Venturi and Tatchell 2000, Geymonat et al. 2002, Lee et al. 1999, Li 1999, Pereira et al. 2000, Shirayama et al. 1994a). In the absence of *LTE1*, cells fail to activate the MEN and do not exit from mitosis at low temperatures (Shirayama et al. 1994a). The absence of the GAP leads to inappropriate MEN activation and mitotic exit in cells arrested in mitosis due to activation of the spindle assembly checkpoint (SAC) or the SPOC (Bardin et al. 2000, Bloecher et al. 2000, Fesquet et al. 1999, Hoyt, Totis and Roberts 1991, Pereira et al. 2000). A single spindle position checkpoint specific regulator of the MEN has also been identified. The protein kinase Kin4 is only required for MEN inhibition in response to spindle position defects(D'Aquino et al. 2005, Pereira and Schiebel 2005). Kin4 localizes to the mother cell cortex throughout most of the cell cycle. During anaphase the protein kinase also localizes to the spindle pole body (SPB) that remains in the mother cell (D'Aquino et al. 2005, Pereira and Schiebel 2005). In cells with mis-positioned spindles, Kin4 associates with both SPBs where it phosphorylates Bfa1(Maekawa et al. 2007, Pereira and Schiebel 2005). This phosphorylation protects the GAP from inhibitory phosphorylation by the Polo kinase, Cdc5, effectively locking Bub2-Bfa1 in an active state thus inhibiting the MEN (Geymonat et al. 2003, Hu et al. 2001, Maekawa et al. 2007). How Kin4 itself is controlled during the cell cycle or in response to spindle position defects is not understood.

Here, we identify the protein phosphatase PP2A-Rts1 as a regulator of Kin4 function. PP2A-Rts1 is required for the dephosphorylation of Kin4 during cell cycle entry and to

maintain Kin4 in the dephosphorylated state during S-phase and mitosis. Furthermore the phosphatase controls the association of Kin4 with SPBs both during the cell cycle and in response to spindle position defects. The importance of this control is underlined by the finding that PP2A-Rts1 is essential for spindle position checkpoint function but not for other mitotic checkpoints. We propose that PP2A-Rts1 is a SPOC component that facilitates Kin4 localization thereby restraining MEN activity.

Results

PP2A-Rts1 regulates Kin4 phosphorylation

Kin4 is essential for spindle position checkpoint function. To determine how the protein kinase is controlled, we focused on its previously observed cell cycle regulated phosphorylation. Phosphorylated Kin4 can be detected as slower migrating species by SDS-PAGE(D'Aquino et al. 2005). Kin4 is phosphorylated in G1, but upon release from a pheromone induced G1-arrest, Kin4 phosphorylation is rapidly lost. The protein remains in a hypophosphorylated state throughout S phase and mitosis, but is rapidly rephosphorylated during exit from mitosis (Figure 1A and (D'Aquino et al. 2005)).

Kin4 is in the dephosphorylated state during the stages of the cell cycle when Kin4 activity is needed to inhibit the MEN in response to potential spindle position defects. This correlation prompted us to investigate the significance of Kin4 phosphorylation by identifying phosphatases responsible for dephosphorylating Kin4. We screened mutants defective in known cell cycle associated phosphatases for effects on Kin4 phosphorylation. Kin4 phosphorylation was examined in cells harboring temperature sensitive alleles of *CDC14 (cdc14-3), SIT4 (sit4-102,*(Wang, Wang and Jiang 2003)), Protein Phosphatase 1 (PP1; *glc7-12*), and a combination of alleles that renders the Protein Phosphatase 2A (PP2A) temperature sensitive (*pph3D, pph21D, pph22-12*; henceforth temperature sensitive PP2A, (Evans and Stark 1997)). We grew the cells to mid exponential phase at permissive temperature (23°C) and followed Kin4 phosphorylation upon shift to the restrictive temperature (37°C). Temperature shift led to a transient accumulation of hyperphosphorylated Kin4 even in wild-type cells, for unknown reasons, which was particularly evident when the ratio of phosphorylated to unphosphorylated Kin4 was determined (Figure 1B, C). After the transient accumulation of hyperphosphorylated Kin4, however, both hyper and hypophosphorylated Kin4 were detected in wild-type and most phosphatase mutants. The *sit4-102* mutant displayed hyperphosphorylation after temperature shift, which was progressively lost during incubation at 37°C (Figure 1B, C). Temperature sensitive PP2A mutants showed a persistence of hyper-phosphorylated Kin4 (Figure 1B-C). Though other phosphatases,

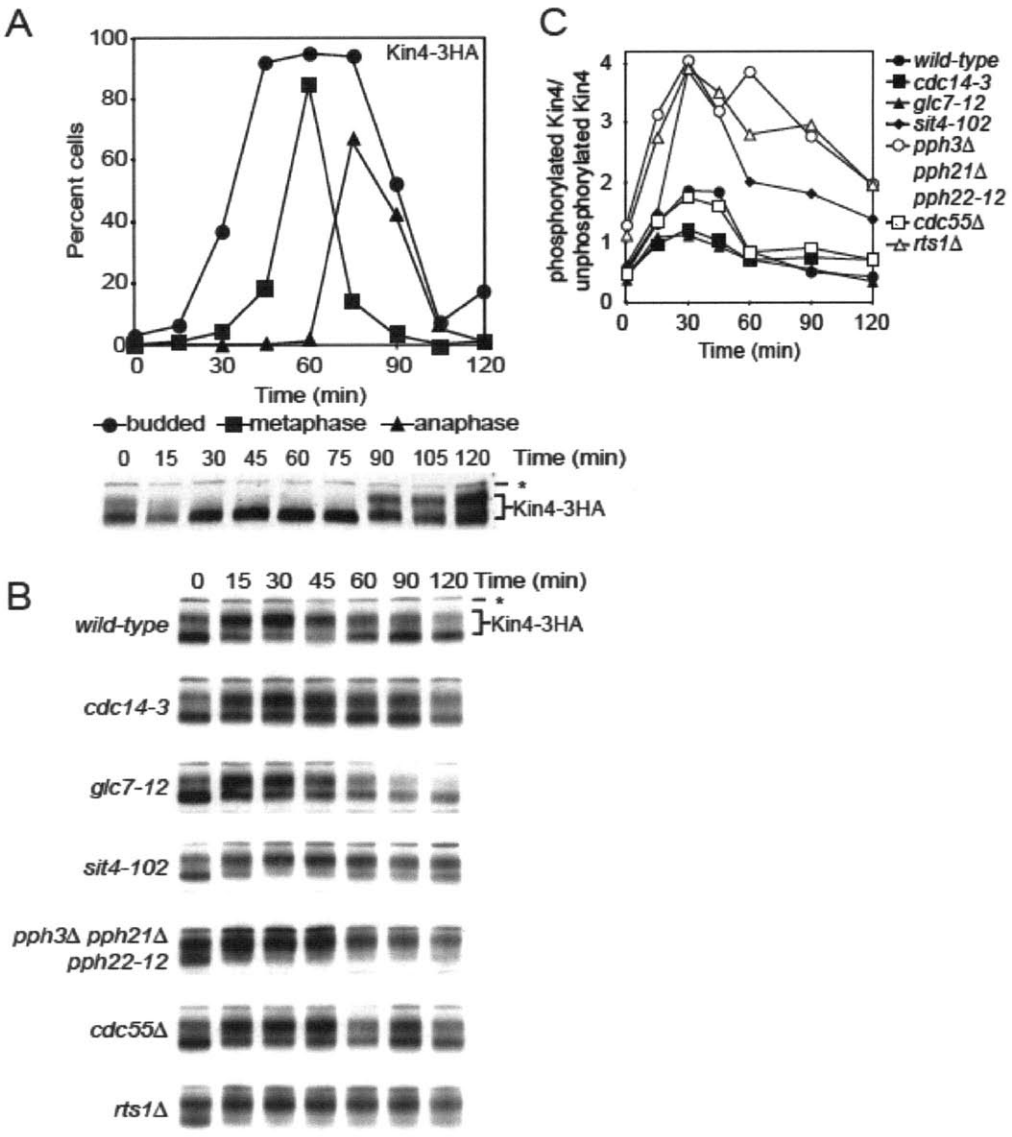

Figure 1. PP2A-Rts1 is necessary for Kin4 dephosphorylation

(A) Wild-type cells expressing a Kin4-3HA fusion (A11779) were arrested in G1 with 5 μg/mL α factor and released into pheromone free media. After 70 minutes, 10 μg/mL α factor was added to prevent entry into a subsequent cell cycle. Cell cycle stage was determined by spindle and bud morphology. Kin4-3HA was monitored by western blot. An asterisk indicates a cross-reacting band with the HA antibody.

(B-C)Wild-type (A11779), *cdc14-3* (A19111), *glc7-12* (A19808), *sit4-102* (A20176), *pph3Δ pph21Δ pph22-12* (A20126), *cdc55Δ* (A19804) and *rts1Δ* (A20187) cells expressing a Kin4-3HA fusion were grow to exponential phase at room temperature and then shifted to 37°C (t=0). Samples were taken at the indicated times to examine Kin4-3HA mobility. An asterisk indicates a cross-reacting band with the HA antibody. Quantification of (B) is shown in (C).

possibly Sit4, contribute to Kin4 dephosphorylation (see also Figure 3B), we conclude that PP2A is primarily required for Kin4 de-phosphorylation.

Budding yeast PP2A is a heterotrimeric enzyme composed of a single scaffolding subunit, Tpd3, a catalytic subunit, Pph21 or Pph22 and a regulatory subunit, Cdc55 (B type-PP2A) or Rts1 (B' type-PP2A) (reviewed in (Jiang 2006)). To determine which regulatory subunit is required for Kin4 dephosphorylation, we examined the phosphorylation status of Kin4 in the *cdc55*Δ and *rts1*Δ mutants. In *cdc55*Δ cells, Kin4 phosphorylation status resembled that of wild-type. In contrast, in the *rts1*Δ strain, Kin4 phosphorylation resembled that of the PP2A mutant (Figure 1B, C). We conclude that PP2A-Rts1 is primarily responsible for Kin4 dephosphorylation.

PP2A-Rts1 is a component of the spindle position checkpoint

If dephosphorylation of Kin4 is important for its checkpoint function, mutants in which Kin4 dephosphorylation is impaired should exhibit spindle position checkpoint defects. To test this possibility, we examined how *PP2A-RTS1* mutants respond to spindle mis-position. Cells lacking cytoplasmic dynein (*dyn1*Δ) exhibit spindle position defects particularly at low temperature (14°C)(Li et al. 1993). As a result, chromosome segregation frequently occurs within the mother cell. This in turn leads to activation of the SPOC, which causes inhibition of the MEN and cell cycle arrest in late anaphase ("arrested" morphology; Figure 2A). *dyn1*Δ cells with an impaired SPOC fail to delay mitotic exit resulting in anucleated and multinucleated cells ("bypassed" morphology; Figure 2A).

After growth at 14°C for 24 hours, 27% of *dyn1*Δ mutants exhibit the "arrested" morphology and only 10% the "bypassed" morphology (Figure 2B), indicating that the SPOC is functional and that the MEN is inhibited. When the SPOC is inactivated by deletion of *KIN4,* 35% of *dyn1*Δ *kin4*Δ double mutant cells exhibit the "bypassed" morphology. Deletion of *RTS1* in the *dyn1*Δ mutant also lead to inactivation of the SPOC with 42% of cells showing the "bypassed" morphology (Figure 2B). Importantly, the *rts1*Δ single mutant did not exhibit spindle position defects indicating that PP2A-Rts1

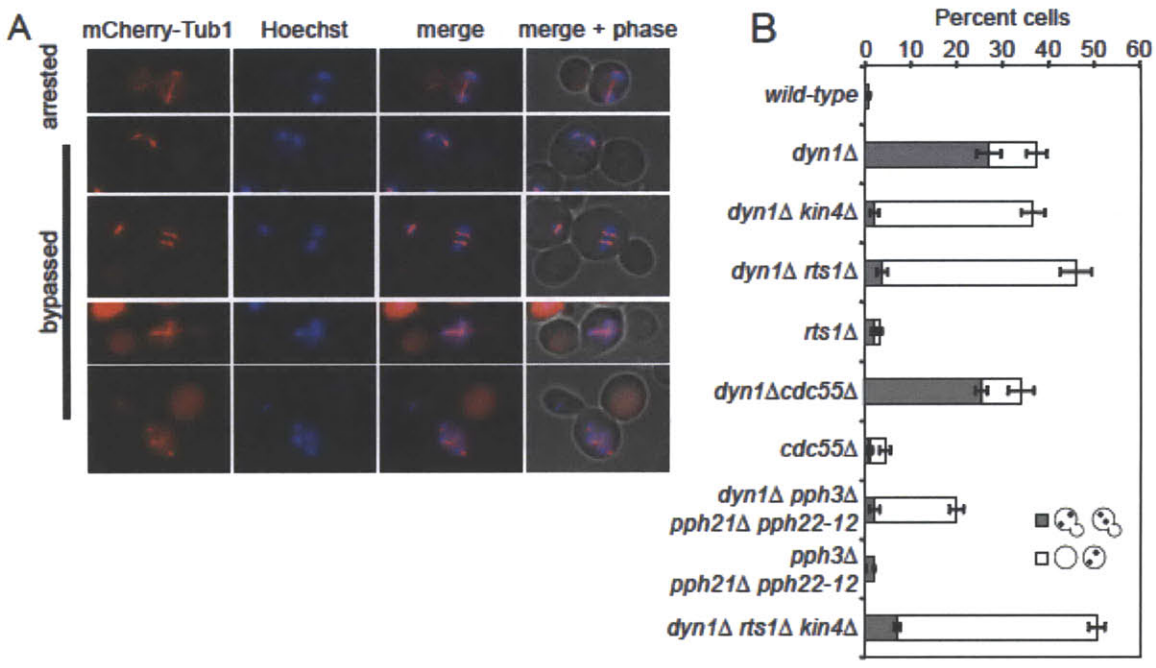

Figure 2. PP2A-Rts1 functions in the spindle position checkpoint

(A) A *dyn1*Δ *rts1*Δ mutant (A21725) carrying a mCherry-Tub1 marker (red) was grown at 14°C for 24 hours. The DNA was visualized by Hoechst staining (blue). Cells with the arrested morphology are budded and have two DNA masses spanned by an anaphase spindle in the mother cell. Cells with the bypassed morphology have no DNA masses or multiple DNA masses but with disassembled spindles or spindles indicative of cell cycle progression after improper mitotic exit.

(B) Wild-type (A2587), *dyn1*Δ (A17349), *dyn1*Δ *kin4*Δ (A17351), *dyn1*Δ *rts1*Δ (20310), *rts1*Δ (A20312), *dyn1*Δ *cdc55*Δ (A21520), *cdc55*Δ (A15396), *dyn1*Δ *pph3*Δ *pph21*Δ *pph22-12* (A21574), *pph3*Δ *pph21*Δ *pph22-12* (A19130) and *dyn1*Δ *rts1*Δ *kin4*Δ (A21538) were grown as described in (A). Cells were stained for tubulin by indirect immuno-fluorescence and the DNA was stained with DAPI. $n \geq 100$ cells per sample. Gray bars represent the percentage of cells with the arrested morphology and white bars represent the percentage of cells with the bypassed morphology. Error bars represent SEM.

likely does not play a role in the actual positioning of the spindle. The spindle position checkpoint defect was specific to PP2A-B' as the *cdc55*Δ *dyn1*Δ mutant displayed no SPOC defect (Figure 2B). We observed a defect in SPOC function in *dyn1*Δ *pph21*Δ *pph22-12 pph3*Δ quadruple mutants although this defect was not as pronounced as in the *dyn1*Δ *rts1*Δ mutant possibly due to the proliferation defect of the quadruple mutant

(Figure 2B). Lastly, we found that deletion of *KIN4* did not enhance the SPOC defect of *dyn1*Δ *rts1*Δ mutants. Taken together, these data indicate that PP2A-Rts1 is a component of the SPOC that likely functions in the same pathway as *KIN4*.

PP2A-Rts1 functions in the SPOC by controlling Kin4 localization to spindle pole bodies

Having established that PP2A-Rts1 is required for SPOC function, we wished to determine whether PP2A-Rts1 acts through Kin4. To this end we examined the effects of deleting *RTS1* on the phenotype associated with *KIN4* overexpression. Overexpression of *KIN4* from the *GAL1-10* promoter terminally arrests cells in anaphase (D'Aquino et al. 2005). Deletion of *RTS1* suppressed the lethality caused by *GAL-KIN4* (Figure 3A) indicating that overexpressed *KIN4* requires PP2A-Rts1 function to exert its inhibitory effects on mitotic exit. Importantly, deletion of *RTS1* did not suppress the lethal anaphase arrest induced by *GAL-BFA1* (Lee et al. 1999, Li 1999) suggesting that *rts1*Δ is not a general suppressor of anaphase arrest but instead shows specificity towards *KIN4*. The rescue of the *GAL-KIN4* lethality by the deletion of *RTS1* was not as complete as that brought about by the deletion of *BUB2*, a gene known to function downstream of *KIN4*, suggesting that the mechanisms of suppression may not be the same ((D'Aquino et al. 2005); Figure 3A).

To determine the relationship between PP2A-Rts1 and Kin4 we examined the effects of deleting *RTS1* on Kin4 phosphorylation, activity and localization. We found that Kin4 is hyper-phosphorylated throughout the cell cycle in the *rts1*Δ mutant (Figure 3B). While we observed a consistent 10 to 15 minute delay in cell cycle progression prior to metaphase spindle assembly, inactivation of *RTS1* did not affect the phosphorylation state of the Bub2-Bfa1 complex, nor the MEN GTPase Tem1, nor the Tem1 activator Lte1, as judged by changes in electrophoretic mobility (Figure 3C – F). These findings suggest that not all SPOC components and its targets are substrates of PP2A-Rts1.

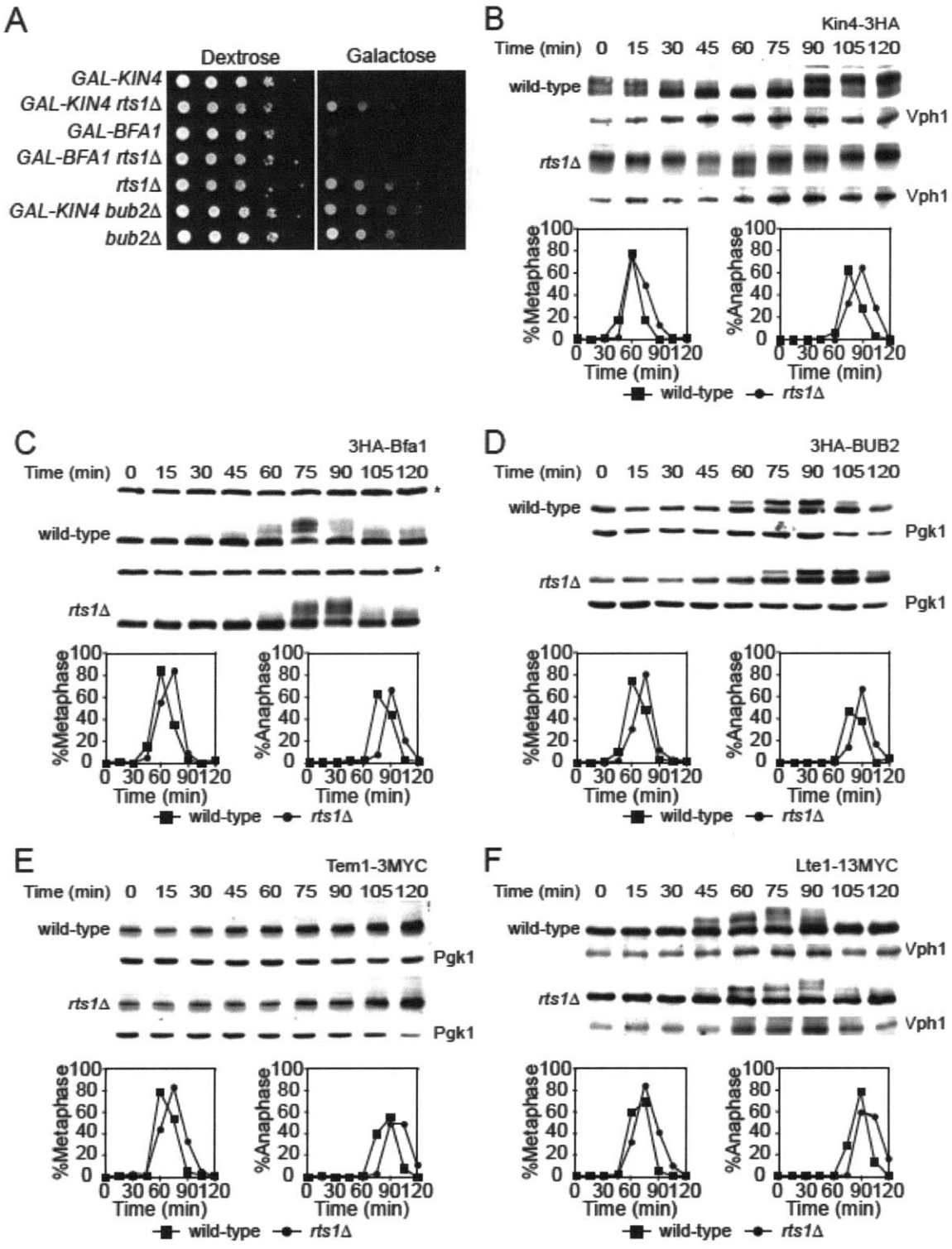

Figure 3. PP2A-Rts1 affects Kin4 phosphorylation but not other MEN components

(A) *GAL-GFP-KIN4* (A11997), *GAL-GFP-KIN4 rts1*Δ (A20893), *GAL-GFP-BFA1* (A3487), *GAL-GFP-BFA1 rts1*Δ (A20892), *rts1*Δ (A20312), *GAL-GFP-KIN4*

*bub2*Δ (A18792) and *bub2*Δ (A1863) cells were spotted on plates containing either dextrose or galactose and raffinose. The first spot represents growth of approximately $3x10^4$ cells and each subsequent spot is a 10 fold serial dilution.

(B-F) Wild-type and *rts1*Δ cells expressing (B) Kin4-3HA (A11779 and A20187), (C) 3HA-Bfa1 (A4378 and A21540), (D) 3HA-Bub2 (A21921 and A22064), (E) Tem1-3MYC (A1828 and A21539) or (F) Lte1-13MYC (A22669 and A22669) were analyzed as described in Figure 1A. Vph1, Pgk1 and a cross reacting band with the HA antibody (labeled with an asterisk) were used as loading controls.

Next we examined whether PP2A-Rts1 affects Kin4 activity, which is essential for checkpoint function (Figure 4A). Kin4 kinase activity was not decreased when isolated from *rts1*Δ mutant cells (Figure 4B-C) indicating that PP2A-Rts1 does not affect Kin4's *in vitro* enzymatic activity.

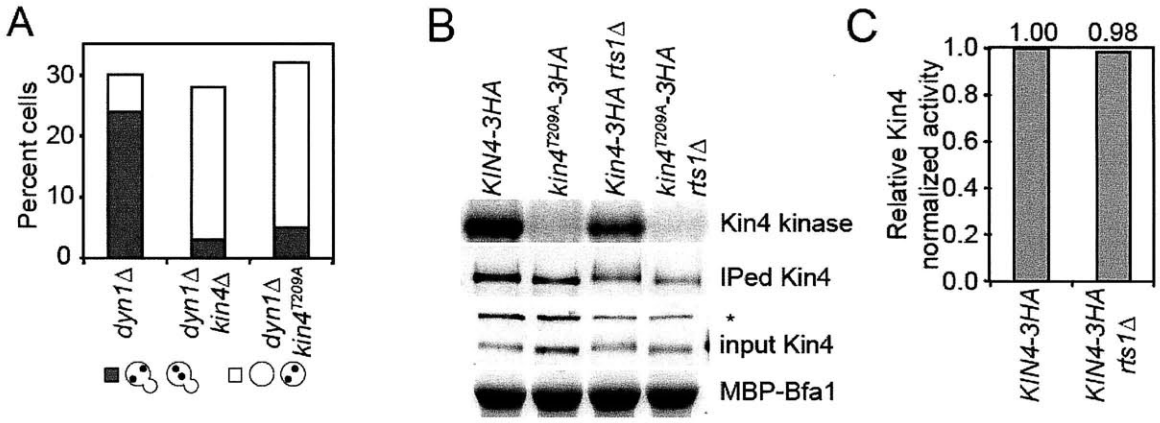

Figure 4. Loss of *RTS1* function does not affect the kinase activity of Kin4

(A) *dyn1*Δ (A17349), *dyn1*Δ *kin4*Δ (A17351) and *dyn1*Δ *kin4*^{T209A}Δ (A22736) cells were grown for 24 hours at 14°C. The DNA was visualized by DAPI staining and microtubules were stained by indirect immuno-fluorescence. Gray bars represent the percentage of cells with the arrested morphology and white bars represent the percentage of cells with the bypassed morphology. $n \geq 100$.

(B) Wild-type cells expressing either a Kin4-3HA or a kin4^{T209A}-3HA (kinase dead) fusion (A11779 or A22119) and *rts1*Δ cells expressing either a Kin4-3HA or a kin4^{T209A}-3HA fusion (A20187 or A22120) were grown to exponential phase and arrested with 15 μg/mL nocodazole for 2 hours. Kin4 associated kinase activity (top, Kin4 kinase), immunoprecipitated Kin4-3HA (second row, IPed Kin4), total amount of Kin4-3HA in extracts (third row, input Kin4) and levels of Bfa1 substrate (as monitored by Coomassie stain) added to the kinase reaction (bottom, Bfa1) is shown. The band that is shown for Kin4 associated kinase activity and total Bfa1 substrate is the first major degradation product of MBP-

Bfa1 as described in Maekawa et al., 2007 and was the dominant signal. An asterisk indicates a cross reacting band with the HA antibody.

(C) Normalized activity of (B) was calculated as kinase activity divided by immunoprecipitated Kin4. Relative activity was calculated as normalized activity of the sample divided by the normalized activity of the wild-type sample.

An intact SPOC not only requires Kin4 kinase activity but also binding of the protein kinase to SPBs (Maekawa et al. 2007). During an unperturbed cell cycle Kin4 localizes to the mother cell cortex. During anaphase, Kin4 also associates with the SPB that remains in the mother cell (mSPB). In cells with mis-positioned anaphase spindles, Kin4 associates with both SPBs. Kin4 mutants that fail to localize to SPBs are checkpoint defective (Maekawa et al. 2007). Furthermore, ectopically targeting Kin4 to SPBs suffices to delay mitotic exit (Maekawa et al. 2007). We monitored the ability of Kin4-GFP to associate with the mSPB during anaphase and observed a strong reduction in mSPB localization in *rts1*Δ cells (Figure 5). Whereas Kin4-GFP localized to the mSPB during anaphase in 54% of wild-type cells, Kin4-GFP was found on mSPBs of only 11% of *rts1*Δ anaphase cells (Figure 5C). Furthermore, in the *rts1*Δ mutant cells that showed Kin4 localization at the mSPB, the signal was weaker (Figure 5A). The loss of Kin4 localization to SPBs was not due to a reduction in *KIN4-GFP* expression in the *rts1*Δ mutant, as levels of Kin4-GFP in these cells are similar to that observed in wild-type cells (Figure 5B). The cortical localization and asymmetry of Kin4 was also reduced in *rts1*Δ cells which was most pronounced in small budded cells (Figure 5A, 7A, D). The basis of this loss in asymmetric localization of Kin4 is currently unclear. Localization of Bub2, Bfa1 and Tem1 was not affected by the deletion of *RTS1* (Figures 6A-C) indicating that loss of *RTS1* function does not alter the overall structure of SPBs nor affects the localization of other SPB-associated MEN proteins. Bud restricted cortical localization of Lte1 was also not affected by deletion of *RTS1* suggesting that overall cell polarity and integrity of the bud neck is maintained in the mutant (Figure 6D). We conclude that PP2A-Rts1 is required for Kin4 function and association of the protein with the mSPB during anaphase.

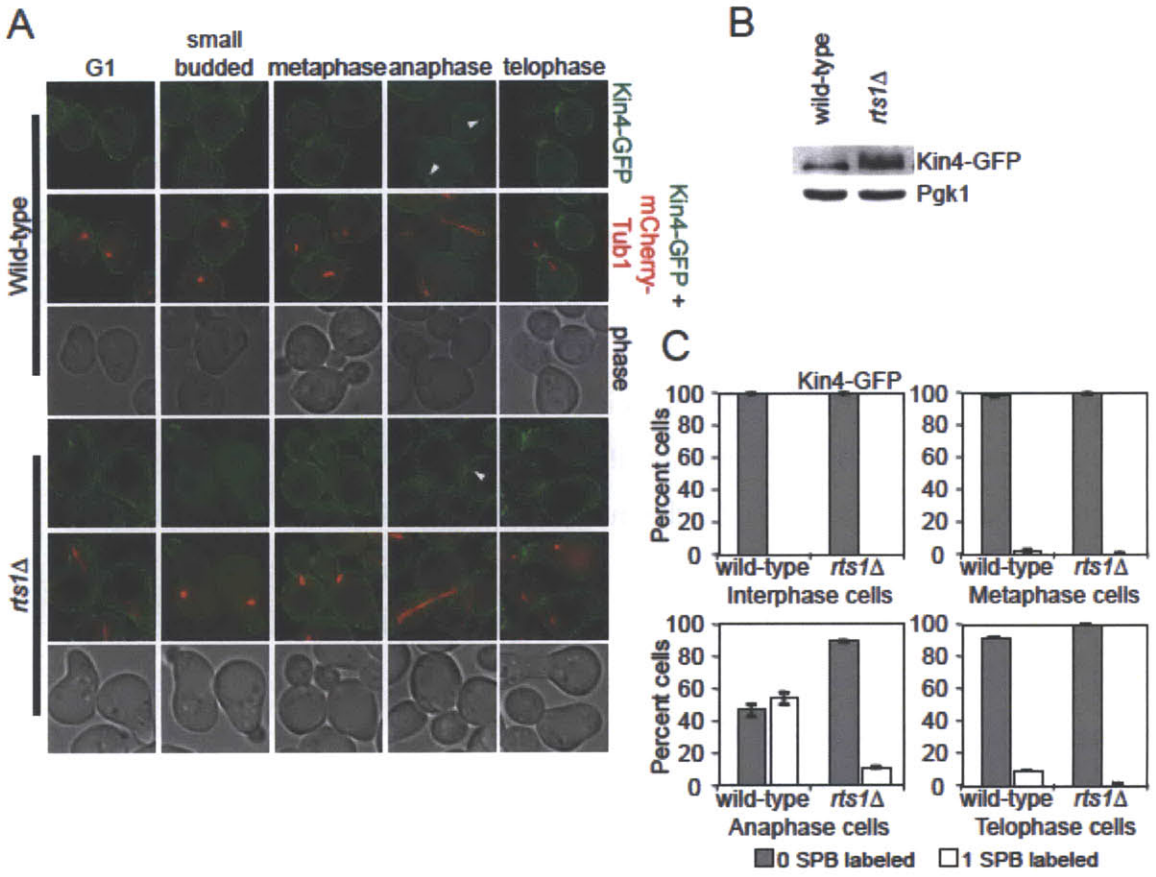

Figure 5. Localization of Kin4 to the mother SPB during anaphase requires *RTS1*

(A-C) Wild-type (A19900) and *rts1*Δ (A20918) cells expressing Kin4-GFP and mCherry-Tub1 fusion proteins were treated as described in Figure 1A. Samples were taken every 15 minutes for 2 hours after release and the cells were imaged live. Serial sections spanning the entire cell were collected to ensure imaging of all spindle poles. Panels in (A) show deconvolved images from 20 serial sections. Kin4-GFP is in green and mCherry-Tub1 is in red. Levels of Kin4-GFP for equal ODs of culture are shown in (B). Pgk1 was used as a loading control. Quantification of Kin4-GFP colocalization with spindle poles is shown in (C). $n \geq 100$ for interphase, metaphase and anaphase cells. $n \geq 40$ for the rarer telophase cells. Error bars represent SEM.

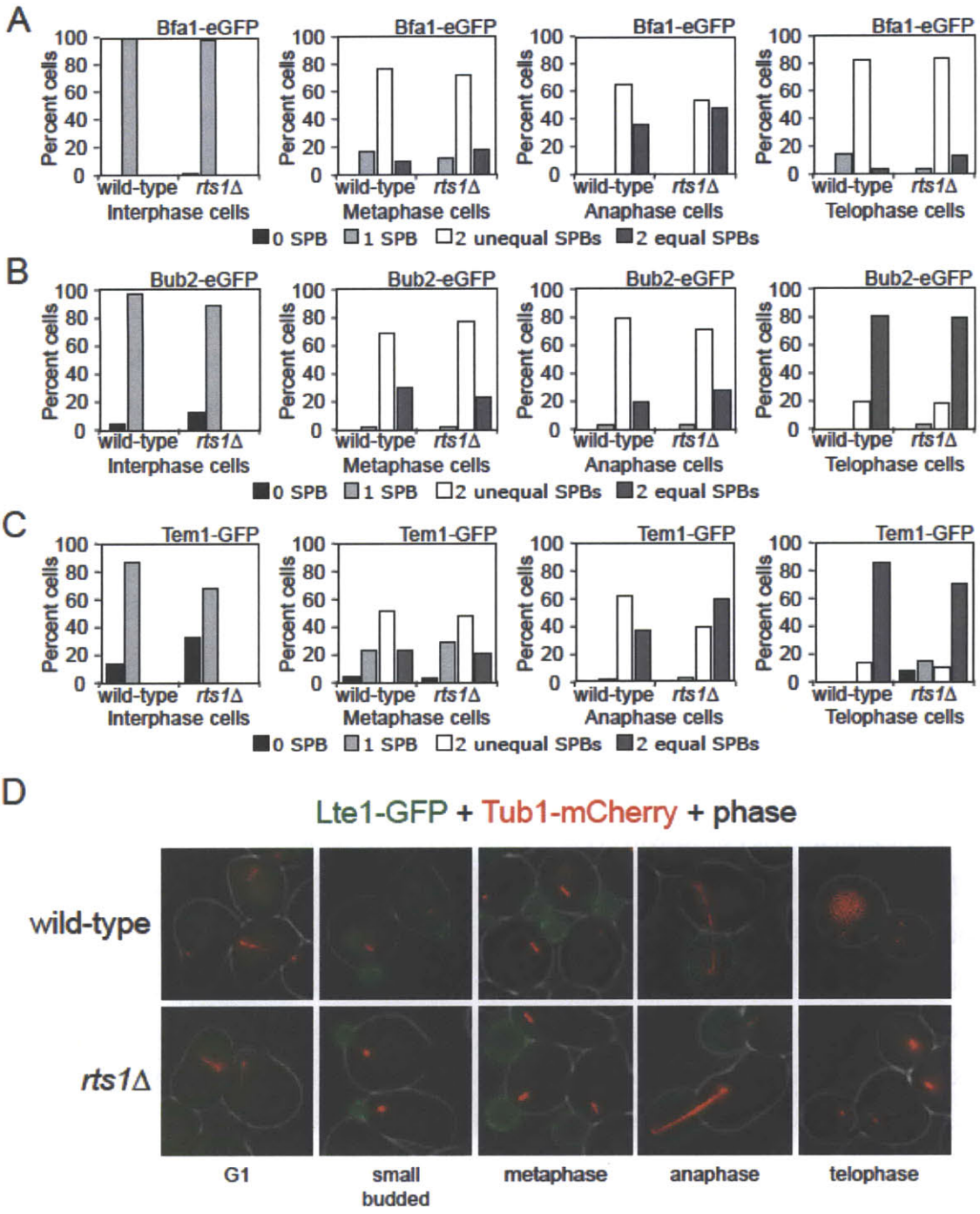

Figure 6. Tem1 and its regulators display normal localization in the *rts1*Δ mutant

(A-C) Wild-type and *rts1*Δ cells expressing mCherry-Tub1 and (A) Bfa1-eGFP (A21608 and A21729), (B) Bub2-eGFP (A21610 and A21730) or (C) Tem1-GFP (A22556 and A22667) were analyzed as described in Figures 5A and 5C.

(D) Wild-type (A22632) and *rts1*Δ (A22631) cells expressing Lte1-GFP and mCherry-Tub1 were analyzed as described in Figure 5A. Panels display typical cells and all localization trends were completely penetrant in all cells examined.

***RTS1* is Required for Efficient SPB Loading of Kin4 in response to SPOC activation**

Having determined that *RTS1* was required for Kin4 localization during an unperturbed cell cycle we next investigated whether *RTS1* also affected Kin4 loading onto SPBs when the spindle is depolymerized or mis-positioned, situations where the SPOC is active and *KIN4* function would be most important. We first examined cells treated with the spindle depolymerizing drug nocodazole. Under these conditions Kin4 associates with SPBs ((Pereira and Schiebel 2005); Figure 7A, B). In contrast, Kin4 association with SPBs was significantly reduced in *rts1*Δ mutants (Figure 7A-B). In the few cells where Kin4 was detected on SPBs the signal intensity was reduced. This loss of SPB association could not be explained by changes in Kin4 expression as Kin4-GFP protein levels were similar in the two strains (Figure 7C). Similar results were obtained in *dyn1*Δ cells with mis-positioned spindles. In such cells Kin4 localizes to both SPBs ((Pereira and Schiebel 2005); Figure 7D, E). In the absence of *RTS1*, Kin4 localization to SPBs was severely impaired (Figure 7D, E).

Overexpression of *KIN4* only partially suppressed the Kin4 SPB loading defect of *rts1*Δ mutants, providing a possible explanation for why deleting *RTS1* suppressed the lethality associated with high levels of Kin4 (Figure 3A). Over-expression of *KIN4* from the *MET25* promoter, which inhibits proliferation (Figure 7F), allowed some Kin4 to associate with SPBs in *rts1*Δ mutants but the number of cells that exhibit Kin4 localization to SPBs was reduced compared to wild-type cells (Figure 7G). Thus in all situations in which Kin4 is known to load onto SPBs (correctly positioned anaphase spindles, spindle depolymerization, mis-positioned anaphase spindles and overexpressed *KIN4*), we observe a defect in SPB loading in the *rts1*Δ mutant.

In cells with a mis-positioned spindle and an intact SPOC, both Bub2 and Bfa1 localize to both SPBs but Tem1 fails to load onto SPBs. When *KIN4* is deleted, Tem1 loads onto SPBs and thus presumably allows for premature exit from mitosis ((D'Aquino et al. 2005); Figure 7J). Consistent with previously observed effects of loss of *KIN4* function on the localization of Tem1 complex components, both Bub2 and Bfa1

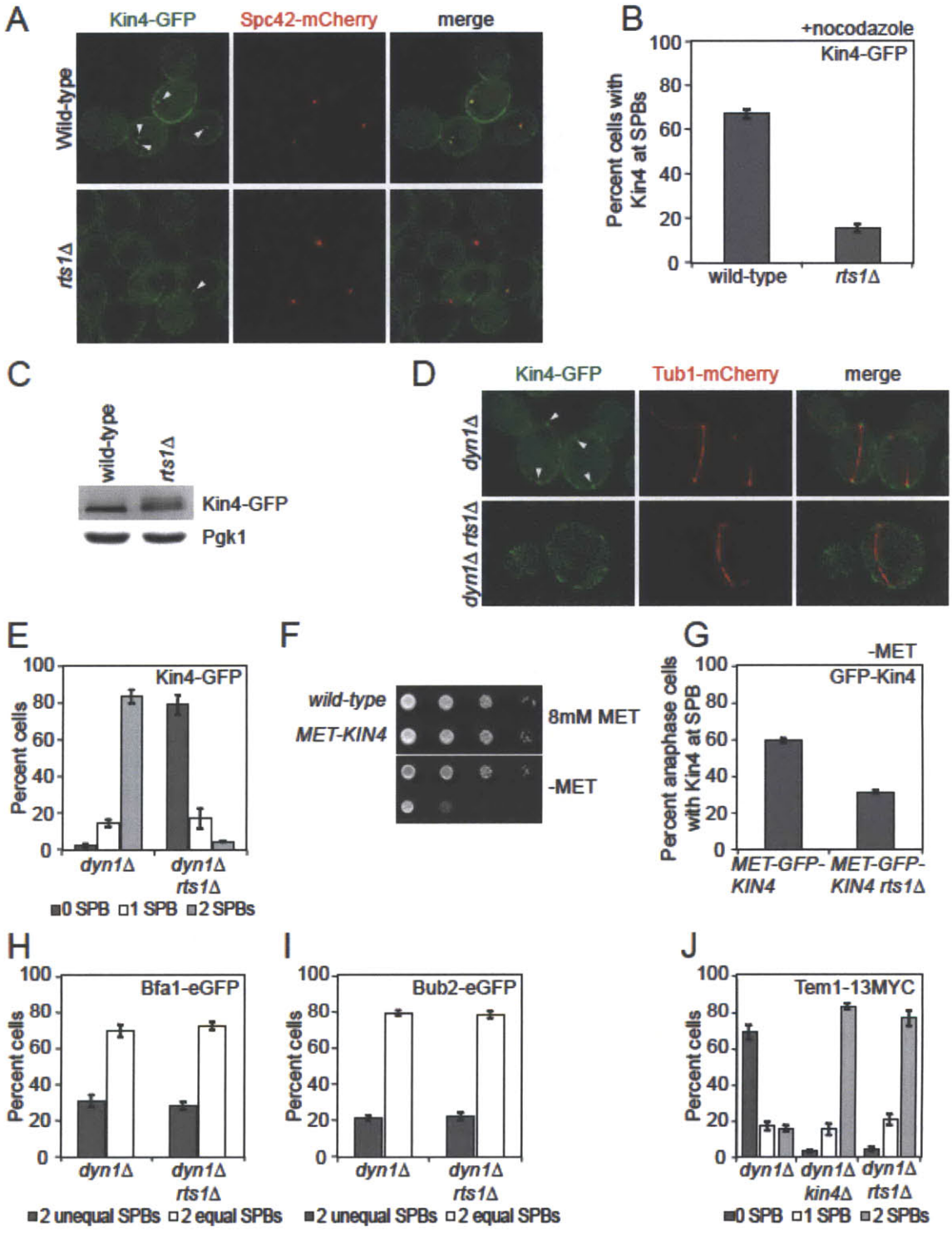

Figure 7. SPOC induced Kin4 localization to spindle poles requires *RTS1*

(A-C) Wild-type (A19902) and *rts1*Δ (A21732) cells expressing Kin4-GFP and SPC42-mCherry fusion proteins were treated with 15 μg/mL nocodazole for 90 minutes. Cells were analyzed as described in Figure 5A. Kin4-GFP is in green

and Spc42-mCherry is in red. Quantification of Kin4-GFP colocalization with the SPC42-mCherry marker is shown in (B). n ≥ 50 for each strain. Error bars represent SEM. Levels of Kin4-GFP for equal ODs of culture are shown in (C). Pgk1 was used as a loading control.

(D-E) *dyn1*Δ (A21720) and *dyn1*Δ *rts1*Δ (A22878) cells expressing Kin4-GFP and mCherry-Tub1 proteins were grown to exponential phase and then shifted to 14°C for 24 hours. Cells were collected and analyzed as described in Figure 5A. Quantification of Kin4-GFP colocalization with spindle poles is shown in (E). n ≥ 50. Error bars represent SEM.

(F) Wild-type (A2587) and *MET-GFP-KIN4* (A23232) were spotted on SC medium supplemented with 8 mM methonine or SC medium lacking methonine and incubated at 30°C for 24 hours. The first spot represents growth of approximately $3x10^4$ cells and each subsequent spot is a 10 fold serial dilution. This overexpression allele was used instead of *GAL-GFP-KIN4* for single cell analysis of the effects of *KIN4* overexpression due to the low viability of *rts1*Δ mutants when grown in raffinose.

(G) *MET-GFP-KIN4* (A23358) and *MET-GFP-KIN4 rts1*Δ (A23357) cells expressing a mCherry-Tub1 fusion protein were grown and arrested with α factor inYePAD + 8 mM methonine. After 2.5 hours of arrest, cells were washed and resuspended in SC –MET + α factor media and the arrest was held for an additional 30 minutes. Cells were then released into pheromone free SC –MET media. Anaphase cells were counted for co-localization of GFP-Kin4 with the ends of the spindle. n ≥100. Error bars represent SEM.

(H-I) *dyn1*Δ and *dyn1*Δ *rts1*Δ cells expressing mCherry-Tub1 and (F) Bfa1-eGFP (A21723 and A21722) or (G) Bub2-eGFP (A21724 and A21725) were analyzed as described in (D) and (E). n ≥ 50. Error bars represent SEM.

(J) *dyn1*Δ (A12123), *dyn1*Δ *kin4*Δ (A12122) and *dyn1*Δ *rts1*Δ (A22636) cells expressing a Tem1-13MYC fusion protein were grown as described in (D) and stained for tubulin and Tem1-13MYC by indirect immuno-fluorescence. n ≥ 50. Error bars represent SEM.

localization were unaffected by deletion of *RTS1* but Tem1 was observed to improperly load on to SPBs of cells with mis-positioned spindles (Figure 7H-J). This improper loading of Tem1 onto SPBs of cells with mis-positioned spindles in the *rts1*Δ mutant indicates that *RTS1* is required for normal *KIN4* function.

RTS1 inhibition of the MEN is spindle position checkpoint specific

Our data show that PP2A-Rts1 inhibits the MEN when the SPOC is active. We next wished to determine whether this inhibition was SPOC specific or whether PP2A-Rts1 was a general MEN inhibitor. To address this question we first examined the importance of MEN activity on SPOC and spindle assembly checkpoint (SAC) activity. We

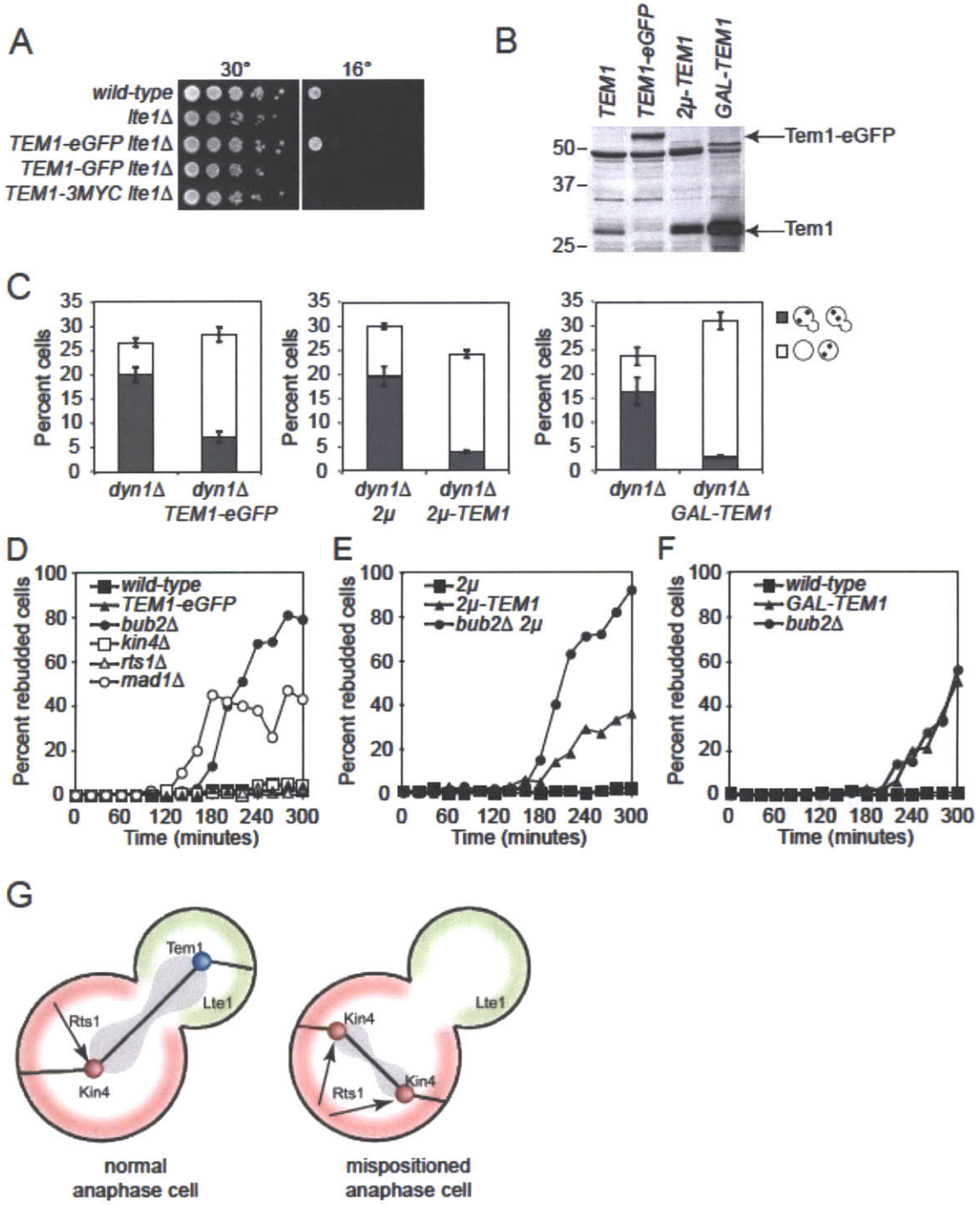

Figure 8. The SPOC and SAC are bypassed by differing levels of MEN activation

(A) Wild-type (A2587), *lte1*Δ (A18591), *lte1*Δ *TEM1-eGFP* (A21483), *lte1*Δ *TEM1-GFP* (A22567) and *lte1*Δ *TEM1-3MYC* (A4365) cells were spotted on YePAD plates and incubated at 30°C and 16°C. Pictures shown represent growth from 2 days for the 30°C condition and 4 days for 16°C. The first spot represents growth

of approximately $3x10^4$ cells and each subsequent spot is a 10 fold serial dilution.

(B) Whole cell lysates from 0.13 ODs of cells were analyzed by western blot for Tem1 levels in the wild-type (A2587), *TEM1-eGFP* (A21089), Yep13-*TEM1* (A23122) and *GAL-TEM1* (A2441) strains. A23122 was grown in SC-LEU for plasmid maintenance and A2441 was pregrown in YePA + 2% raffinose and induced with addition of 2% galactose for 2 hours.

(C) *dyn1*Δ (A17349), *dyn1*Δ *TEM1-eGFP* (A22811), *dyn1*Δ YEp13 (A23125), *dyn1*Δ YEp13-*TEM1* (A19104) and *dyn1*Δ *GAL-TEM1* (A23117) were grown and analyzed as described in Figures 2A and 2B with the following modifications: strains carrying YEp13 plasmids were pregrown in SC-LEU and then transferred to YePAD medium prior to temperature shift and strains A17349 and A23117 for the experiment in the third panel were pregrown in YePA + 2% raffinose and the GAL promoter was induced two hours prior to temperature shift with the addition of 2% galactose. $n \geq 100$ and error bars represent SEM.

(D) Wild-type (A2587), *mad1*Δ (A928), *bub2*Δ (A1863), *kin4*Δ (A17865), *rts1*Δ (A20312) and *TEM1-eGFP* (A21089) cells were grown and arrested in G1 as described in Figure 1A and subsequently released into media containing 15 μg/mL nocodazole. Additional 7.5 μg/mL nocodazole was added at 220 minutes after release to maintain the metaphase block. Samples were taken every 20 minutes for microscopic analysis. $n \geq 100$.

(E) YEp13 (A23121), Yep13-*TEM1* (A23122) and YEp13 *bub2*Δ (A23120) cells were grown and analyzed as in 1A and 7D with the following modification: strains were pregrown in SC-LEU to maintain the plasmid and then transferred to YePAD medium prior to pheromone arrest.

(F) Wild-type (A2587), *GAL-TEM1* (A2441) and *bub2*Δ (A1863) cells were grown and analyzed as in 1A and 7D with the following modifications: strains were grown and arrested in YePA + 2% raffinose and the GAL promoter was induced half an hour prior to release with the addition of 2% galactose.

(G) Model for the role of *RTS1* in the control of *KIN4*. See discussion for further details.

constructed a series of hypermorphic alleles of *TEM1* and tested their behavior in response to challenges to both spindle assembly and spindle positioning. We isolated a hypermorphic allele of *TEM1*, *TEM1-eGFP*. *TEM1-eGFP* suppresses the growth defect of *lte1*Δ cells at 16°C. Other C-terminal tagged alleles of *TEM1* do not display this suppression (Figure 8A). This allele produces about two fold more protein than wild-type *TEM1* (Figure 8B). In addition we examined two overexpression constructs of *TEM1*. *TEM1* expressed from a multi copy 2micron plasmid expressed approximately six fold more than wild-type *TEM1* and *TEM1* expressed from the *GAL1-10* promoter produced about 50 fold more protein (Figure 8B). We then tested the ability of these *TEM1* alleles

to hyperactivate the MEN and thus bypass the cell cycle arrests caused by the SAC and the SPOC. All three hypermorphic alleles of *TEM1* bypassed the cell cycle arrest caused by spindle position defects to a similar degree (Figure 8C). Cells treated with the spindle poison, nocodazole, activate the SAC which in turn prevents both entry into anaphase and MEN activation in response to microtubule – kinetochore attachment defects (reviewed in (Lew and Burke 2003)). Indeed, deletion of *BUB2* leads to inappropriate activation of the MEN and exit from mitosis in cells treated with nocodazole (Figure 8D; (Fraschini et al. 1999)). This is evident from examining the ability of cells to form small buds (termed rebudding) in the presence of nocodazole (Figure 8D;(Fraschini et al. 1999, Hoyt et al. 1991, Li and Murray 1991)). Tem1-eGFP failed to bypass the nocodazole-induced cell cycle arrest (Figure 8D) whereas the intermediate strength allele, 2micron-*TEM1*, displayed an intermediate level of bypass (Figure 8E). The strongest allele, *GAL-TEM1*, displayed the greatest degree of bypass of the nocodazole induced arrest (Figure 8F).

Having established this series of hyperactive *TEM1* alleles, we then compared these alleles to mutants of known SPOC components. Cells lacking *RTS1* or *KIN4* resembled *TEM1-eGFP* cells. The SAC was intact in these cells but the SPOC was not ((D'Aquino et al. 2005, Pereira and Schiebel 2005); Figure 8D). In contrast, *bub2*Δ cells most resembled *GAL-TEM1* cells, exhibiting both SAC and SPOC defects (Figure 8F). This finding indicates that like *KIN4*and unlike *BUB2*, *RTS1* is not a general inhibitor of the MEN but only exerts its inhibitory function in the SPOC. Additionally, our results suggest that higher levels of MEN activity are required to bypass the SAC than the SPOC.

Discussion

PP2A-Rts1 is a component of the spindle position checkpoint

Previous studies identified the protein kinase Kin4 as an inhibitor of MEN activity in response to spindle position defects. How the protein kinase was controlled however, was not understood. Based on the correlation between phosphorylation status and presumptive time of *KIN4* function during the cell cycle, we hypothesized that dephosphorylated Kin4 was active and that phosphatases that promoted accumulation of this form would be required for Kin4 function. To test this hypothesis we screened known phosphatases implicated in cell cycle control and identified PP2A and its regulatory subunit Rts1 as being required for Kin4 dephosphorylation. Consistent with the idea that dephosphorylation of Kin4 is indeed required for the protein's function we found that cells lacking PP2A-Rts1 failed to delay exit from mitosis in response to spindle position defects. Our studies also shed light on the mechanism whereby PP2A-Rts1 restrains the MEN when spindles are mis-positioned. The phosphatase does not appear to affect Kin4 kinase activity but instead promotes its association with SPBs, which was previously shown to be essential for SPOC activity (Maekawa et al. 2007).

Several lines of evidence indicate that PP2A-Rts1 is not a general inhibitor of the MEN but specifically functions in the SPOC by regulating Kin4 localization. Deletion of *RTS1*, like deletion of *KIN4,* leads to a bypass of the spindle position checkpoint arrest but not the nocodazole-induced cell cycle arrest. In contrast, deletion of the MEN inhibitor and target of Kin4, Bub2-Bfa1, leads to a bypass of both checkpoint arrests. The specificity of PP2A-Rts1 towards Kin4 regulation is revealed by the observations that (i) deletion of *KIN4* does not enhance the SPOC defect of the *dyn1*Δ *rts1*Δ mutant, that (ii) loss of *RTS1* function only alters the phosphorylation state and localization of Kin4 and not other MEN components and that (iii) loss of *RTS1* function suppresses the lethality of overexpression of *KIN4* but not *BFA1*. Attempts to test whether targeting Kin4 to SPBs was the sole function of PP2A-Rts1 in the spindle position checkpoint failed because a *KIN4* allele previously described to constitutively localize to SPBs (*KIN4-SPC72(177-622);* (Maekawa et al. 2007)*)* is not functional in the checkpoint (Figure 9).

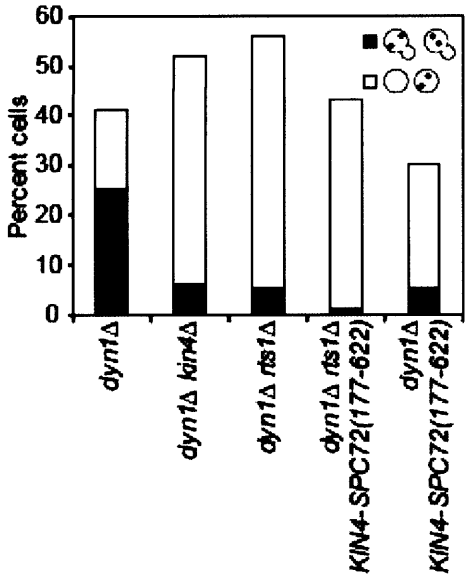

Figure 9. *KIN4-SPC72(177-622)* is a loss of function allele of *KIN4*

*dyn1*Δ (A17349), *dyn1*Δ *kin4*Δ (A17351) *dyn1*Δ *rts1*Δ (A20310) *dyn1*Δ *rts1*Δ *KIN4-SPC72(177-622)* (A22062) and *dyn1*Δ *KIN4-SPC72(177-622)* (A22063) cells were grown and analyzed as described in Figures 2A and 2B. $n \geq 100$.

PP2A-Rts1 regulation of Kin4 – an additional layer of control in the spindle position checkpoint

Based on the localization patterns of the MEN activator Lte1 and MEN inhibitor Kin4, we and others previously proposed that bud restricted Lte1 creates a zone of MEN activation in the bud and mother cell restricted Kin4 generates a zone of MEN inhibition in the mother cell ((Bardin et al. 2000, D'Aquino et al. 2005, Pereira et al. 2000); Figure 8G). Because components of the MEN localize to SPBs, movement of the MEN-bearing SPB into the bud would lead to MEN activation and exit from mitosis. In principle, this division of the cell into mitotic exit restrictive and permissive zones would be sufficient to ensure that exit from mitosis only occurs when one SPB and hence half of the nucleus moves into the bud. Our studies described here show that an additional layer of control exists where PP2A-Rts1 controls the association of Kin4 with SPBs that are located in the mother cell. This additional layer of control could provide temporal control over Kin4, restricting access of the kinase to its target to the time when a spindle is present in cells, specifically mitosis. This hypothesis would be consistent with the observed cell cycle regulation of Kin4 phosphorylation.

We do not yet understand how *RTS1* promotes Kin4 loading onto SPBs. PP2A-Rts1 could mobilize Kin4 at the cortex and facilitate its association with SPBs (Figure 8G). Whether the phosphatase does so by dephosphorylating Kin4 or a Kin4 receptor at SPBs is also not known. PP2A-Rts1 not only affects the ability of Kin4 to associate with SPBs in the mother cell but also its association with the mother cell cortex. In wild-type cells Kin4 is restricted to the mother cell cortex during S-phase and early mitosis. In cells lacking *RTS1* less Kin4 is observed at the cortex and localization is not restricted to the mother cell. It is therefore also possible that PP2A-Rts1 plays an important role in the establishment or maintenance of specific Kin4 localization to the mother cell cortex and that perhaps this localization is a prerequisite for Kin4 to load onto SPBs (Figure 8G). Indeed we observe that Kin4 mutants that fail to associate with the mother cell cortex also fail to associate with SPBs during anaphase (L. Y. C. unpublished observations).

A key question raised by the observation that Kin4 phosphorylation changes during the cell cycle is whether PP2A-Rts1 itself is cell cycle and SPOC regulated or whether it is a yet to be identified kinase(s) whose ability to phosphorylate Kin4 is regulated. Despite intense efforts, we have been unsuccessful in identifying kinases that affect phosphorylation and function of Kin4. Regardless of whether the Kin4 kinase(s) is cell cycle regulated, is there evidence that PP2A-Rts1 activity changes during the cell cycle? We do not detect any changes in Rts1 binding to the scaffolding subunit of PP2A, Tpd3, during the cell cycle (Figure 10), arguing against cell cycle regulated changes in PP2A subunit composition. There is however evidence that PP2A-Rts1 localization is cell cycle regulated. The protein localizes to centromeric DNA upon cell cycle entry and remains there until anaphase entry. The phosphatase also localizes to the bud neck during late mitosis where it regulates septin dynamics (L. Y. C. unpublished observations, (Dobbelaere et al. 2003, Gentry and Hallberg 2002)). Rts1 is not detected on SPBs (L. Y. C. unpublished observations, (Gentry and Hallberg 2002)) arguing against a model where Rts1 association with its targets at the SPB is part of SPOC control. Rather we favor the model where Rts1 is required for robust localization of Kin4 to the mother cell cortex, which is itself a requirement for SPB localization.

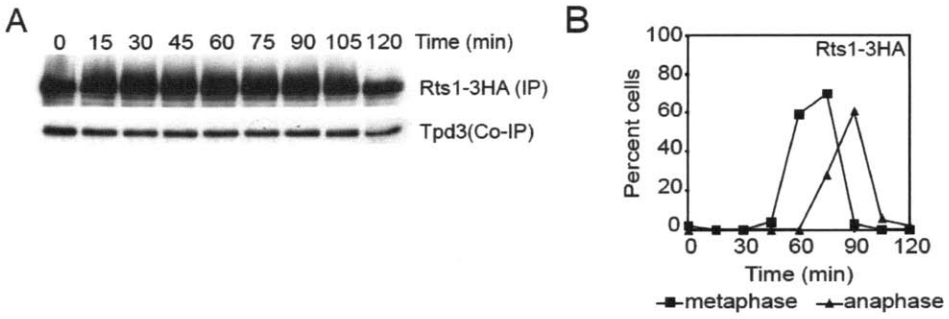

Figure 10. Rts1 and Tpd3 are associated throughout the cell cycle

(A-B) Wild-type cells expressing an Rts1-3HA (A20757) fusion protein were grown as described in Figure 1A. Rts1-3HA was immunoprecipitated using an HA antibody and the ability to co-immunoprecipitate Tpd3 was examined by western blot with an antibody against Tpd3. Cell cycle progression was monitored by spindle morphology (B).

PP2A – a key regulator of chromosome segregation fidelity

PP2A has previously been implicated in mitotic checkpoint control. The phosphatase together with its targeting subunit Cdc55 is required for cell cycle arrest upon triggering the SAC(Minshull et al. 1996). Our studies now show that the same phosphatase but with a different targeting subunit is essential for SPOC-induced cell cycle arrest. PP2A however has many other roles in mitotic progression. In controlling chromosome segregation, PP2A-Cdc55 controls the activity of the protein phosphatase Cdc14 during early anaphase as part of the FEAR network and also potentially controls the activity of the APC/C at the metaphase to anaphase transition(Chiroli et al. 2007, Queralt et al. 2006, Tang and Wang 2006, Wang and Burke 1997, Yellman and Burke 2006). During meiosis, PP2A-Rts1 controls the chromosome segregation factor Sgo1(Tang et al. 2006). In all instances where mechanisms are at least partly understood, PP2A control involves the targeted action of the phosphatase at specific locations in the cell. In the case of the SPOC it is possibly the cell cortex, during meiosis the kinetochore and in the case of the FEAR network the nucleolus. It thus appears that the recurring theme in PP2A control of mitosis is regulation by targeted localization.

Experimental Procedures

Yeast Strains and Growth Conditions

All strains are derivatives of W303 (A2587) with the following exceptions: A20126 and A21574 are derivatives of DEY100 (A19130) and A20176 is a derivative of Y398 (A19926). All strains are listed in Table 1. Lte1-GFP, Tem1-GFP, Rts1-3HA, *rts1*Δ, Spc42-mCherry and *MET-GFP-KIN4* were constructed by standard PCR based methods(Hentges et al. 2005, Longtine et al. 1998, Snaith, Samejima and Sawin 2005). *kin4*^{T209A} was constructed by a two-step gene replacement using the *URA3* gene from *Kluyveromyces lactis*. Growth conditions are described in the figure legends.

Plasmid Construction

The plasmid used to construct the *HIS3MX6:MET-GFP-KIN4* allele, pFA6a-*HIS3MX6:pMET25-GFP* (pA1758), was constructed by digesting pFA6a-*HIS3MX6:pGAL-GFP* (Longtine et al. 1998) and a PCR product containing the *MET25* promoter with BglII and PacI and ligating the two fragments together.

Immunoblot Analysis

Immunoblot analysis to determine total amount of Kin4-3HA, 3HA-Bfa1, Tem1-3MYC and Lte1-13MYC were performed as described(Bardin et al. 2000, D'Aquino et al. 2005, Seshan, Bardin and Amon 2002). For immunoblot analysis of Kin4-GFP, 3HA-Bub2 and Tem1, cells were incubated for a minimum of 10 minutes in 5% trichloroacetic acid. The acid was washed away with acetone and cells were pulverized with glass beads in 100 μL of lysis buffer (50 mM Tris-Cl pH7.5, 1 mM EDTA, 2.75 mM DTT and complete protease inhibitor cocktail [Roche]) using a bead mill. Sample buffer was added and the cell homogenates were boiled. Kin4-GFP was detected using an anti-GFP antibody (Clontech, JL-8) at 1:1000, 3HA-Bub2 was detected using an anti-HA antibody (Covance, HA.11) at 1:1000 and Tem1 was detected with an anti-Tem1 antibody at 1:1500. Semi-quantitative measurements of relative protein levels of Tem1 and levels of phosphorylated and unphosphorylated Kin4-3HA were made using ECL Plus (GE Healthcare) and fluorescence imaging. Quantification was performed using NIH Image

Quant software. Rts1-3HA was detected using the same anti-HA antibody at 1:1000 and Tpd3 was detected with a rabbit anti-Tpd3 antibody at 1:2000.

Antibody generation

An anti-Tem1 antibody was raised in rabbits against the peptide, CKKLTIPEINEIGDPLLIYKHL. The antibody was then affinity purified using immobilized antigen peptides (Covance).

Fluorescence Microscopy

Indirect in situ immunofluorescence methods and antibody concentrations for Tub1 and Tem1-13MYC were as previously described(D'Aquino et al. 2005, Kilmartin and Adams 1984). For simultaneous visualization of nuclei and the mCherry-Tub1 fusion protein, cells were prepared as described (Monje-Casas et al. 2007) with the following modifications: cells were permeabilized with 1% Triton X-100 for 5 minutes and the cells were resuspended in 1 μg/mL Hoechst 3342. For live cell microscopy, cells were grown in YePAD, harvested, resuspended in SC and immediately imaged using a Zeiss Axioplan 2 microscope and a Hamamatsu OCRA-ER digital camera. Deconvolution was performed with Openlab 4.0.2 software. For quantifications, Z-stacks were taken and the localization was determined.

Spindle position checkpoint assay

Cells were grown to mid-exponential phase and then incubated at 14°C for 24 hours. Cells were fixed, stained for the nuclei and spindle and examined for endpoint morphology. Cells that were anucleated, multinucleated or budded with two nuclei in the mother cell body but with a disassembled spindle were counted as bypassed. Budded cells with two nuclei in the mother cell body with an intact anaphase spindle were counted as arrested.

Kin4 Kinase Assays

Kin4 kinase assays were performed as previously (D'Aquino et al. 2005)with the following modifications: 30 μL of anti-HA affinity matrix bead slurry (Roche) were used,

3.5 mg of total protein were used per immunoprecipitation, kinase reactions were allowed to run for one hour and the substrate was a mix of 1 μg myelin basic protein and about 5 μg of recombinant MBP-BFA1. MBP-BFA1 was purified as previously described(Geymonat et al. 2002). Kinase signal was determined by phosphorimaging and immunoblot signal was determined using ECL Plus (GE Healthcare) and fluorescence imaging. Quantification was performed using NIH Image Quant software.

Co-Immunoprecipitation assays

Approximately 12 OD units of cells were collected, washed once with 10mM Tris-Cl pH7.5 and then lysed with glass beads in a bead mill with lysis buffer (50mM Tris-Cl pH7.5, 150mM NaCl, 1% NP-40, 60mM β-glycerolphosphate, 0.1mM sodium orthovanadate, 15mM para-nitrophenlylphosphate, 1mM DTT and complete protease inhibitor cocktail [Roche]). 1 μg anti-HA antibody (Covance, HA.11) was added to 900 μg of total protein and incubated for 1 hour. 10 μL of pre-swelled protein-G bead slurry (Pierce) were then added to each sample and agitated for 2 hours at 4°C. Beads were then washed six times with wash buffer (50 mM Tris-Cl pH7.5, 150 mM NaCl, 1% NP-40). Sample buffer was added to the beads that were then boiled.

Table 1: Yeast Strains

Strain	Relevant genotype	Source
928	*MATa mad1Δ::URA3*	
1828	*MATa TEM1-3MYC*	
1863	*MATa bub2Δ::HIS3MX6*	
2441	*MATa ura3:GAL-TEM1:URA3*	
2587	*MATa ade2-1 leu2-3 ura3 trp1-1 his3-11,15 can1-100 GAL+ psi+*	
3487	*MATa HIS3MX6:GAL-GFP-BFA1*	
4365	*MATa lte1Δ::KanMX6 TEM1-3MYC*	
4378	*MATa 3HA-BFA1*	
11779	*MATa KIN4-3HA:KanMX6*	
11997	*MATa HIS3MX6:GAL-GFP-KIN4*	
12122	*MATa dyn1Δ::URA3 TEM1-13MYC:HIS3MX6 3HA-CDC14 kin4Δ::KanMX6*	
12123	*MATa dyn1Δ::URA3 TEM1-13MYC:HIS3MX6 3HA-CDC14*	
15396	*MATa cdc55Δ::KanMx6*	
17349	*MATa dyn1Δ::URA3*	
17351	*MATa kin4Δ::KanMX6 dyn1Δ::URA3*	
17865	*MATa kin4Δ::KanMX6*	
18591	*MATa lte1Δ::KanMX6*	
18792	*MATa HIS3MX6:GAL-GFP-KIN4 bub2Δ::HIS3MX6*	
19104	*MATa dyn1Δ::URA3 Yep13-TEM1*	
19111	*MATa KIN4-3HA:KanMX6 cdc14-3*	
19130	*MATa pph21Δ1::HIS3 pph22-12 pph3Δ1::LYS2 ssd1-d2*	DEY100[1]
19804	*MATa KIN4-3HA:TRP1 cdc55Δ::KanMX6*	
19808	*MATa trp1-1:glc7-12:TRP1 glc7Δ::LEU2 KIN4-3HA:KanMX6*	
19900	*MATa ura3:mCherry-TUB1:URA3 KIN4-GFP:HIS3MX6*	
19902	*MATa SPC42-mCherry:NatMX6 KIN4-GFP:HIS3MX6*	
19926	*MATa sit4Δ::HIS3 ssd1-d1 Ycp50-sit4-102 (URA/CEN)*	Y398[2]
20126	*MATa pph21Δ1::HIS3 pph22-12 pph3Δ1::LYS2 ssd1-d2 KIN4-3HA:KanMX6*	
20176	*MATa sit4Δ::HIS3 ssd1-d1 KIN4-3HA:KanMX6 Ycp50-sit4-102 (URA/CEN)*	
20187	*MATa KIN4-3HA::KanMX6 rts1Δ::NatMX6*	
20310	*MATa rts1Δ::NatMX6 dyn1Δ::URA3*	
20312	*MATa rts1Δ::NatMX6*	
20757	*MATa RTS1-3HA:KanMX6*	
20892	*MATa HIS3MX6:GAL-GFP-BFA1 rts1Δ::NatMX6*	
20893	*MATa HIS3MX6:GAL-GFP-KIN4 rts1Δ::NatMX6*	
20918	*MATa ura3:mCherry-TUB1:URA3 KIN4-GFP:HIS3MX6*	

	rts1Δ::NatMX6	
21089	*MATa TEM1-yEGFP:HIS3MX6*	
21483	*MATa lte1Δ::KanMX6 TEM1-yEGFP:HIS3MX6*	
21520	*MATa cdc55Δ::KanMX6 dyn1Δ::URA3*	
21538	*MATa rts1Δ::NatMX6 kin4Δ::TRP1 dyn1Δ::URA3*	
21539	*MATa TEM1-3 rts1Δ::NatMX6*	
21540	*MATa rts1Δ::NatMX6 3HA-BFA1*	
21574	*MATa pph21Δ1::HIS3 pph22-12 pph3Δ1::LYS ssd1-d2 dyn1Δ::NatMX6*	
21608	*MATa ura3:mCherry-TUB1:URA3 BFA1-yEGFP:KanMX6*	
21610	*MATa ura3:mCherry-TUB1:URA3 BUB2-yEGFP:KanMX6*	
21720	*MATa ura3:mCherry-TUB1:URA3 KIN4-GFP:HIS3MX6 dyn1Δ::URA3*	
21722	*MATa ura3:mCherry-TUB1:URA3 BFA1-yEGFP:KanMX6 dyn1Δ::URA3 rts1Δ::NatMX6*	
21723	*MATa ura3:mCherry-TUB1:URA3 BFA1-yEGFP:KanMX6 dyn1Δ::URA3*	
21724	*MATa ura3:mCherry-TUB1:URA3 BUB2-yEGFP:KanMX6 dyn1Δ::URA3*	
21725	*MATa ura3:mCherry-TUB1:URA3 BUB2-yEGFP:KanMX6 dyn1Δ::URA3 rts1Δ::NatMX6*	
21729	*MATa ura3:mCherry-TUB1:URA3 BFA1-yEGFP:KanMX6 rts1Δ::NatMX6*	
21730	*MATa ura3:mCherry-TUB1:URA3 BUB2-yEGFP:KanMX6 rts1Δ::NatMX6*	
21732	*MATa SPC42-mCherry:NatMX6 KIN4-GFP:HIS3MX6 rts1Δ::NatMX6*	
21921	*MATa 3HA-BUB2*	yFH649-2[3]
22062	*MATa dyn1Δ::URA3 rts1Δ::NatMx6 LEU2:KIN4 -SPC72(177-622):kin4Δ::KL-URA3:Kin4'3'UTR:KanMX6*	
22063	*MATa dyn1Δ::URA3 LEU2:KIN4-SPC72(177-622): kin4Δ::KL-URA3:Kin4'3'UTR:KanMX6*	
22064	*MATa 3HA-BUB2 rts1Δ::NatMX6*	
22119	*MATa Kin4T209A-3HA:KanMX6*	
22120	*MATa Kin4T209A-3HA:KanMX6 rts1Δ::NatMX6*	
22556	*MATa ura3:mCherry-TUB1:URA3 TEM1-GFP:HIS3MX6*	
22567	*MATa lte1Δ::NatMX6 TEM1-GFP:HIS3MX6*	
22631	*MATa ura3:mCherry-TUB1:URA3 LTE1-GFP:KanMX6 rts1Δ::NatMX6*	
22632	*MATa ura3:mCherry-TUB1:URA3 LTE1-GFP:KanMX6*	
22636	*MATa dyn1Δ::URA3 TEM1-13MYC:HIS3MX6 rts1Δ::NatMX6*	
22667	*MATa ura3:mCherry-TUB1:URA3 TEM1-GFP:HIS3MX6 rts1Δ::NatMX6*	
22668	*MATa LTE1-13MYC:KanMX6*	
22669	*MATa LTE1-13MYC:KanMX6 rts1Δ::NatMX6*	

22736 *MATa KIN4T209A:Kin4-3'UTR:KanMX6 dyn1Δ::URA3*
22811 *MATa dyn1Δ::URA3 TEM1-yEGFP:HIS3MX6*
22878 *MATa ura3:mCherry-TUB1:URA3 KIN4-GFP:HIS3MX6 dyn1Δ::HIS3MX6 rts1Δ::NatMX6*
23117 *MATa dyn1Δ::URA3 ura3:GAL-TEM1:URA3*
23120 *MATa Yep13 bub2Δ::HIS3MX6*
23121 *MATa Yep13*
23122 *MATa Yep13-TEM1*
23125 *MATa dyn1Δ*::URA3 Yep13
23232 *MATa HIS3MX6:MET-GFP-KIN4*
23357 *MATa HIS3MX6:MET-GFP-KIN4 ura3:mCherry-TUB1:URA3 rts1Δ::NatMX6*
23358 *MATa HIS3MX6:MET-GFP-KIN4 ura3:mCherry-TUB1:URA3*

[1] Evans, D. R. and M. J. Stark (1997). "Mutations in the Saccharomyces cerevisiae type 2A protein phosphatase catalytic subunit reveal roles in cell wall integrity, actin cytoskeleton organization and mitosis." Genetics **145**(2): 227-41.

[2] Wang, H., X. Wang, et al. (2003). "Interaction with Tap42 is required for the essential function of Sit4 and type 2A phosphatases." Mol Biol Cell **14**(11): 4342-51.

[3] Hu, F. and S. J. Elledge (2002). "Bub2 is a cell cycle regulated phospho-protein controlled by multiple checkpoints." Cell Cycle **1**(5):351-355.

References

Bardin, A. J., R. Visintin & A. Amon (2000) A mechanism for coupling exit from mitosis to partitioning of the nucleus. *Cell,* 102, 21-31.

Bloecher, A., G. M. Venturi & K. Tatchell (2000) Anaphase spindle position is monitored by the BUB2 checkpoint. *Nat Cell Biol,* 2, 556-8.

Cheng, J., N. Turkel, N. Hemati, M. T. Fuller, A. J. Hunt & Y. M. Yamashita (2008) Centrosome misorientation reduces stem cell division during ageing. *Nature,* 456, 599-604.

Chiroli, E., V. Rossio, G. Lucchini & S. Piatti (2007) The budding yeast PP2ACdc55 protein phosphatase prevents the onset of anaphase in response to morphogenetic defects. *J Cell Biol,* 177, 599-611.

D'Aquino, K. E., F. Monje-Casas, J. Paulson, V. Reiser, G. M. Charles, L. Lai, K. M. Shokat & A. Amon (2005) The protein kinase Kin4 inhibits exit from mitosis in response to spindle position defects. *Mol Cell,* 19, 223-34.

Dobbelaere, J., M. S. Gentry, R. L. Hallberg & Y. Barral (2003) Phosphorylation-dependent regulation of septin dynamics during the cell cycle. *Dev Cell,* 4, 345-57.

Evans, D. R. & M. J. Stark (1997) Mutations in the Saccharomyces cerevisiae type 2A protein phosphatase catalytic subunit reveal roles in cell wall integrity, actin cytoskeleton organization and mitosis. *Genetics,* 145, 227-41.

Fesquet, D., P. J. Fitzpatrick, A. L. Johnson, K. M. Kramer, J. H. Toyn & L. H. Johnston (1999) A Bub2p-dependent spindle checkpoint pathway regulates the Dbf2p kinase in budding yeast. *Embo J,* 18, 2424-34.

Fraschini, R., E. Formenti, G. Lucchini & S. Piatti (1999) Budding yeast Bub2 is localized at spindle pole bodies and activates the mitotic checkpoint via a different pathway from Mad2. *J Cell Biol,* 145, 979-91.

Gentry, M. S. & R. L. Hallberg (2002) Localization of Saccharomyces cerevisiae protein phosphatase 2A subunits throughout mitotic cell cycle. *Mol Biol Cell,* 13, 3477-92.

Geymonat, M., A. Spanos, S. J. Smith, E. Wheatley, K. Rittinger, L. H. Johnston & S. G. Sedgwick (2002) Control of mitotic exit in budding yeast. In vitro regulation of Tem1 GTPase by Bub2 and Bfa1. *J Biol Chem,* 277, 28439-45.

Geymonat, M., A. Spanos, P. A. Walker, L. H. Johnston & S. G. Sedgwick (2003) In vitro regulation of budding yeast Bfa1/Bub2 GAP activity by Cdc5. *J Biol Chem,* 278, 14591-4.

Hentges, P., B. Van Driessche, L. Tafforeau, J. Vandenhaute & A. M. Carr (2005) Three novel antibiotic marker cassettes for gene disruption and marker switching in Schizosaccharomyces pombe. *Yeast,* 22, 1013-9.

Hoyt, M. A., L. Totis & B. T. Roberts (1991) S. cerevisiae genes required for cell cycle arrest in response to loss of microtubule function. *Cell,* 66, 507-17.

Hu, F., Y. Wang, D. Liu, Y. Li, J. Qin & S. J. Elledge (2001) Regulation of the Bub2/Bfa1 GAP complex by Cdc5 and cell cycle checkpoints. *Cell,* 107, 655-65.

Jaspersen, S. L., J. F. Charles & D. O. Morgan (1999) Inhibitory phosphorylation of the APC regulator Hct1 is controlled by the kinase Cdc28 and the phosphatase Cdc14. *Curr Biol,* 9, 227-36.

Jiang, Y. (2006) Regulation of the cell cycle by protein phosphatase 2A in Saccharomyces cerevisiae. *Microbiol Mol Biol Rev,* 70, 440-9.
Kilmartin, J. V. & A. E. Adams (1984) Structural rearrangements of tubulin and actin during the cell cycle of the yeast Saccharomyces. *J Cell Biol,* 98, 922-33.
Lee, J., H. S. Hwang, J. Kim & K. Song (1999) Ibd1p, a possible spindle pole body associated protein, regulates nuclear division and bud separation in Saccharomyces cerevisiae. *Biochim Biophys Acta,* 1449, 239-53.
Lee, S. E., L. M. Frenz, N. J. Wells, A. L. Johnson & L. H. Johnston (2001) Order of function of the budding-yeast mitotic exit-network proteins Tem1, Cdc15, Mob1, Dbf2, and Cdc5. *Curr Biol,* 11, 784-8.
Lew, D. J. & D. J. Burke (2003) The spindle assembly and spindle position checkpoints. *Annu Rev Genet,* 37, 251-82.
Li, R. (1999) Bifurcation of the mitotic checkpoint pathway in budding yeast. *Proc Natl Acad Sci U S A,* 96, 4989-94.
Li, R. & A. W. Murray (1991) Feedback control of mitosis in budding yeast. *Cell,* 66, 519-31.
Li, Y. Y., E. Yeh, T. Hays & K. Bloom (1993) Disruption of mitotic spindle orientation in a yeast dynein mutant. *Proc Natl Acad Sci U S A,* 90, 10096-100.
Longtine, M. S., A. McKenzie, 3rd, D. J. Demarini, N. G. Shah, A. Wach, A. Brachat, P. Philippsen & J. R. Pringle (1998) Additional modules for versatile and economical PCR-based gene deletion and modification in Saccharomyces cerevisiae. *Yeast,* 14, 953-61.
Luca, F. C., M. Mody, C. Kurischko, D. M. Roof, T. H. Giddings & M. Winey (2001) Saccharomyces cerevisiae Mob1p is required for cytokinesis and mitotic exit. *Mol Cell Biol,* 21, 6972-83.
Maekawa, H., C. Priest, J. Lechner, G. Pereira & E. Schiebel (2007) The yeast centrosome translates the positional information of the anaphase spindle into a cell cycle signal. *J Cell Biol,* 179, 423-36.
Mah, A. S., J. Jang & R. J. Deshaies (2001) Protein kinase Cdc15 activates the Dbf2-Mob1 kinase complex. *Proc Natl Acad Sci U S A,* 98, 7325-30.
Minshull, J., A. Straight, A. D. Rudner, A. F. Dernburg, A. Belmont & A. W. Murray (1996) Protein phosphatase 2A regulates MPF activity and sister chromatid cohesion in budding yeast. *Curr Biol,* 6, 1609-20.
Monje-Casas, F., V. R. Prabhu, B. H. Lee, M. Boselli & A. Amon (2007) Kinetochore orientation during meiosis is controlled by Aurora B and the monopolin complex. *Cell,* 128, 477-90.
O'Connell, C. B. & Y. L. Wang (2000) Mammalian spindle orientation and position respond to changes in cell shape in a dynein-dependent fashion. *Mol Biol Cell,* 11, 1765-74.
Pereira, G., T. Hofken, J. Grindlay, C. Manson & E. Schiebel (2000) The Bub2p spindle checkpoint links nuclear migration with mitotic exit. *Mol Cell,* 6, 1-10.
Pereira, G. & E. Schiebel (2005) Kin4 kinase delays mitotic exit in response to spindle alignment defects. *Mol Cell,* 19, 209-21.
Queralt, E., C. Lehane, B. Novak & F. Uhlmann (2006) Downregulation of PP2A(Cdc55) phosphatase by separase initiates mitotic exit in budding yeast. *Cell,* 125, 719-32.

Seshan, A., A. J. Bardin & A. Amon (2002) Control of Lte1 localization by cell polarity determinants and Cdc14. *Curr Biol,* 12, 2098-110.

Shirayama, M., Y. Matsui, K. Tanaka & A. Toh-e (1994a) Isolation of a CDC25 family gene, MSI2/LTE1, as a multicopy suppressor of ira1. *Yeast,* 10, 451-61.

Shirayama, M., Y. Matsui & E. A. Toh (1994b) The yeast TEM1 gene, which encodes a GTP-binding protein, is involved in termination of M phase. *Mol Cell Biol,* 14, 7476-82.

Shou, W., J. H. Seol, A. Shevchenko, C. Baskerville, D. Moazed, Z. W. Chen, J. Jang, A. Shevchenko, H. Charbonneau & R. J. Deshaies (1999) Exit from mitosis is triggered by Tem1-dependent release of the protein phosphatase Cdc14 from nucleolar RENT complex. *Cell,* 97, 233-44.

Snaith, H. A., I. Samejima & K. E. Sawin (2005) Multistep and multimode cortical anchoring of tea1p at cell tips in fission yeast. *Embo J,* 24, 3690-9.

Tang, X. & Y. Wang (2006) Pds1/Esp1-dependent and -independent sister chromatid separation in mutants defective for protein phosphatase 2A. *Proc Natl Acad Sci U S A,* 103, 16290-5.

Tang, Z., H. Shu, W. Qi, N. A. Mahmood, M. C. Mumby & H. Yu (2006) PP2A is required for centromeric localization of Sgo1 and proper chromosome segregation. *Dev Cell,* 10, 575-85.

Visintin, R., K. Craig, E. S. Hwang, S. Prinz, M. Tyers & A. Amon (1998) The phosphatase Cdc14 triggers mitotic exit by reversal of Cdk-dependent phosphorylation. *Mol Cell,* 2, 709-18.

Visintin, R., E. S. Hwang & A. Amon (1999) Cfi1 prevents premature exit from mitosis by anchoring Cdc14 phosphatase in the nucleolus. *Nature,* 398, 818-23.

Wang, H., X. Wang & Y. Jiang (2003) Interaction with Tap42 is required for the essential function of Sit4 and type 2A phosphatases. *Mol Biol Cell,* 14, 4342-51.

Wang, Y. & D. J. Burke (1997) Cdc55p, the B-type regulatory subunit of protein phosphatase 2A, has multiple functions in mitosis and is required for the kinetochore/spindle checkpoint in Saccharomyces cerevisiae. *Mol Cell Biol,* 17, 620-6.

Yeh, E., R. V. Skibbens, J. W. Cheng, E. D. Salmon & K. Bloom (1995) Spindle dynamics and cell cycle regulation of dynein in the budding yeast, Saccharomyces cerevisiae. *J Cell Biol,* 130, 687-700.

Yellman, C. M. & D. J. Burke (2006) The role of Cdc55 in the spindle checkpoint is through regulation of mitotic exit in Saccharomyces cerevisiae. *Mol Biol Cell,* 17, 658-66.

Zachariae, W., M. Schwab, K. Nasmyth & W. Seufert (1998) Control of cyclin ubiquitination by CDK-regulated binding of Hct1 to the anaphase promoting complex. *Science,* 282, 1721-4.

Chapter III: Spindle position is coordinated with cell cycle progression through establishment of mitotic exit activating and inhibitory zones

Submitted for publication as a manuscript: *Chan L.Y. and Amon A. 2010.*

Summary

The spindle position checkpoint (SPOC) prevents exit from mitosis until each daughter cell has received a complete genetic complement. In budding yeast the SPOC does so by inhibiting the Mitotic Exit Network (MEN), a signaling pathway that promotes exit from mitosis. Here we show that spindle position is sensed by a system composed of MEN inhibitory and activating zones and a sensor that moves between them. The MEN inhibitory zone is located in the mother cell, the MEN activating zone in the bud. The spindle pole body (SPB), where the components of the MEN reside, functions as the sensor. Only when the MEN bearing SPB escapes the MEN inhibitor Kin4 in the mother cell and moves into the bud where the MEN activator Lte1 resides can exit from mitosis occur. In this manner, spatial information is sensed and translated into a chemical signal.

Introduction

Polarized cell division, the process of dividing the cell along a predetermined axis, is central to the development of complex biological systems. Cell intrinsic and/or extrinsic cues establish these axes and the mitotic spindle must be positioned along them to ensure that each daughter cell receives a full genomic complement. Feedback mechanisms have been identified in cultured rat kidney cells and *Drosophila* germline stem cells that delay the cell cycle in response to defects in spindle position, but this mechanism is best understood in budding yeast (Cheng et al. 2008, O'Connell and Wang 2000, Yeh et al. 1995). In yeast, the site of bud formation and therefore cytokinesis is determined during G1. Thus, the axis of division is defined prior to mitosis and the mitotic spindle must be aligned along this mother – bud axis during every cell division. When this process fails, a surveillance mechanism known as the spindle position checkpoint (SPOC) delays mitotic exit to provide the cell with an opportunity to reposition the spindle and thus partition the genetic material equally prior to spindle disassembly and cytokinesis. When this surveillance mechanism fails, cells that mis-position their spindles give rise to mitotic products with too many or too few nuclei (Yeh et al. 1995).

Mitotic exit is controlled by a signaling pathway known as the Mitotic Exit Network (MEN). The central switch of the MEN is the small GTPase, Tem1, which localizes to spindle pole bodies (SPBs, yeast centrosomes) during mitosis (Shirayama, Matsui and Toh 1994b, Bardin, Visintin and Amon 2000, Molk et al. 2004, Pereira et al. 2000). At the SPB, activated Tem1 (presumably Tem1-GTP) transduces a signal through a two kinase cascade ultimately resulting in the activation of the phosphatase, Cdc14. Cdc14 brings about the inactivation of mitotic cyclin-dependent kinases, which results in spindle disassembly, cytokinesis and, ultimately, resetting of the cell to a G1-like state (Jaspersen, Charles and Morgan 1999, Visintin et al. 1998, Zachariae et al. 1998).

Tem1 is positively regulated by the bud cortex localized protein, Lte1, and negatively by the two-component GTPase activating protein (GAP) complex, Bub2 - Bfa1 (Bardin et al. 2000, Bloecher, Venturi and Tatchell 2000, Geymonat et al. 2002, Lee et al. 1999, Li 1999, Pereira et al. 2000, Shirayama et al. 1994a). The GAP complex in turn is inhibited

by the Polo-like kinase, Cdc5 (Geymonat et al. 2003, Hu et al. 2001). During metaphase, Tem1 and the GAP complex localize to both SPBs; during anaphase they become concentrated at the SPB that migrates into the bud (Bardin et al. 2000, Fraschini et al. 1999, Lee et al. 1999, Li 1999, Pereira et al. 2000, Molk et al. 2004).

The SPOC inhibits the MEN at the level of Tem1 activation. The protein kinase Kin4 and the protein phosphatase PP2A-Rts1 are essential for SPOC function (Chan and Amon 2009, D'Aquino et al. 2005, Pereira and Schiebel 2005). Kin4 localizes to the mother cell cortex throughout the cell cycle and at the mother spindle pole body in mid-anaphase where it phosphorylates Bfa1 and protects the GAP complex from inhibitory phosphorylation by Cdc5 (Maekawa et al. 2007). In cells with mis-positioned spindles, Kin4 associates with both anaphase SPBs, phosphorylates the GAP complex at both SPBs and thus inhibits the MEN (Maekawa et al. 2007, Pereira and Schiebel 2005). The protein phosphatase PP2A-Rts1 regulates Kin4's phosphorylation state and promotes the loading of Kin4 onto SPBs, which is essential for SPOC function (Chan and Amon 2009).

How the cell monitors spindle position and translates this spatial information to regulate MEN is only partially understood. Emergence of a Tem1 bearing SPB into the bud where Lte1 resides ensures that Tem1 activation by Lte1 only occurs when the spindle elongates along the mother-bud axis (Bardin et al. 2000, Pereira et al. 2000). The importance of spatial restriction of Lte1 to the bud is underscored by experiments that inappropriately place Lte1 in the mother cell thus leading to premature mitotic exit when the spindle is mispositioned (Bardin et al. 2000, Castillon et al. 2003, Geymonat et al. 2009). Fission yeast appears to promote activation of the Tem1 homolog, Spg1, through a strikingly similar mechanism (Garcia-Cortes and McCollum 2009).

However, restricting Lte1 to the bud cannot be the only mechanism that regulates Tem1 in response to spindle position because Lte1 is only essential for mitotic exit at low temperatures (Adames, Oberle and Cooper 2001, Shirayama et al. 1994a). Many other mechanisms have been proposed to act in addition to Lte1 (Adames et al. 2001, D'Aquino

et al. 2005, Fraschini et al. 2006). We have proposed the key parallel mechanism to be Kin4 mediated MEN inhibition (D'Aquino et al. 2005) and based on the restriction of Kin4 to the mother cell cortex and Lte1 to the daughter cell cortex, put forward a "zone model" that states that in order for the MEN to signal, a Tem1 bearing SPB must first escape the zone of inhibition or the mother cell where Kin4 resides and then enter the zone of activation or the daughter cell where Lte1 resides. This proposed function of Kin4 has however not been tested.

To shed light on whether and how Kin4 is regulated by spindle position defects we have defined the regions within Kin4 that mediate its MEN inhibitory function and its cortical localization in the mother cell. This analysis identified a C-terminal cortical localization domain and a single amino acid, serine 508, that is necessary for restriction to the mother cell cortex. Mutation of this serine did not affect Kin4 activity or protein levels but led to the association of Kin4 with both the mother and daughter cell cortices, allowing us to test the validity of the zone model of Kin4 function. We find that symmetrically localized Kin4 inhibits the MEN in the absence of spindle position defects but only in the absence of the MEN activator Lte1. These data not only demonstrate that when present in the same compartment, Lte1's MEN promoting activity dominates over Kin4's MEN inhibitory activity but also show that Kin4 establishes a MEN inhibitory zone in the mother cell that the MEN bearing SPB must escape in order to promote exit from mitosis. Our data further indicate that Kin4 is not activated by spindle position defects but that Kin4 is active in every cell cycle to restrain MEN signaling in the mother cell. Exit from mitosis can only occur when a MEN bearing SPB escapes this inhibitory zone. Thus, cells ensure the accurate partitioning of the genetic material between mother and daughter cells by establishing zones of MEN inhibition and activation that allows the translation of spatial cues into a cell cycle signal.

Results

KIN4 acts in every cell cycle

The zone model, where spindle position is sensed and translated by a sensor (Tem1) that moves from an inhibitory (Kin4) to an activating (Lte1) zone makes the following predictions: (1) Kin4 and Lte1 should not be regulated by spindle position but should control the MEN during every cell cycle, (2) targeting Lte1 to the mother cell should promote mitotic exit in cells with mis-positioned spindles (this was indeed found to be the case, (Bardin et al. 2000, Castillon et al. 2003, Geymonat et al. 2009)), and (3) targeting Kin4 to both the mother cell and the bud should inhibit mitotic exit. We tested prediction (1) first. The Cdc14 early anaphase release (FEAR) network is a non-essential pathway that acts in parallel to the MEN to promote timely mitotic exit. Simultaneous deletion of *LTE1* and FEAR network components such as *SPO12* results in lethality (Stegmeier, Visintin and Amon 2002). The observation that *kin4*Δ suppresses the lethality of *lte1*Δ *spo12*Δ double mutants indicated that *KIN4* restrains MEN activity even in an unperturbed cell cycle (D'Aquino et al. 2005). The analysis of *lte1*Δ *kin4*Δ double mutants further confirmed this notion. *lte1*Δ mutants are unable to proliferate at temperatures below 18°C because of an inability to exit from mitosis (Shirayama et al. 1994a) (Figure 1A). Deletion of *KIN4* completely suppressed this proliferation defect of the *lte1*Δ mutant, similar to deletion of *BUB2* (Pereira and Schiebel 2005, Yoshida, Ichihashi and Toh-e 2003) (Figure 1A). Furthermore, we found that the 15 minute delay in mitotic exit observed in *lte1Δ* cells at room temperature was fully suppressed by the deletion of *KIN4* (note that this result also demonstrates that *LTE1* is required for efficient mitotic exit during every cell cycle) (Adames et al. 2001, Bardin et al. 2000, Jensen et al. 2004) (Figure 1B). The extent of the suppression was similar to that caused by deletion of *BUB2* (Figure 1B). Our data indicate that *KIN4* antagonizes mitotic exit during every cell cycle.

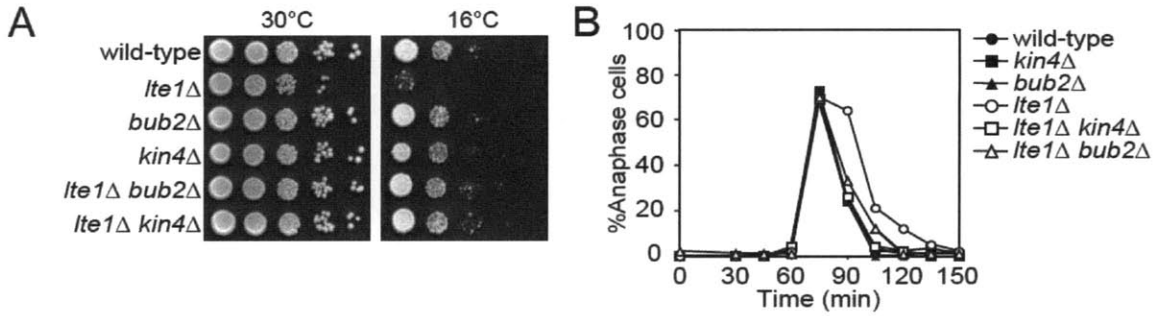

Figure 1. Kin4 Inhibits the MEN in every Cell Cycle

(A) Wild-type (A2587), *lte1*Δ (A24807), *bub2*Δ (A23045), *kin4*Δ (A17865), *lte1*Δ *bub2*Δ (A24808) and *lte1*Δ *kin4*Δ (A24806) cells were spotted on YePAD plates and incubated at 30°C and 16°C. Pictures shown represent growth from 2 days for the 30°C condition and 10 days for 16°C. The first spot represents growth of approximately $3x10^4$ cells and each subsequent spot is a 10 fold serial dilution.

(B) Cells in (A) were arrested in G1 with 5 μg/mL α factor and released into pheromone free media at room temperature. After 70 minutes, 10 μg/mL α factor was added to prevent entry into the subsequent cell cycle. Cells were collected every 15 minutes and stained for tubulin by indirect immuno-fluorescence and for the DNA with DAPI. Anaphase was determined by spindle and nuclear morphology. $n \geq 100$ cells.

The N-terminal kinase domain of Kin4 mediates inhibition of mitotic exit

To test the prediction that symmetric targeting of Kin4 inhibits mitotic exit, we first needed to create an allele of *KIN4* that localizes to both the mother cell and bud while retaining its MEN inhibitory function. To this end, we characterized the functional domains of Kin4. The kinase activity of Kin4 is absolutely required for its ability to inhibit the MEN (Chan and Amon 2009). During spindle mis-position, Kin4 must phosphorylate the GAP complex and protect it from inhibitory phosphorylation by Cdc5 to maintain a cell cycle arrest (Maekawa et al. 2007). Previous findings have suggested that the inhibition of the MEN by the SPOC and thus Kin4 is quite potent. Cells that misposition their spindles were observed to delay mitotic exit for over three hours (Yeh et al. 1995). Additionally, overexpression of Kin4 arrests cells in anaphase and is suppressed by *bub2*Δ indicating that Kin4 is a potent inhibitor of the MEN (D'Aquino et al. 2005) (Figure 2B). We find that overexpression of the kinase domain alone is sufficient to mediate this lethality. We truncated Kin4 C-terminal to the kinase domain at amino acid position 341 (kin4(1-341)) and overexpressed it from the *GAL1-10* promoter

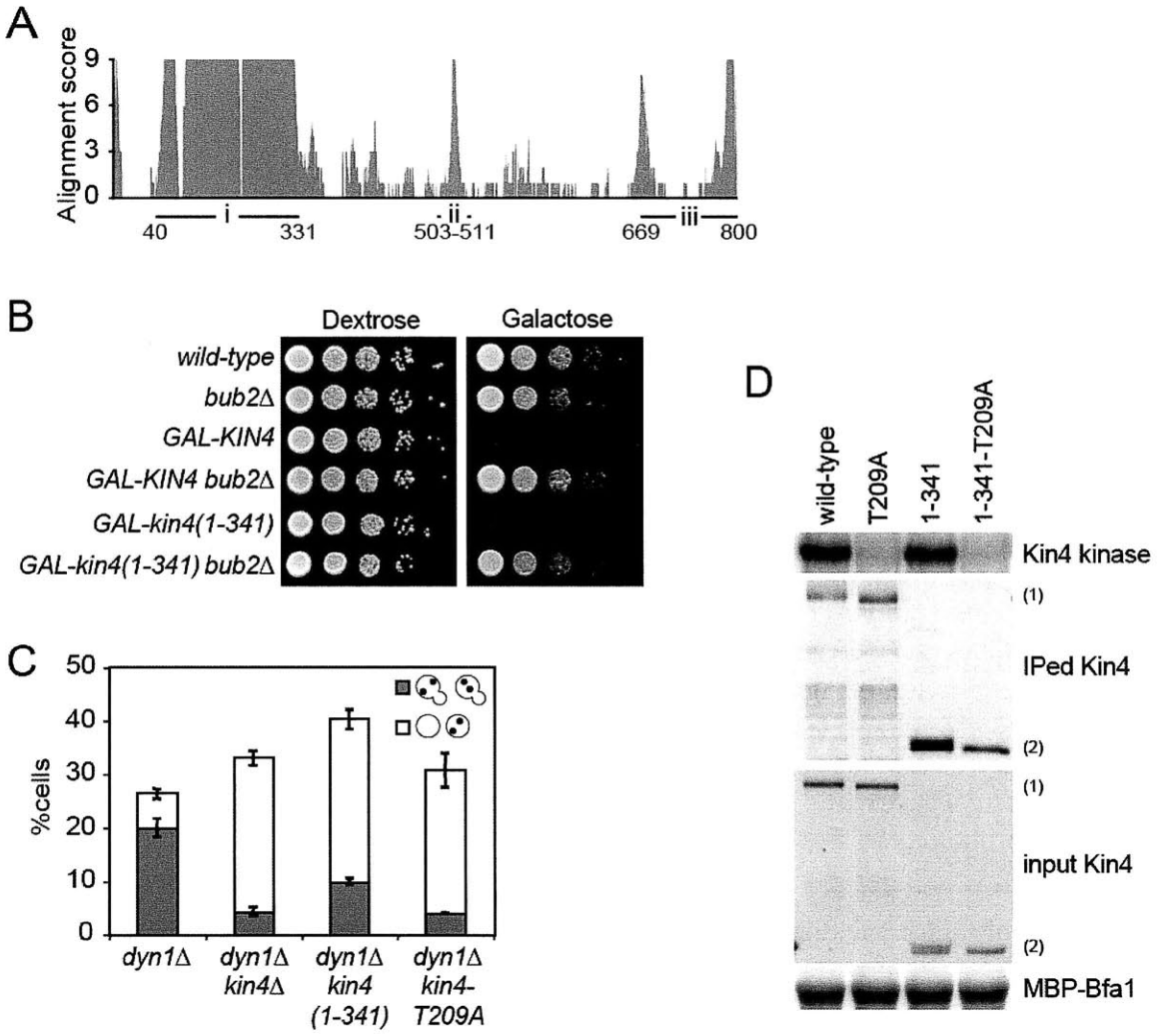

Figure 2. The N-terminal kinase domain of Kin4 mediates MEN inhibition

(A) The amino acid sequence of Kin4 and its orthologs were aligned using T-Coffee and the alignment score was plotted against the amino acid position. The three major regions of conservation are labeled i, ii and iii with the amino acid positions marked.

(B) Wild-type (A2587), *bub2Δ* (A1863), *pGAL1-10-GFP-KIN4* (A11997), *pGAL1-10-GFP-KIN4 bub2Δ* (A18792), *pGAL1-10-GFP-kin4(1-341)* (A23250) and *pGAL1-10-GFP- kin4(1-341) bub2Δ* (A24113) cells were spotted on plates containing either glucose or galactose and raffinose. The first spot represents growth of approximately $3x10^4$ cells and each subsequent spot is a 10 fold serial dilution.

(C) *dyn1Δ* (A17349), *dyn1Δ kin4Δ* (A17351), *dyn1Δ kin4(1-341)* (A22262) and *dyn1Δ kin4-T209A* (A22736) were grown at 14°C for 24 hours. Cells were stained for tubulin by indirect immuno-fluorescence and for the DNA with DAPI. $n \geq 100$ cells per sample. Gray bars represent the percentage of cells with

the arrested morphology and white bars represent the percentage of cells with the bypassed morphology. Error bars represent SEM.

(D) Cells expressing Kin4-3HA (A11779), kin4-T209A-3HA (kinase dead) (A22119), kin4(1-341)-3HA (A14052) or kin4(1-341)-T209A-3HA (A22278) were grown to exponential phase and arrested with 15 μg/mL nocodazole for 2 hours. Kin4 associated kinase activity (top, Kin4 kinase), immunoprecipitated Kin4-3HA (second row, IPed Kin4), total amount of Kin4-3HA in extracts (third row, input Kin4) and levels of Bfa1 substrate (as monitored by Coomassie stain) added to the kinase reaction (bottom, MBP-Bfa1) are shown. The band that is shown for Kin4 associated kinase activity and total Bfa1 substrate is the first major degradation product of MBP-Bfa1 as described in Maekawa et al., 2007 and was the dominant signal. (1) denotes full length and (2) denotes the kinase domain alone.

(Figure 2A, region i). We found that overexpression of kin4(1-341) is lethal. This lethality is due to an inability to exit mitosis as deletion of *BUB2* restored the viability of *GAL1-10-kin4(1-341)* cells (Figure 2B).

Despite retaining the ability to inhibit the MEN when overexpressed, we found that kin4(1-341) was unable support checkpoint function when expressed at endogenous levels. Cells lacking dynein (*dyn1*Δ) frequently mis-position their spindles (particularly at cold temperatures, 14°C) and delay exit from mitosis (Li et al. 1993). Thus *dyn1*Δ cultures accumulate cells with a mispositioned anaphase spindle bridging the two nuclei entirely in the mother cell body ("arrested" morphology). *KIN4* function is required for this delay in exit from mitosis as *kin4Δ* cells with mis-positioned spindles exit from mitosis prematurely and produce anucleate and multi-nucleated cells ("bypassed" morphology) (D'Aquino et al. 2005, Pereira and Schiebel 2005). *dyn1*Δ cultures grown at 14°C for 24 hours accumulated 20% of cells with the arrested morphology and 6.3% of cells with the bypassed morphology (Figure 2C). In *dyn1*Δ *kin4*Δ double mutant cultures, 4.3% of cells exhibited the arrested morphology and 28.7% of cells exhibited the bypassed morphology (Figure 2C). As previously reported, the kinase dead mutant of *KIN4*, *kin4-T209A*, also failed as a checkpoint component (Chan and Amon 2009) (Figure 2C). The *dyn1*Δ *kin4(1-341)* mutant behaved as the *dyn1*Δ *kin4*Δ or *dyn1*Δ *kin4-T209A* mutant (Figure 2C). This failure of kin4(1-341) to function in the SPOC could not be attributed to defects in kinase activity as levels of associated kinase activity were

similar between the full length and truncation constructs as judged by *in vitro* immuno-precipitation kinase assays (Figure 2D). We conclude that the kinase domain alone of Kin4 is a potent inhibitor of the MEN but that critical regions required for regulating its function must reside in Kin4 C-terminal to the kinase domain.

The C-terminus of Kin4 mediates cortical localization

To identify regions of Kin4 outside the kinase domain that might be important for Kin4 function, we aligned the sequence of Kin4 and its orthologs in other members of the Saccharomycetaceae family. This alignment revealed three major regions of high conservation. The highly conserved amino acids 43-313 encode the kinase domain (region i, Figure 2A). Residues 503-511 (region ii) and the C-terminus of the protein (region iii) also contained highly conserved regions (Figure 2A).

To examine the functions of the C-terminal region, we generated truncations of *KIN4* that lack the C-terminal 146 amino acids (*kin4(1-654)*) and that contain only the C-terminal 146 amino acids (*kin4(655-800)*) and found that they expressed well (Figure 3B). We fused kin4(1-654) to GFP and observed several localization defects. Kin4 normally localizes to the mother cell cortex throughout the cell cycle (D'Aquino et al. 2005, Pereira and Schiebel 2005) (Figure 3A). Interestingly, kin4(1-654) did not localize to the mother cell cortext but the bud cortex in small budded cells, but this localization did not persist in later stages of the cell cycle (Figure 3A). Full length Kin4 also localizes to the mother cell spindle pole body (mSPB) during anaphase but kin4(1-654) did not (Pereira and Schiebel 2005) (Figure 3A).

kin4(655-800) displayed a different set of localization defects. We observed that kin4(655-800) localized to both the mother and daughter cell cortices in all phases of the cell cycle but failed to load onto either SPB in anaphase (Figure 3A). We next identified a key residue in this C-terminal domain, F793, which is essential for its cortical localization. We mutated three strictly conserved residues in the highly conserved tail of Kin4 and found that when F793 was mutated to alanine, the C-terminal domain no longer localized to the cortex (Figures 3C, 3D and 3E). We introduced this mutation into the full

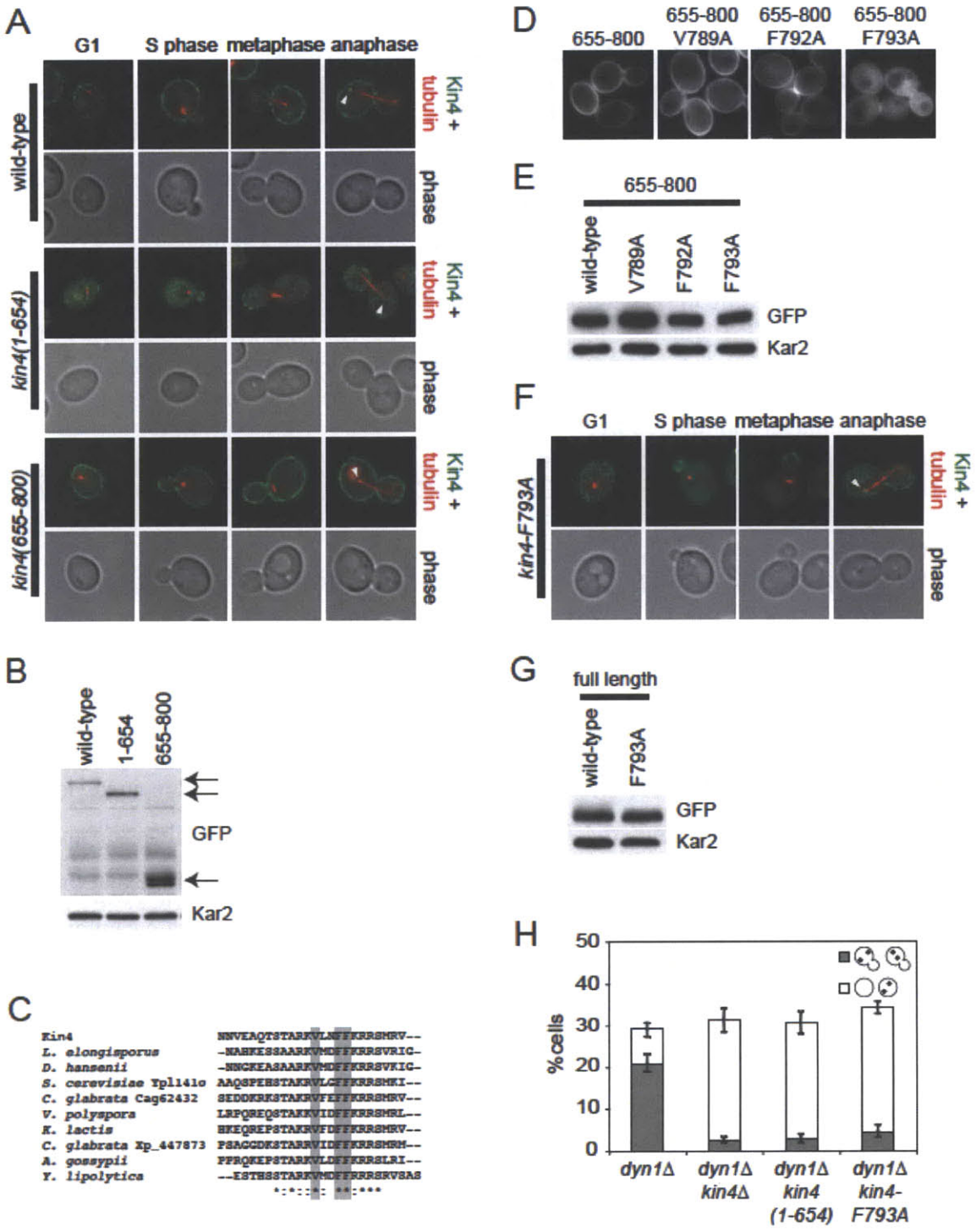

Figure 3. The C-terminus of Kin4 controls cortical localization.

(A) Cells expressing an mCherry-Tub1 fusion protein and Kin4-GFP (A19900) or kin4(1-654)-GFP (A21575) or kin4(655-800)-GFP (A21576) were grown to exponential phase and imaged live. The deconvolved GFP signal shown is from

8-10 serial sections. Kin4-GFP is shown in green, mCherry-Tub1 in red. Arrowheads indicate the position of the mother SPB.

(B) Cells in (A) were lysed and analyzed for expression of the GFP fusion protein by western blot. Arrows indicate the relevant bands. Kar2 was used as a loading control.

(C) The sequence of the last 24 amino acids of Kin4 and its orthologs were aligned using T-Coffee. The residues V789, F792 and F793 are highlighted. An asterisk denotes a strictly conserved residue and a colon denotes a similarly conserved residue.

(D) Cells expressing GFP-kin4(655-800) (A18463), GFP-Kin4(655-800)-V789A (A18452), GFP-kin4(655-800)-F792A (A18451) or GFP-kin4(655-800)-F793A (A18450) from the galactose inducible promoter were grown to exponential phase in YePA + 2% raffinose and induced with the addition of 2% galactose for 90 minutes and imaged live.

(E) Cells in (D) were analyzed as in (B).

(F) Cells expressing kin4-F793A-GFP and mCherry-Tub1 (A21556) were analyzed as in (A).

(G) Cells in (F) were analyzed as in (B).

(H) *dyn1*Δ (A17349), *dyn1*Δ *kin4*Δ (A17351), *dyn1*Δ *kin4(1-654)* (A22263) and *dyn1*Δ *kin4-F793A* (A21298) were analyzed as in Figure 2C.

length protein and found that kin4-F793A expressed as well as the wild-type and displayed a localization pattern similar to that of kin4(1-654) (Figures 3F and 3G). To test if cortical localization is important for SPOC function, we examined the checkpoint function of the *kin4(1-654)* and *kin4-F793A* alleles. We found that both alleles behaved as deletion of *KIN4* with respect to SPOC function (Figure 3H). We conclude that the C-terminus of Kin4 contains a cortical localization domain but that this domain cannot mediate mother cell restricted cortical localization or SPB localization. Furthermore, this domain is required for Kin4's checkpoint function.

Amino acids 503-511 are necessary for asymmetric cortical association of Kin4

To determine the function of the conserved nine amino acids at position 503-511 (region ii, Figure 2A), we examined the consequences of deleting this region on Kin4 localization. We found that like wild-type, kin4(Δ503-511) associated with the cortex in G1 cells. However, in small budded cells, the protein was transiently enriched at the bud cortex and was evenly distributed between the mother and bud cortices during the remainder of the cell cycle (Figure 4A). Association of Kin4 with the mSPB was not affected by this internal deletion (Figure 4A). An alanine scan of this region identified a

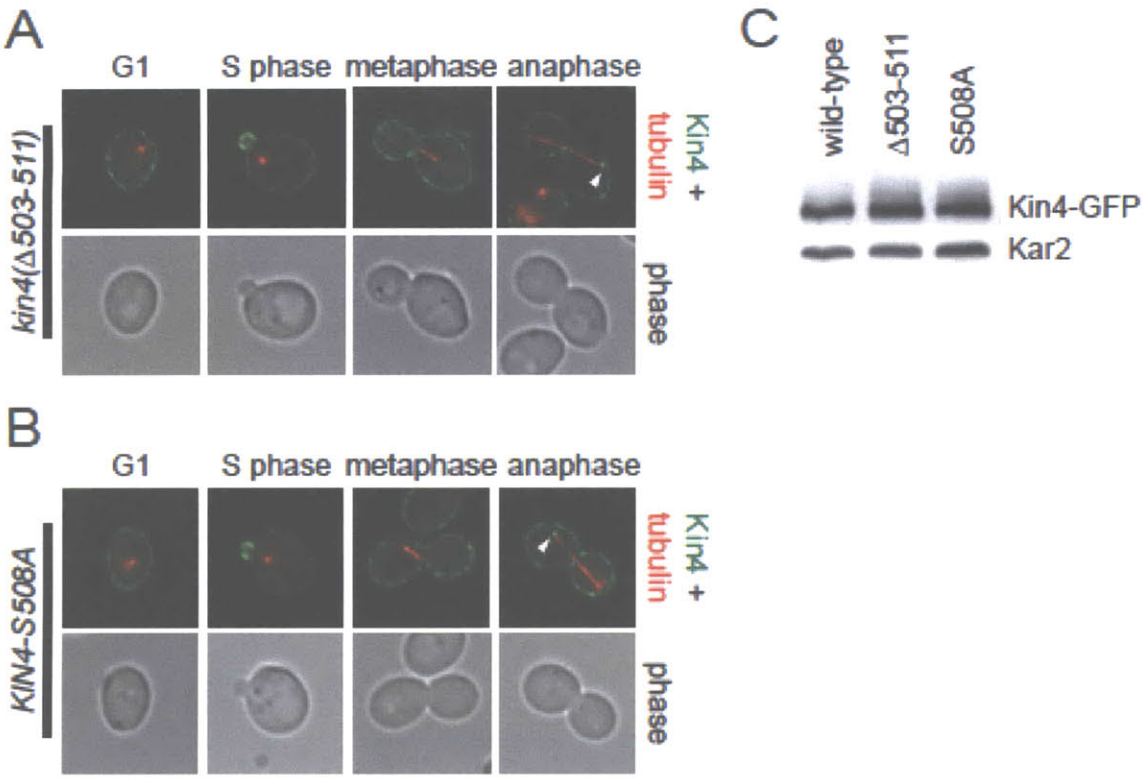

Figure 4. Serine 508 is required for restricting Kin4 to the mother cell cortex.

(A-B) Cells expressing mCherry-Tub1 and (A) kin4(Δ503-511)-GFP (A21555) or (B) Kin4-S508A (A21557) were analyzed as in Figure 3A.
(C) Cells expressing mCherry-Tub1 and Kin4-GFP (A19900), kin4(Δ503-511)-GFP (A21555) or Kin4-S508A-GFP (A21557) were analyzed as in Figure 3B.

single amino acid substitution that resulted in the same symmetric cortical localization at serine 508 (Figure 4B). This symmetric cortical localization cannot be attributed to increases in protein abundance as kin4(Δ503-511) and Kin4-S508A expressed similarly to wild-type (Figure 4C). We conclude that amino acids 503-511 and specifically S508 are necessary for asymmetric cortical localization of Kin4.

Symmetric Kin4 Delays Mitotic Exit in the absence of *LTE1*

If a Tem1 bearing SPB must escape the zone of Kin4 influence to activate the MEN, then a symmetrically localized Kin4 should delay or prevent exit from mitosis. To test this prediction of the zone model, we released wild-type and *KIN4-S508A* mutant cells from a pheromone-induced G1 arrest and monitored anaphase entry and exit by spindle

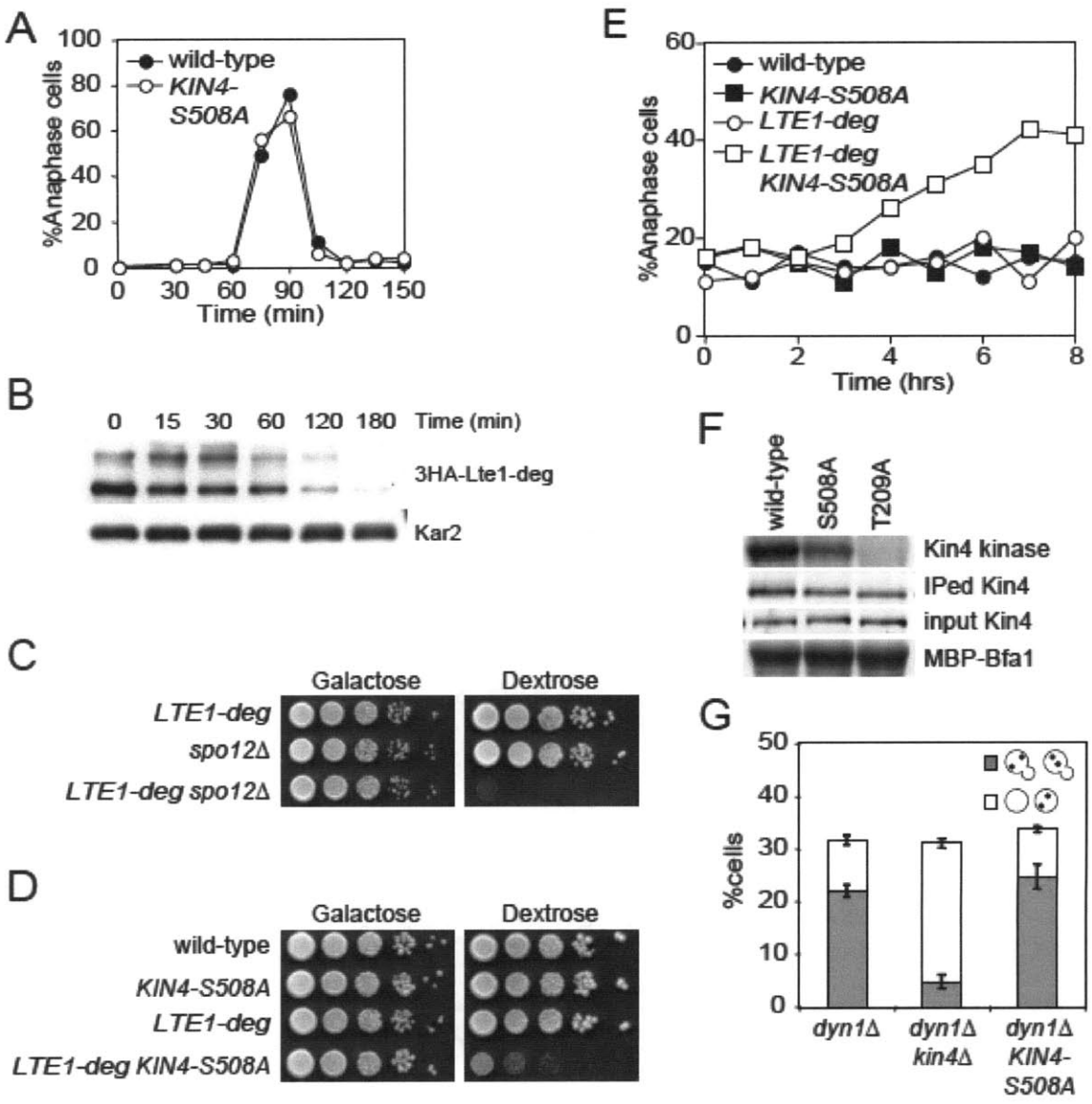

Figure 5. Kin4 localization in the bud delays mitotic exit in *lte1Δ* cells.

(A) Wild-type (A2587) and *KIN4-S508A* (A21299) cells were analyzed as in Figure 1B.

(B) Cells expressing a URL-3HA-Lte1 fusion protein (A23686) from the galactose inducible promoter were grown in YePA + 2% raffinose + 2% galactose to exponential phase. 2% glucose was added to the media at time = 0 to repress the *GAL* promoter and samples were collected for western blot analysis. Kar2 was used as a loading control.

(C) *pGAL1-10-URL-3HA-LTE1* (*LTE1-deg)* (A23686), *spo12*Δ (A4874) and *LTE1-deg spo12*Δ (A24543) cells were spotted on plates containing either glucose or galactose and raffinose. The first spot represents growth of approximately $3x10^4$ cells and each subsequent spot is a 10 fold serial dilution.

(D) Wild-type (A2587), *KIN4-S508A* (A21299), *LTE1-deg* (A23686) and *KIN4-S508A LTE1-deg* (A24084) cells were analyzed as in (C).
(E) Cells in (D) were grown to exponential phase in YePA + 2% raffinose + 2% galactose at room temperature. At t = 0, 2% glucose was added to the culture media to repress the *GAL1-10* promoter and samples were collected and analyzed for spindle and nuclear morphology.
(F) Cells expressing either Kin4-3HA (A11779), Kin4-S508A-3HA (A20608) or kin4-T209A-3HA (A22119) were analyzed as in Figure 2D.
(G) *dyn1*Δ (A17349), *dyn1*Δ *kin4*Δ (A17351), and *dyn1*Δ *KIN4-S508A* (A21301) were analyzed as in Figure 2C.

morphology. Inconsistent with the prediction, cells expressing *KIN4-S508A* as the sole source of *KIN4* progressed through the cell cycle with wild-type kinetics (Figure 5A).

Previous experiments localizing Lte1 to the mother cell showed that this mis-localization is sufficient to bypass the SPOC and prematurely activate the MEN. These experiments not only demonstrated the importance of restricting Lte1 to the bud, but also imply that when Lte1 and Kin4 are in the same cellular compartment, the mitotic exit promoting activity of Lte1 dominates over the mitotic exit inhibitory effects of Kin4. In light of this observation, symmetric Kin4 should not inhibit mitotic exit since Lte1 is still present in the bud. However, if the zone model is correct, symmetrically localized Kin4 should inhibit mitotic exit in cells lacking *LTE1*. To test this hypothesis, we first constructed a conditional allele of *LTE1* by fusing the degradation tag, ubiquitin-arginine-lacZ, to the coding sequence of *LTE1* and placed the fusion under the control of the *GAL1-10* promoter (*LTE1-deg*). This fusion protein was efficiently depleted after three hours in glucose at room temperature (Figure 5B). Consistent with efficient depletion, we find that depletion of Lte1 led to loss of viability in cells lacking the FEAR network component *SPO12* (Figure 5C).

Under conditions of Lte1 depletion (glucose), *KIN4-S508A* and *LTE1-deg* single mutants grew similarly to wild-type cells, but proliferation was severely hampered in the double mutant (Figure 5D). To determine if this proliferation defect was due to a defect in exit from mitosis, we monitored accumulation of anaphase cells in single and double mutants. In glucose, both *KIN4-S508A* and *LTE1-deg* cultures behaved as the wild-type and

accumulated 10-20% anaphase cells at any given time (Figure 5E). In contrast, *LTE1-deg KIN4-S508A* double mutant cultures accumulated cells with anaphase spindles over time, with 40% of cells arresting in anaphase after eight hours in glucose (Figure 5E). The mitotic exit inhibitory effect of the *KIN4-S508A* allele cannot be attributed to increased protein abundance or kinase activity. Kin4 protein levels and kinase activity were similar in *KIN4-S508A* and wild-type cells (Figures 4C and 5F). Our results show that symmetric Kin4 inhibits mitotic exit in the absence of *LTE1*. Furthermore, these data indicate that Lte1's MEN promoting function dominates over Kin4's MEN inhibitory function. With respect to sensing spindle position, our data show that the daughter bound SPB must escape the zone of Kin4 influence in order for the MEN to signal.

The zone model also predicts that a symmetrically localized Kin4 should have no effect on SPOC function. Since the SPBs of a mispositioned spindle never escape the mother cell, symmetric localization of Kin4 is inconsequential. Indeed, we found that *KIN4-S508A* retained full checkpoint function (Figure 5G). The findings that symmetric Kin4 inhibits mitotic exit in the absence of Lte1 and retains full checkpoint function support the zone model.

Kar9 and Clb4 prevent Kin4 from loading onto the daughter SPB

Kin4 association with SPBs is critical for its MEN inhibitory function (Maekawa et al. 2007). Analysis of Kin4-S508A localization revealed that despite the protein associating with the bud cortex, Kin4-S508A loaded onto the daughter cell SPB (dSPB) in only 3.8% of anaphase cells (Figures 4B and 6A). In contrast Kin4-S508A associated with the mSPB in 51% of anaphase cells (Figure 6A). This finding indicates that additional layers of regulation must exist to exclude Kin4 from the dSPB. The microtubule motor dynein (Dyn1), the cytoskeletal adapter protein Kar9 and the B-type cyclin Clb4 have all previously been implicated in regulating the asymmetric distribution of proteins between mother and daughter SPBs

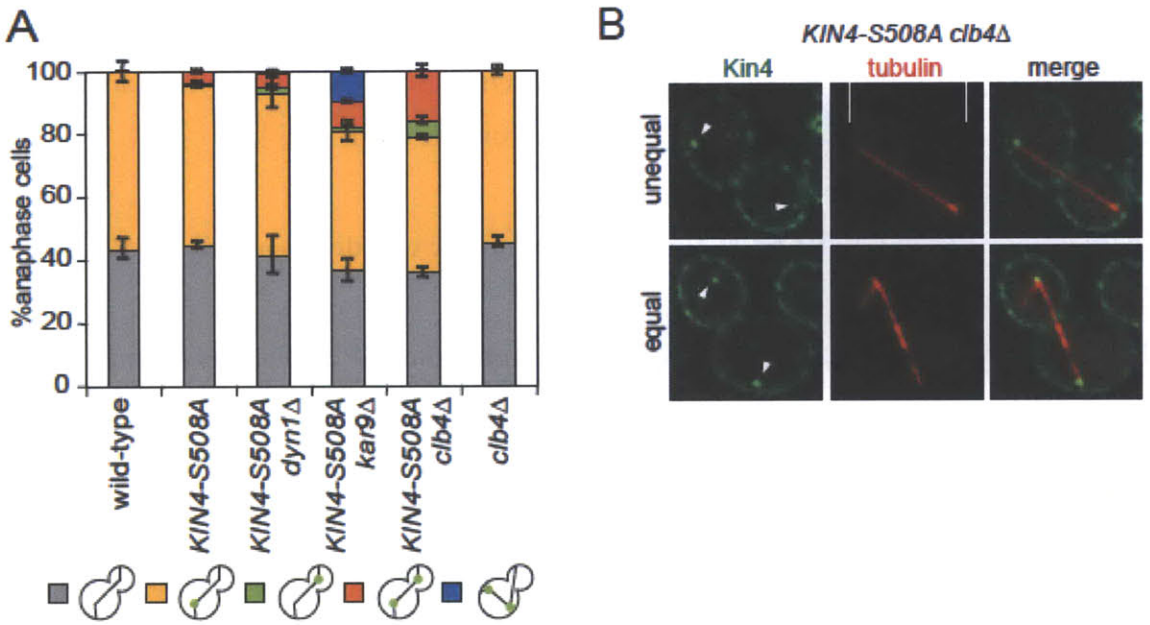

Figure 6. Kar9 and Clb4 prevent symmetric Kin4 from loading to the daughter SPB

(A) Cells expressing GFP tagged Kin4 and mCherry-Tub1 with the following genetic backgrounds: wild-type (A19900), *KIN4-S508A* (A21557), *KIN4-S508A dyn1*Δ (A23052), *KIN4-S508A kar9*Δ (A23051), *KIN4-S508A clb4*Δ (A23055) and *clb4*Δ (A23249) were analyzed over a single cell cycle as described in Figure 1B. Samples were taken at 60, 75, 90 and 105 minutes post release and imaged live. Serial sections spanning the entire cell were collected to ensure imaging of all spindle poles. Loading of Kin4 to the SPBs was judged by co-localization of Kin4-GFP with the ends of the anaphase spindle. $n \geq 100$ cells and error bars represent SEM.

(B) Representative *KIN4-S508A clb4*Δ cells with symmetric Kin4 localization to the SPBs. The top cell shows an unequal SPB loading pattern whereas the bottom cells shows equal Kin4-GFP intensity at both SPBs. The deconvolved GFP signal shown is from 10 serial sections.

(Lee, Oberle and Cooper 2003, Liakopoulos et al. 2003, Maekawa and Schiebel 2004, Maekawa et al. 2003). We therefore tested whether deletion of any of these factors affected the association of Kin4-S508A with SPBs. We found no increase in the number of cells with Kin4-S508A at both SPBs in the *dyn1*Δ mutant (4.5%), a modest increase in the *kar9*Δ mutant (8%) and the largest increase in the *clb4*Δ mutant cells (16%; Figure 6A). In cells with Kin4-S508A localizing to both SPBs we often observed the GFP signal to be stronger on the mSPB suggesting that Kar9 and Clb4 are not the only factors that mediate Kin4 exclusion from SPBs (Figure 6B). Wild-type Kin4 did not load onto dSPBs

in *clb4*Δ mutants suggesting that Kin4 first needs to be targeted to the daughter cell to load onto the dSPB (Figure 6A). We conclude that the dSPB specific factors, Kar9 and Clb4 contribute to the exclusion of Kin4-S508A from the dSPB.

Increased dSPB loading of Kin4 enhances the mitotic exit defect of *KIN4-S508A LTE1-deg* cells

To test whether increased loading of Kin4-S508A onto the dSPB enhances the mitotic exit defect of cells lacking Lte1 and containing symmetric Kin4, we examined the consequences of deleting *KAR9* or *CLB4* on *KIN4-S508A LTE1-deg* cells. Deletion of *KAR9* mildly enhanced the proliferation defect of *KIN4-S508A LTE1-deg* mutants (Figure 7A). Deletion of *CLB4* enhanced the proliferation defect of *KIN4-S508A LTE1-deg* cells by 10 fold (Figure 7A, compare rows 2 and 4). Neither *KIN4-S508A clb4*Δ nor *LTE1-deg clb4*Δ double mutants displayed any proliferative defects consistent with the notions that Lte1 dominates over Kin4's inhibition of the MEN and that Kin4 must load onto both SPBs to inhibit mitotic exit (Figure 7A, rows 6 and 7). Deletion of *BUB2* fully suppressed the proliferative defect of *KIN4-S508A LTE1-deg clb4*Δ mutants indicating that the proliferation defect is due to MEN inhibition (Figure 7A, row 5). Cytological examination of cells confirmed this. We observed a severe anaphase delay in the *KIN4-S508A LTE1-deg clb4*Δ mutant that was completely suppressed by deletion of *BUB2* (Figure 7B).

A fusion construct between Kin4 and a fragment of the SPB resident protein, Spc72 (kin4-Spc72(177-622), henceforth kin4-SPB) was previously constructed and cells expressing this fusion protein displayed a very subtle delay in mitotic exit but failed to inhibit the MEN in response to spindle position defects (Chan and Amon 2009, Maekawa et al. 2007). Consistent with the subtle cell cycle delay, we observed no detectable loss in proliferative capacity in the *kin4-SPB* mutant (Figure 7C, row 2). When combined with the *LTE1-deg* allele, *kin4-SPB* led to a subtle proliferation defect that was not nearly as severe as that observed in *KIN4-S508A LTE1-deg* or *KIN4-S508A LTE1-deg clb4*Δ cells (Figure 7C, row 4). This finding suggests that while *kin4-SPB* is hyper-morphic for SPB loading, it is also hypo-morphic for MEN inhibition once at the SPB.

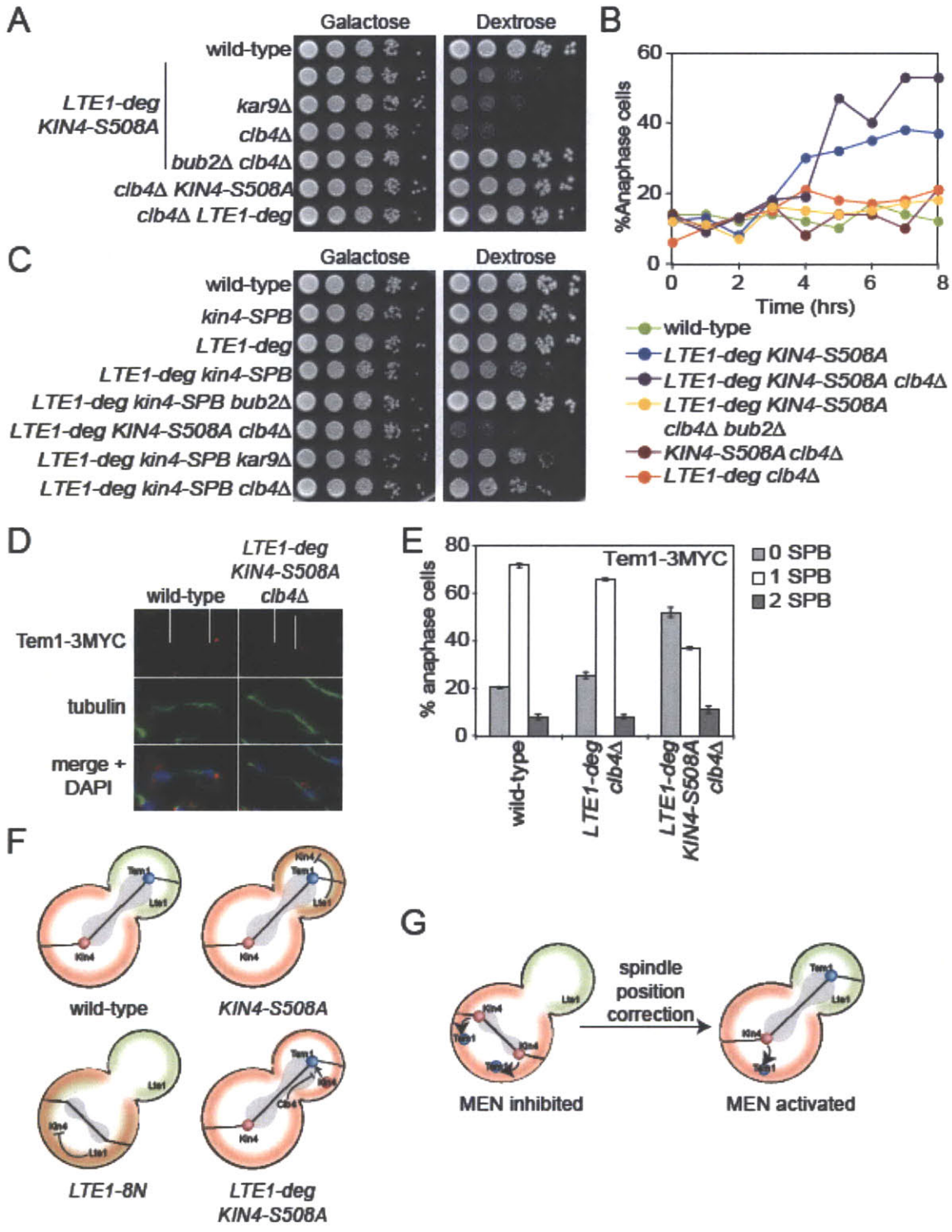

Figure 7. Loading of Kin4 onto both SPBs arrests cells in anaphase

(A) Wild-type (A2587), *LTE1-deg KIN4-S508A* (A24084), *LTE1-deg KIN4-S508A kar9Δ* (A24816), *LTE1-deg KIN4-S508A clb4Δ* (A24086), *LTE1-deg KIN4-*

S508A clb4Δ bub2Δ (A24346), *KIN4-S508A clb4Δ* (A24083) and *LTE1-deg clb4Δ* (A24085) cells were analyzed as in Figure 5C.

(B) Wild-type (A2587), *LTE1-deg KIN4-S508A* (A24084), *LTE1-deg KIN4-S508A clb4Δ* (A24086), *LTE1-deg KIN4-S508A clb4Δ bub2Δ* (A24346), *KIN4-S508A clb4Δ* (A24083) and *LTE1-deg clb4Δ* (A24085) cells were analyzed as in Figure 5E.

(C) Wild-type (A2587), *kin4-SPC72(177-622)* (*kin4-SPB*) (A24586), *LTE1-deg* (A23686), *LTE1-deg kin4-SPB* (A24587), *LTE1-deg kin4-SPB bub2Δ* (A24588), *LTE1-deg KIN4-S508A clb4Δ* (A24086), *LTE1-deg kin4-SPB kar9Δ* (A24817) and *LTE1-deg kin4-SPB clb4Δ* (A24858) cells were analyzed as in Figure 5C.

(D-E) Wild-type (A1828), *LTE1-deg clb4Δ* (A24805) and *LTE1-deg KIN4-S508A clb4Δ* (A24761) cells expressing a Tem1-3MYC fusion protein were grown as in Figure 5E. Cells were collected seven hours post glucose addition and stained for tubulin (green) and Tem1-3MYC (red) by indirect immuno-fluorescence and the DNA (blue) was stained with DAPI. Tem1 loading was judged by colocalization of Tem1-3MYC with the ends of the anaphase spindle. $n \geq 100$ cells and error bars represent SEM.

(F) Layers of Kin4 control. See text for further details.

(G) The zone model of SPOC function. See text for further details.

This loss-of-function is likely due to the effects of the protein fusion (Figure 7C, row 4). Importantly, the *kar9Δ* and *clb4Δ* mutations did not enhance the growth defect of *LTE1-deg kin4-SPB* mutants indicating that the phenotypic enhancement these mutations lend to the *KIN4-S508A LTE1-deg* mutant is caused by enhanced loading of Kin4-S508A to dSPBs (Figure 7C, rows 7 and 8).

To further characterize the effects of loading Kin4 onto both SPBs on MEN function, we examined the localization of Tem1. Tem1 localizes to the dSPB in anaphase. Its loss from this organelle correlates well with Kin4 inhibition of the MEN. In cells with a mis-positioned spindle, Tem1 fails to load onto either SPB. Without *KIN4*, such cells inappropriately load Tem1 onto both SPBs, presumably triggering premature mitotic exit (D'Aquino et al. 2005). Cells that over-express *KIN4* and arrest in anaphase also fail to load Tem1 onto either SPB (D'Aquino et al. 2005). Accordingly, Tem1 association with dSPBs was reduced in *KIN4-S508A LTE1-deg clb4Δ* mutants during anaphase (Figures 7D and 7E). We conclude that even in the absence of spindle mis-position, Kin4 targeted to both cell cortices and SPBs inhibits mitotic exit in the absence of *LTE1*.

Discussion

Multiple control mechanisms ensure that Kin4 inhibits the MEN only in the mother cell

The N-terminal kinase domain of Kin4 mediates MEN inhibition. Overexpression of this region of the protein alone is sufficient to inhibit the MEN and hence exit from mitosis. This potent MEN inhibitory activity requires multiple control mechanisms to ensure that inhibition only occurs when the mitotic spindle is mis-positioned and the MEN bearing SPBs are in the mother cell. These regulatory mechanisms are:

(i) Lte1 dominates over Kin4. When both proteins are present in the same cellular compartment, Lte1's MEN promoting effects trump the MEN inhibitory effects of Kin4. The Lte1-8N allele, which localizes to both the mother cell and bud cortices, promotes exit from mitosis in the mother cell even in the presence of Kin4 (Geymonat et al. 2009). Conversely, the *KIN4-S508A* mutant only inhibits mitotic exit in the absence of *LTE1* (Figure 7F).

(ii) Kin4 is restricted to the mother cell cortex by unknown mechanisms.

(iii) Kin4 is excluded from the daughter cell SPB. The dSPB specific factors Clb4 and Kar9 inhibit binding of Kin4-S508A to the dSPB suggesting that SPB asymmetry contributes an additional layer to Kin4 regulation (Figure 7F).

While such multiple overlapping mechanisms make their dissection difficult, they highlight the biological importance of restricting Kin4 function.

If Kin4 function is largely governed by localization, how is Kin4 localization controlled? The C-terminal 146 amino acids of Kin4 harbor sequences sufficient for association with the cell cortex. We do not yet know how this region mediates cortex association. It is, however, interesting to note that this cortical localization mechanism is operative in mammalian cells. Kin4 and kin4(655-800) localizes to the cell cortex in 293T cells while the point mutant, kin4(655-800)-F793A failed to do so suggesting that the localization mechanisms are the same in yeast and mammalian cells (Figures 8A and 8B). Identifying the binding partners of Kin4's C-terminal domain will be important for understanding how Kin4 is localized at the cortex and potentially why this is important for maintenance of asymmetry and loading of Kin4 onto the SPB.

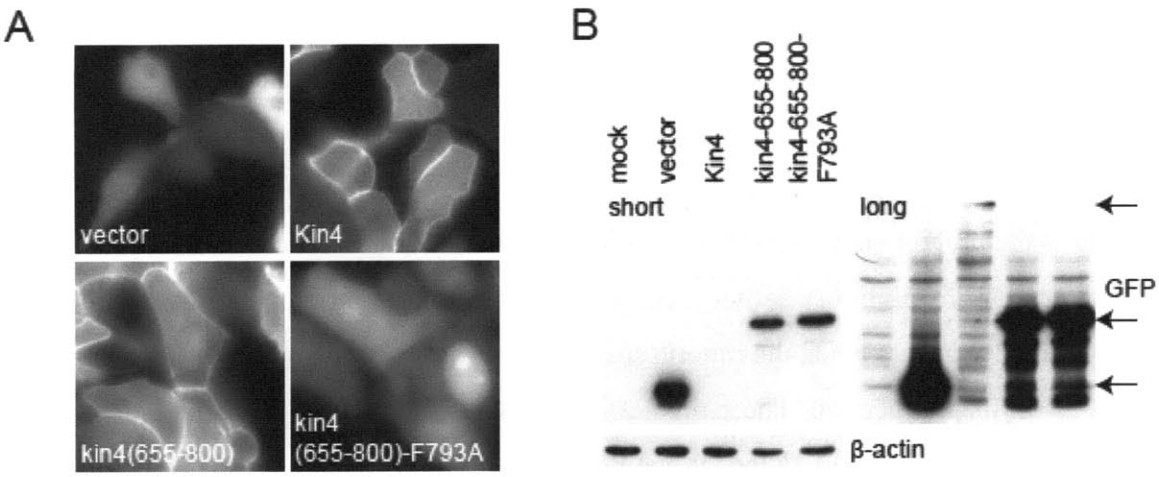

Figure 8. Expression of Kin4 constructs in mammalian cells

(A) 293T cells were transiently transfected with plasmids expressing eGFP (pAM50), eGFP-Kin4 (pAM51), eGFP-kin4(655-800) (pAM52) or eGFP-kin4(655-800)-F793A (pAM53) and imaged live. The exposure times are approximately 5ms for eGFP, 100ms for eGFP-Kin4 and 20ms for eGFP-kin4(655-800) and eGFP-kin4(655-800)-F793A.

(B) Cells in (A) were lysed and analyzed for expression of the GFP fusion protein by western blot. A short and long exposure are shown due to the lower expression of eGFP-Kin4. Arrows indicate the relevant bands. Levels of β-actin were used as a loading control.

How is asymmetry at the cortex established? Full length Kin4 very transiently localizes to the bud tip during nascent bud formation but subsequently associates with the mother cell cortex (Figure 9A). This suggests that Kin4 is initially targeted to the nascent bud cortex possibly before the machinery that generates asymmetry can exclude additional bud localization. The N-terminal domain of Kin4 appears to contain a bud-cortex targeting domain. kin4(1-341) was found to be associated with the bud cortex throughout the cell cycle (Figure 9B). Perhaps kin4(1-341) harbors the signals necessary for initial bud cortex association but lacks the sequences necessary to re-direct Kin4 to the mother cortex and/or clear the protein from the bud cortex. Residues 503-511 appear to contain such sequences. In their absence, Kin4 is present throughout the mother and bud cortices. Determining the cellular machinery that recognizes this region will be critical to understanding how the MEN inhibitory zone is established and maintained in the mother cell. It is important to note that while many proteins localize exclusively to the bud, only

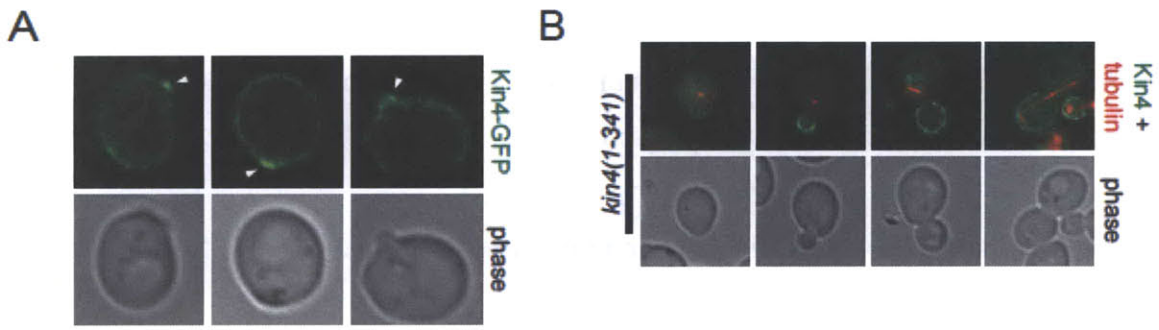

Figure 9. Localization of Kin4 in nascent budded cells

(A) Cells expressing Kin4-GFP (A19900) were grown to exponential phase and imaged live. The deconvolved GFP signal shown is from 8 serial sections. Arrows indicate the position of the nascent bud.

(B) Cells expressing an mCherry-Tub1 fusion protein and kin4(1-341)-GFP (A23410) were grown to exponential phase and imaged live. The deconvolved GFP signal shown is from 8-10 serial sections. Kin4-GFP is in green and mCherry-Tub1 is in red.

a few proteins show mother cortex selectivity. Such proteins must either defy vectorial transport that directs most newly synthesized proteins to the bud and/or be redirected back to the mother cell by unknown mechanisms (perhaps by selective proteolysis) to yield this unusual localization pattern.

The machinery that restricts Kin4 to the mother cell is not completely efficient. Low levels of Kin4 can be detected in the daughter cell, particularly in anaphase (L. Chan unpublished observations). However, additional mechanisms are in place that prevent leaky Kin4 from inappropriately inhibiting the MEN at SPBs. The dSPB-associated proteins Clb4 and to a lesser extent Kar9 exclude Kin4 from the SPB in the bud. Due to Kar9's critical role in loading Clb4 onto the dSPB, we favor a model where Clb4 rather than Kar9 regulates Kin4's association with dSPBs (Maekawa and Schiebel 2004). Clb4 could modify SPB components or Kin4 itself to prevent Kin4 from binding to the daughter cell SPB. Alternatively, Clb4's role could be indirect. The interactions between cytoplasmic microtubules and the bud cortex are increased in *clb4*Δ mutants (Maekawa and Schiebel 2004). If symmetric Kin4 loads from the bud cortex to the dSPB via cytoplasmic microtubules, it is possible that increased cortex-microtubule interactions could lead to an increase in Kin4-S508A loading to the dSPB. Much needs to be

discovered about the factors responsible for Kin4's unusual localization pattern, but our domain analysis of Kin4 already demonstrates that their function will be critical for coordinating cell cycle progression and spindle position.

A bud-localized MEN activating zone and a mother cell-localized MEN inhibitory zone drive spindle position sensing

Our results and those of others demonstrate that SPOC function is at least in part based on the spatial restriction of the MEN regulators Kin4 and Lte1. In this "zone model", for the MEN to become active and to promote exit from mitosis, one of the MEN bearing SPBs must escape the zone of inhibition or the mother cell where Kin4 resides and enter the zone of activation or the daughter cell where Lte1 resides (Figure 7G). Perturbation of either zone leads to mis-regulation of the MEN. When Lte1 is localized in the mother cell, either by overexpression, crippling of the septin ring diffusion barrier or mutations within Lte1, cells with mis-positioned spindles prematurely exit from mitosis (Bardin et al. 2000, Castillon et al. 2003, Geymonat et al. 2009). Conversely, symmetric targeting of Kin4 inhibits exit from mitosis. The observation that Kin4 could only do so in the absence of Lte1 not only indicates that Lte1's MEN promoting activity dominates over Kin4's inhibitory effects, it also raises the interesting possibility that in addition to its role in promoting timely mitotic exit, Lte1 restrains any spurious effects of Kin4 that leaks into the bud.

Our analysis of the *KIN4-S508A* allele has important implications for how we think about the SPOC. The *KIN4-S508A* allele does not appear to affect Kin4 protein levels or associated kinase activity. Only protein localization is affected in that the protein is present at both the mother cell and bud cortices. The observation that in the absence of *LTE1*, this allele inhibits exit from mitosis even in cells with correctly positioned anaphase spindles, demonstrates that a spindle mis-position event is not a prerequisite for Kin4's ability to inhibit the MEN (Figure 7F). Thus, Kin4 is not a sensor of spindle position. Rather it is the MEN bearing SPBs and ultimately the GTPase switch, Tem1, that moves and senses its position in space relative to its regulators, Lte1 and Kin4, that allows the MEN to monitor spindle position. The idea that MEN is activated by

movement of a SPB out of the Kin4 inhibitory zone and into the bud is supported by several other observations. Tem1 becomes concentrated on the dSPB upon anaphase spindle elongation and is further enhanced by Lte1 (Bardin et al. 2000, Molk et al. 2004, Pereira et al. 2000). Also, the MEN inhibitor, Bub2, is lost from the dSPB after it emerges into the bud (Molk et al. 2004). Perhaps by employing multiple SPOC mechanisms, the cell achieves more robust coupling of spindle position to mitotic exit than employing any single mechanism alone.

Several other models have been proposed for how the MEN is activated and how the SPOC functions to shut down the MEN in response to spindle position defects. A model where disappearance of the Bub2-Bfa1 GAP complex from the mSPB triggers mitotic exit is inconsistent with the demonstration that Kin4 association with SPBs inhibits MEN signaling (Chan and Amon 2009, Fraschini et al. 2006, Maekawa et al. 2007, Pereira and Schiebel 2005). An alternate model proposes that the presence of cytoplasmic microtubules in the bud neck contribute to SPOC function (Adames et al. 2001, Moore et al. 2009). While it is possible that cytoplasmic microtubule-bud neck interactions contribute to triggering and/or maintenance of the SPOC, it is important to note that loss of cytoplasmic microtubules as is observed in *bim1*Δ, *cnm67*Δ and *tub2-401* mutants abolishes checkpoint function in only about 20% of cells that misposition their spindles (Adames et al. 2001). This indicates that the presence of cytoplasmic microtubules in the bud neck is not the major mechanism whereby spindle position defects affect MEN signaling. In contrast, misdirecting Lte1 or Kin4 to the wrong compartment leads to an almost complete bypass of the SPOC and anaphase arrest, respectively.

We do not yet know how Kin4 and Lte1 ultimately control the MEN GTPase Tem1. Kin4 phosphorylates Bfa1 thereby preventing inactivation of the GAP complex by Cdc5 (Maekawa et al. 2007). While this explains how Tem1 activity is controlled it does not explain how Tem1's association with SPBs is regulated. How Lte1 activates Tem1 is also unclear. Lte1 contains putative guanine nucleotide exchange factor (GEF) domains and it has been proposed that Lte1 may activate MEN signaling by acting as a GEF for Tem1 (Bardin et al. 2000, Pereira et al. 2000). A recent study has cast doubt on this hypothesis.

No *in vitro* GEF activity could be detected for Lte1 against Tem1 (Geymonat et al. 2009). Elucidating mechanistically how Tem1 receives signals from Kin4 and Lte1 and the role of the GAP complex in this process are important next steps in understanding MEN activation and SPOC function.

Kin4 and Lte1 are not the sole regulators of the MEN

Our data indicate that Kin4 functions during every cell cycle to restrain MEN activity. Deletion of *KIN4* abolished the mitotic exit delay associated with deleting *LTE1* and suppresses the synthetic lethality of *lte1Δ* FEAR network double mutants (D'Aquino et al. 2005). *LTE1* is also required during every cell cycle for timely mitotic exit and is essential for the transition at low temperatures (Adames et al. 2001, Bardin et al. 2000, Jensen et al. 2004, Shirayama et al. 1994a). However, it is also clear that other mechanisms must exist to restrict MEN signaling to anaphase. In the absence of *LTE1* and *KIN4*, SPOC regulation of the MEN is lost but mitotic exit proceeds with proper timing in cells with correctly positioned spindles. Thus, additional mechanisms must exist that only allow the MEN to be active during anaphase. Identifying these will be critical for understanding how MEN activation is integrated with other cell cycle events.

Sensing activating and inhibitory zones – a general theme in checkpoint signaling?

The tension sensing aspect of the spindle assembly checkpoint (SAC) shares striking similarities with the SPOC model proposed here (Liu et al. 2009, Tanaka et al. 2002). The SAC senses whether kinetochores are attached to microtubules and whether these attachments are under tension and thus properly bi-oriented. When this is not the case, the SAC arrests cells in metaphase (Lew and Burke 2003). The conserved protein kinase, Aurora B, severs microtubule-kinetochore attachments that are not under tension by phosphorylating the major microtubule binding activity at kinetochores, the KMN network (Cheeseman et al. 2006, DeLuca et al. 2006). The resulting unattached kinetochores are recognized by the SAC, which shuts down cell cycle progression in metaphase. Aurora B resides at the inner centromere (Liu et al. 2009, Tanaka et al. 2002). When sister kinetochores are not attached by microtubules to opposite poles of the spindle and hence not under tension, the KMN network proteins reside in the Aurora B

zone where they are phosphorylated and lose their ability to bind microtubules. When sister kinetochores are properly bi-oriented and thus under tension, they are pulled away from the inner centromere and Aurora B can no longer access its kinetochore substrates (Liu et al. 2009, Tanaka et al. 2002). Thus, kinetochore-microtubule attachments are stabilized and proper bi-orientation is achieved. By analogy to the zone model for spindle position sensing proposed here, Aurora B is not activated by tensionless kinetochores, rather, Aurora B is always active but restricted to a zone where tensionless kinetochores (by virtue of not being under tension) reside. Here too, a cell cycle checkpoint relies on the establishment of a regulatory zone to translate spatial information into a chemical signal.

Experimental Procedures

Yeast Strains and Growth Conditions

All strains are derivatives of W303 (A2587) and are listed in Table 1. *KIN4-3'UTR:KanMx6, lte1Δ::NatMx4, bub2Δ::KanMx6, kin4(1-341), kin4(1-341)-GFP, kin4(1-341)-3HA, GAL-GFP-kin4(1-341), kin4(1-341)-T209A-3HA, kin4(1-654), kin4(1-654)-GFP, kin4-F793A-GFP, kin4(Δ503-511)-GFP, KIN4-S508A-GFP, KIN4-S508A-3HA, GAL-URL-3HA-LTE1, kin4-SPC72(177-622)* and *clb4Δ::NatMx4* were constructed by standard PCR based methods (Goldstein and McCusker 1999, Longtine et al. 1998). *kin4(Δ503-511), kin4-F793A* and *KIN4-S508A* were constructed by two-step gene replacement using the *URA3* gene from *Kluyveromyces lactis* and PCR products derived from plasmids pA1607, pA1608 and pA1609 respectively. pA1419, pA1425, pA1426 and pA1427 were digested with EcoRV and integrated at the *TRP1* locus to generate *pGAL1-10-GFP-kin4(655-800)-[V789A, F792A, F793A]* alleles. pA1624 was integrated as above to generate the *kin4(655-800)-GFP* allele. Growth conditions are described in the figure legends.

Plasmid Construction

All plasmids used in this study are listed in Table 2. pA1419 was constructed by digesting YIplac204 and a PCR product containing *pGAL1-10-GFP-kin4(655-800)* with BamHI and SacI and ligating the two fragments together. pA1425 - pA1427 were constructed by site directed mutagenesis of pA1419. pA1607 was constructed by digesting pA1207 (D'Aquino et al. 2005) and a PCR fragment containing the Δ503-511 deletion (constructed by PCR mediated ligation of two overlapping fragments spanning the deletion) with BsrGI and MscI and ligating the two fragments together. pA1608 and pA1609 were generated by site directed mutagenesis of pA1207. pA1624 was generated by sequential cloning into YIplac204 of the promoter of *KIN4* (1kb upstream of the start codon) with HindIII and then a PCR fragment containing *kin4(655-800)-GFP* with SphI and SacI. pA1760 was generated by digesting pFA6a-3HA-KanMx6 and a PCR fragment containing *SPC72(177-622)* (Maekawa et al. 2007) with AscI and PacI and ligating the two fragments together. pAM51 and pAM52 were constructed by digesting pAM50 (pEGFP-C1 [Clontech]) with EcoRI and ligating in PCR fragments containing *KIN4* and

kin4(655-800) digested with MfeI respectively. pAM53 was generated by site directed mutagenesis of pAM52.

Immunoblot Analysis

Immunoblot analysis to determine total amount of Kin4-GFP and Kin4-3HA were as previously described (Chan and Amon 2009). For immunoblot analysis of Kar2 and 3HA-Lte1, cell lysates were prepared as previously described (Chan and Amon 2009). Kar2 was detected using a rabbit anti-Kar2 anti-serum (Rose, Misra and Vogel 1989) at 1:200,000 and 3HA-Lte1 was detected using an anti-HA antibody (Covance, HA.11) at 1:1000. For immunoblot analysis of mammalian cell lysates, cells were harvested, washed once in PBS (100mM sodium phosphate pH7.2, .9% NaCl), resuspended in lysis buffer (PBS + 1% NP-40, .5% sodium deoxycholate, .1% SDS, 100 μg/mL Benzonase [Novagen], 100 mM DTT and complete protease inhibitor cocktail [Roche]), incubated on ice for 30 minutes and then boiled after the addition of sample buffer. GFP fusion proteins were detected using a mouse anti-GFP antibody cocktail [Roche] at 1:2000 and β-actin was detected using a mouse anti-β-actin antibody [Sigma AC-74] at 1:15,000.

Fluorescence Microscopy

Indirect *in situ* immunofluorescence methods for Tub1 were as previously described (Kilmartin and Adams 1984). For immunofluorescence detection of Tem1-3MYC, cells were fixed for 15 minutes in 3.7% formaldehyde, 100mM potassium phosphate pH6.4 buffer and prepared for staining as above. Cells were incubated with a mouse anti-MYC [Covance, 9E10] antibody at 1:1000 dilution for 2 hours and an anti-mouse-Cy3 [Jackson] secondary antibody at 1:1500 for 2 hours. Live cell imaging techniques are as previously described (Chan and Amon 2009). Imaging of 293T cells is as follows. Cells were seeded on a poly-lysine coated coverslip and transfected with the appropriate plasmid (see below for transfection details). Cells were imaged live 24 hours post transfection on a Zeiss Observer.Z1 inverted scope with a 40X objective. Images were collected with a Hammamatsu ORCA-ER C4742-80 digital CCD camera and analyzed with Metamorph software [Molecular Devices].

Kin4 Kinase Assays

Kin4 kinase assays were performed as previously described (Chan and Amon 2009).

Sequence Alignment

Kin4 orthologs were identified by BLAST (Altschul et al. 1997) and sequence alignment analysis was carried out using T-Coffee (Notredame, Higgins and Heringa 2000).

Mammalian Cell Growth and Transfection

293T cells were cultured in DMEM supplemented with 10%NBCS, 4 mM glutamine, 100 U/mL penicillin and 100 μg/mL streptomycin. Cells were plated at a density of $1x10^5$ cells/cm^2 24 hours prior to transfection. Cells were transfected using TransIT-LT1 transfection reagent [Mirus] according to the manufacturer's recommendations. Cells were imaged and harvested for immunoblot analysis 24 hours post transfection.

Table 1: Yeast Strains

A1828	*MATa TEM1-3MYC*
A1863	*MATa bub2Δ::HIS3*
A2587	*MATa ade2-1 leu2-3 ura3 trp1-1 his3-1115 can1-100 GAL [phi+] (W303)*
A4874	*MATa spo12Δ::HIS3*
A11779	*MATa KIN4-3HA:KanMx6*
A11997	*MATa His3Mx6:pGAL1-10-GFP-KIN4*
A14052	*MATa kin4(1-341)-3HA:His3Mx*
A17349	*MATa dyn1Δ::URA3*
A17351	*MATa kin4Δ::KanMx6 dyn1Δ::URA3*
A17865	*MATa kin4Δ::KanMx6*
A18450	*MATa trp1:pGAL1-10-GFP-kin4(655-800)-F793A:TRP1*
A18451	*MATa trp1:pGAL1-10-GFP-kin4(655-800)-F792A:TRP1*
A18452	*MATa trp1:pGAL1-10-GFP-kin4(655-800)-V789A:TRP1*
A18463	*MATa trp1:pGAL1-10-GFP-kin4(655-800):TRP1*
A18792	*MATa His3Mx6:pGAL1-10-GFP-KIN4 bub2Δ::HIS3*
A19900	*MATa ura3:mCherry-TUB1:URA3 KIN4-GFP:His3Mx6*
A20608	*MATa KIN4-S508A-3HA:KanMx6*
A21298	*MATa kin4-F793A:KIN4-3'UTR:KanMx6 dyn1Δ::URA3*
A21299	*MATa KIN4-S508A:KIN4-3'UTR:KanMx6*
A21301	*MATa KIN4-S508A:KIN4-3'UTR:KanMx6 dyn1Δ::URA3*
A21555	*MATa kin4(Δ503-511)-GFP:His3Mx6 ura3:mCherry-TUB1:URA3*
A21556	*MATa kin4-F793A-GFP:His3Mx6 ura3:mCherry-TUB1:URA3*
A21557	*MATa KIN4-S508A-GFP:His3Mx6 ura3:mCherry-TUB1:URA3*
A21575	*MATa kin4(1-654)-GFP:His3Mx6 ura3:mCherry-TUB1:URA3*
A21576	*MATa trp1:kin4(655-800)-GFP:TRP1 ura3:mCherry-TUB1:URA3*
A22119	*MATa kin4-T209A-3HA:KanMx6*
A22262	*MATa kin4(1-341):KanMx6 dyn1Δ::URA3*
A22263	*MATa kin4(1-654):KanMx6 dyn1Δ::URA3*
A22278	*MATa kin4(1-341)-T209A-3HA:His3Mx6*
A22736	*MATa kin4-T209A:KIN4-3'UTR:KanMx6 dyn1Δ::URA3*
A23045	*MATa bub2Δ::KanMx6*
A23051	*MATa KIN4-S508A-GFP:His3Mx6 ura3:mCherry-TUB1:URA3 kar9Δ::His3Mx6*
A23052	*MATa KIN4-S508A-GFP:His3Mx6 ura3:mCherry-TUB1:URA3 dyn1Δ::His3Mx6*
A23055	*MATa KIN4-S508A-GFP:His3Mx6 ura3:mCherry-TUB1:URA3 clb4Δ::His3Mx6*
A23249	*MATa KIN4-GFP:His3Mx6 ura3:mCherry-TUB1:URA3 clb4Δ::HIS3*
A23250	*MATa His3Mx6:pGal1-10-GFP-kin4(1-341):KanMx6*
A23410	*MATa kin4(1-341)-GFP:HIS3Mx6 ura3:mCherry-TUB1:URA3*
A23686	*MATa KanMx6:pGAL1-10-URL-3HA-LTE1*
A24083	*MATa KIN4-S508A:KIN4-3'UTR:KanMx6 clb4Δ::HIS3*
A24084	*MATa KanMx6:pGAL1-10-URL-3HA-LTE1 KIN4-S508A:KIN4-*

3'UTR:KanMx6

A24085 *MATa KanMx6:pGAL1-10-URL-3HA-LTE1 clb4Δ::HIS3*

A24086 *MATa KanMx6:pGAL1-10-URL-3HA-LTE1 KIN4-S508A:KIN4-3'UTR:KanMx6 clb4Δ::HIS3*

A24113 *MATa His3Mx6:pGAL1-10-GFP-kin4(1-341):KanMx6 bub2Δ::HIS3*

A24346 *MATa KanMx6:pGAL1-10-URL-3HA-LTE1 KIN4-S508A:KIN4-3'UTR:KanMx6 clb4Δ::NatMx4 bub2Δ::HIS3*

A24543 *MATa KanMx6:pGAL1-10-URL-3HA-LTE1 spo12Δ::HIS3*

A24586 *MATa kin4-SPC72(177-622):KanMX6*

A24587 *MATa kin4-SPC72(177-622):KanMX6 KanMx6:pGAL1-10-URL-3HA-LTE1*

A24588 *MATa kin4-SPC72(177-622):KanMX6 KanMx6:pGAL1-10-URL-3HA-LTE1 bub2Δ::HIS3*

A24761 *MATa KIN4-S508A:KIN4-3'UTR:CaURA3Mx4 clb4Δ::NatMx4 KanMx6:pGAL1-10-URL-3HA-LTE1 TEM1-3MYC*

A24805 *MATa clb4Δ::NatMx4 KanMx6:pGAL1-10-URL-3HA-LTE1 TEM1-3MYC*

A24806 *MATa kin4Δ::KanMx6 lte1Δ::NatMx4*

A24807 *MATa lte1Δ::NatMx4*

A24808 *MATa bub2Δ::KanMx6 lte1Δ::NatMx4*

A24816 *MATa KanMx6:pGAL1-10-URL-3HA-LTE1 KIN4-S508A:KIN4-3'UTR:KanMx6 kar9Δ::His3Mx6*

A24817 *MATa kin4-SPC72(177-622):KanMX6 KanMx6:pGAL1-10-URL-3HA-LTE1 kar9Δ::His3Mx6*

A24858 *MATa kin4-SPC72(177-622):KanMX6 KanMx6:pGAL1-10-URL-3HA-LTE1 clb4Δ::HIS3*

Table 2: Plasmids

pA1419	YIplac204-*pGAL1-10-GFP-kin4(655-800)*
pA1425	YIplac204-*pGAL1-10-GFP-kin4(655-800)-F793A*
pA1426	YIplac204-*pGAL1-10-GFP-kin4(655-800)-F792A*
pA1427	YIplac204-*pGAL1-10-GFP-kin4(655-800)-V789A*
pA1607	YIplac211-*kin4(Δ503-511)-3HA*
pA1608	YIplac211-*kin4-F793A-3HA*
pA1609	YIplac211-*KIN4-S508A-3HA*
pA1624	YIplac204-*kin4(655-800)-GFP*
pA1760	pFA6a-*SPC72(177-622)-KanMx6*
pAM50	pEGFP-C1
pAM51	pEGFP-C1-*KIN4*
pAM52	pEGFP-C1-*kin4(655-800)*
pAM53	pEGFP-C1-*kin4(655-800)-F793A*

References

Adames, N. R., J. R. Oberle & J. A. Cooper (2001) The surveillance mechanism of the spindle position checkpoint in yeast. *J Cell Biol,* 153, 159-68.

Altschul, S. F., T. L. Madden, A. A. Schaffer, J. Zhang, Z. Zhang, W. Miller & D. J. Lipman (1997) Gapped BLAST and PSI-BLAST: a new generation of protein database search programs. *Nucleic Acids Res,* 25, 3389-402.

Bardin, A. J., R. Visintin & A. Amon (2000) A mechanism for coupling exit from mitosis to partitioning of the nucleus. *Cell,* 102, 21-31.

Bloecher, A., G. M. Venturi & K. Tatchell (2000) Anaphase spindle position is monitored by the BUB2 checkpoint. *Nat Cell Biol,* 2, 556-8.

Castillon, G. A., N. R. Adames, C. H. Rosello, H. S. Seidel, M. S. Longtine, J. A. Cooper & R. A. Heil-Chapdelaine (2003) Septins have a dual role in controlling mitotic exit in budding yeast. *Curr Biol,* 13, 654-8.

Chan, L. Y. & A. Amon (2009) The protein phosphatase 2A functions in the spindle position checkpoint by regulating the checkpoint kinase Kin4. *Genes Dev,* 23, 1639-49.

Cheeseman, I. M., J. S. Chappie, E. M. Wilson-Kubalek & A. Desai (2006) The conserved KMN network constitutes the core microtubule-binding site of the kinetochore. *Cell,* 127, 983-97.

Cheng, J., N. Turkel, N. Hemati, M. T. Fuller, A. J. Hunt & Y. M. Yamashita (2008) Centrosome misorientation reduces stem cell division during ageing. *Nature,* 456, 599-604.

D'Aquino, K. E., F. Monje-Casas, J. Paulson, V. Reiser, G. M. Charles, L. Lai, K. M. Shokat & A. Amon (2005) The protein kinase Kin4 inhibits exit from mitosis in response to spindle position defects. *Mol Cell,* 19, 223-34.

DeLuca, J. G., W. E. Gall, C. Ciferri, D. Cimini, A. Musacchio & E. D. Salmon (2006) Kinetochore microtubule dynamics and attachment stability are regulated by Hec1. *Cell,* 127, 969-82.

Fraschini, R., C. D'Ambrosio, M. Venturetti, G. Lucchini & S. Piatti (2006) Disappearance of the budding yeast Bub2-Bfa1 complex from the mother-bound spindle pole contributes to mitotic exit. *J Cell Biol,* 172, 335-46.

Fraschini, R., E. Formenti, G. Lucchini & S. Piatti (1999) Budding yeast Bub2 is localized at spindle pole bodies and activates the mitotic checkpoint via a different pathway from Mad2. *J Cell Biol,* 145, 979-91.

Garcia-Cortes, J. C. & D. McCollum (2009) Proper timing of cytokinesis is regulated by Schizosaccharomyces pombe Etd1. *J Cell Biol,* 186, 739-53.

Geymonat, M., A. Spanos, G. de Bettignies & S. G. Sedgwick (2009) Lte1 contributes to Bfa1 localization rather than stimulating nucleotide exchange by Tem1. *J Cell Biol,* 187, 497-511.

Geymonat, M., A. Spanos, S. J. Smith, E. Wheatley, K. Rittinger, L. H. Johnston & S. G. Sedgwick (2002) Control of mitotic exit in budding yeast. In vitro regulation of Tem1 GTPase by Bub2 and Bfa1. *J Biol Chem,* 277, 28439-45.

Geymonat, M., A. Spanos, P. A. Walker, L. H. Johnston & S. G. Sedgwick (2003) In vitro regulation of budding yeast Bfa1/Bub2 GAP activity by Cdc5. *J Biol Chem,* 278, 14591-4.

Goldstein, A. L. & J. H. McCusker (1999) Three new dominant drug resistance cassettes for gene disruption in Saccharomyces cerevisiae. *Yeast,* 15, 1541-53.
Hu, F., Y. Wang, D. Liu, Y. Li, J. Qin & S. J. Elledge (2001) Regulation of the Bub2/Bfa1 GAP complex by Cdc5 and cell cycle checkpoints. *Cell,* 107, 655-65.
Jaspersen, S. L., J. F. Charles & D. O. Morgan (1999) Inhibitory phosphorylation of the APC regulator Hct1 is controlled by the kinase Cdc28 and the phosphatase Cdc14. *Curr Biol,* 9, 227-36.
Jensen, S., A. L. Johnson, L. H. Johnston & M. Segal (2004) Temporal coupling of spindle disassembly and cytokinesis is disrupted by deletion of LTE1 in budding yeast. *Cell Cycle,* 3, 817-22.
Kilmartin, J. V. & A. E. Adams (1984) Structural rearrangements of tubulin and actin during the cell cycle of the yeast Saccharomyces. *J Cell Biol,* 98, 922-33.
Lee, J., H. S. Hwang, J. Kim & K. Song (1999) Ibd1p, a possible spindle pole body associated protein, regulates nuclear division and bud separation in Saccharomyces cerevisiae. *Biochim Biophys Acta,* 1449, 239-53.
Lee, W. L., J. R. Oberle & J. A. Cooper (2003) The role of the lissencephaly protein Pac1 during nuclear migration in budding yeast. *J Cell Biol,* 160, 355-64.
Lew, D. J. & D. J. Burke (2003) The spindle assembly and spindle position checkpoints. *Annu Rev Genet,* 37, 251-82.
Li, R. (1999) Bifurcation of the mitotic checkpoint pathway in budding yeast. *Proc Natl Acad Sci U S A,* 96, 4989-94.
Li, Y. Y., E. Yeh, T. Hays & K. Bloom (1993) Disruption of mitotic spindle orientation in a yeast dynein mutant. *Proc Natl Acad Sci U S A,* 90, 10096-100.
Liakopoulos, D., J. Kusch, S. Grava, J. Vogel & Y. Barral (2003) Asymmetric loading of Kar9 onto spindle poles and microtubules ensures proper spindle alignment. *Cell,* 112, 561-74.
Liu, D., G. Vader, M. J. Vromans, M. A. Lampson & S. M. Lens (2009) Sensing chromosome bi-orientation by spatial separation of aurora B kinase from kinetochore substrates. *Science,* 323, 1350-3.
Longtine, M. S., A. McKenzie, 3rd, D. J. Demarini, N. G. Shah, A. Wach, A. Brachat, P. Philippsen & J. R. Pringle (1998) Additional modules for versatile and economical PCR-based gene deletion and modification in Saccharomyces cerevisiae. *Yeast,* 14, 953-61.
Maekawa, H., C. Priest, J. Lechner, G. Pereira & E. Schiebel (2007) The yeast centrosome translates the positional information of the anaphase spindle into a cell cycle signal. *J Cell Biol,* 179, 423-36.
Maekawa, H. & E. Schiebel (2004) Cdk1-Clb4 controls the interaction of astral microtubule plus ends with subdomains of the daughter cell cortex. *Genes Dev,* 18, 1709-24.
Maekawa, H., T. Usui, M. Knop & E. Schiebel (2003) Yeast Cdk1 translocates to the plus end of cytoplasmic microtubules to regulate bud cortex interactions. *EMBO J,* 22, 438-49.
Molk, J. N., S. C. Schuyler, J. Y. Liu, J. G. Evans, E. D. Salmon, D. Pellman & K. Bloom (2004) The differential roles of budding yeast Tem1p, Cdc15p, and Bub2p protein dynamics in mitotic exit. *Mol Biol Cell,* 15, 1519-32.

Moore, J. K., V. Magidson, A. Khodjakov & J. A. Cooper (2009) The Spindle Position Checkpoint Requires Positional Feedback from Cytoplasmic Microtubules. *Curr Biol.*

Notredame, C., D. G. Higgins & J. Heringa (2000) T-Coffee: A novel method for fast and accurate multiple sequence alignment. *J Mol Biol,* 302, 205-17.

O'Connell, C. B. & Y. L. Wang (2000) Mammalian spindle orientation and position respond to changes in cell shape in a dynein-dependent fashion. *Mol Biol Cell,* 11, 1765-74.

Pereira, G., T. Hofken, J. Grindlay, C. Manson & E. Schiebel (2000) The Bub2p spindle checkpoint links nuclear migration with mitotic exit. *Mol Cell,* 6, 1-10.

Pereira, G. & E. Schiebel (2005) Kin4 kinase delays mitotic exit in response to spindle alignment defects. *Mol Cell,* 19, 209-21.

Rose, M. D., L. M. Misra & J. P. Vogel (1989) KAR2, a karyogamy gene, is the yeast homolog of the mammalian BiP/GRP78 gene. *Cell,* 57, 1211-21.

Shirayama, M., Y. Matsui, K. Tanaka & A. Toh-e (1994a) Isolation of a CDC25 family gene, MSI2/LTE1, as a multicopy suppressor of ira1. *Yeast,* 10, 451-61.

Shirayama, M., Y. Matsui & E. A. Toh (1994b) The yeast TEM1 gene, which encodes a GTP-binding protein, is involved in termination of M phase. *Mol Cell Biol,* 14, 7476-82.

Stegmeier, F., R. Visintin & A. Amon (2002) Separase, polo kinase, the kinetochore protein Slk19, and Spo12 function in a network that controls Cdc14 localization during early anaphase. *Cell,* 108, 207-20.

Tanaka, T. U., N. Rachidi, C. Janke, G. Pereira, M. Galova, E. Schiebel, M. J. Stark & K. Nasmyth (2002) Evidence that the Ipl1-Sli15 (Aurora kinase-INCENP) complex promotes chromosome bi-orientation by altering kinetochore-spindle pole connections. *Cell,* 108, 317-29.

Visintin, R., K. Craig, E. S. Hwang, S. Prinz, M. Tyers & A. Amon (1998) The phosphatase Cdc14 triggers mitotic exit by reversal of Cdk-dependent phosphorylation. *Mol Cell,* 2, 709-18.

Yeh, E., R. V. Skibbens, J. W. Cheng, E. D. Salmon & K. Bloom (1995) Spindle dynamics and cell cycle regulation of dynein in the budding yeast, Saccharomyces cerevisiae. *J Cell Biol,* 130, 687-700.

Yoshida, S., R. Ichihashi & A. Toh-e (2003) Ras recruits mitotic exit regulator Lte1 to the bud cortex in budding yeast. *J Cell Biol,* 161, 889-97.

Zachariae, W., M. Schwab, K. Nasmyth & W. Seufert (1998) Control of cyclin ubiquitination by CDK-regulated binding of Hct1 to the anaphase promoting complex. *Science,* 282, 1721-4.

Chapter 4: Discussion, Questions and Future Directions

How does *PP2A-RTS1* promote Kin4 function?

RTS1 appears to promote the checkpoint function of Kin4. Kin4 does not efficiently load onto spindle pole bodies (SPBs) in *rts1*Δ mutants. Moreover, *RTS1* is required for Kin4 mediated exclusion of Tem1 from SPBs. However, we do not understand mechanistically how Rts1 promotes Kin4 function. Because PP2A-Rts1 promotes the dephosphorylation of Kin4, the answer to how Rts1 promotes Kin4 function may lie in understanding the functional importance of Kin4 phosphorylation. We have mapped a subset of Kin4 phosphorylation sites and generated the corresponding phospho-mutants but have failed to observe any striking defects in localization or checkpoint function. Moreover, we have failed to observe a genetic interaction between such phospho-mutations and *rts1*Δ (discussed in full in Appendix I: Characterization and Regulation of Kin4 Phosphorylation).

It is interesting to note that Kin4 localization is defective in the *rts1*Δ mutant for much more than SPB loading. Kin4 signal at the cortex was noticeably weaker in the *rts1*Δ mutant. The reason for this weaker signal is not known but it is possible that cortical localization is a prerequisite for SPB loading and could explain the inefficient SPB loading of Kin4 in *rts1*Δ mutants. In agreement with this notion, alleles of *KIN4* that fail to localize to the cortex also fail to load onto SPBs. Kin4 also fails to be asymmetrically restricted to the mother cell cortex in *rts1*Δ mutants. The nature of this defect is not understood but it is important to note that Lte1 localization was not defective in *rts1*Δ mutants suggesting that overall cell polarization is not defective.

It is possible that various pools of Kin4 phosphorylation sites control various aspects of its function such as cortical localization, SPB loading and asymmetric cortical restriction. PP2A-Rts1 may simply be a phosphatase that generally acts on Kin4 and is not selective for any particular phosphorylation pool. A more thorough map of Kin4 phosphorylation sites would enable the generation of additional phospho-site mutants to examine the functional importance of Kin4 phosphorylation and thus the role of Rts1 in Kin4 regulation. Based on the Kin4 localization defects we observe in *rts1*Δ mutants, one

would expect Kin4 phosphorylation to play roles in asymmetric cortical restriction, SPB loading and/or cortex anchorage.

Is there a role for *RTS1* in MEN inhibition downstream of Kin4?

Despite strong evidence that *PP2A-RTS1* acts upstream of *KIN4*, it is still possible that *PP2A-RTS1* has additional roles in MEN inhibition downstream of *KIN4*. Suppression of *GAL-KIN4* by *rts1*Δ superficially supports such a role. However, interpretation of epistasis experiments where gain of function alleles are involved is especially tricky. No single pathway can be ruled out with such an experiment. The reciprocal epistasis experiment where we could test the suppression of a gain of function phenotype of *RTS1* by *kin4*Δ mutation would help to eliminate possible pathways. However, such an experiment cannot be performed due to the lack of any gain of function alleles for *RTS1*. This is a general problem in the field of multi-subunit phosphatases. Simple overexpression of a single subunit has complex results often times generating the loss of function phenotype associated with a competing subunit.

RTS1 was placed upstream of *KIN4* based on the defects in Kin4 localization in the *rts1*Δ mutant. While genetic experiments did not support a definitive ordering of these two genes, it is important to note that suppression of *GAL-KIN4* by *rts1*Δ is not complete. *GAL-KIN4 rts1*Δ double mutants grew more poorly than *rts1*Δ mutants alone. Contrast this with mutations in *BUB2*, a factor mechanistically known to be downstream of *KIN4*. Suppression of *GAL-KIN4* by *bub2*Δ was complete in that the *GAL-KIN4 bub2*Δ grew equally well as the *bub2*Δ mutant. This implies that if *RTS1* is downstream of *KIN4*, then *KIN4* cannot be acting solely through *RTS1*.

In contrast to *GAL-KIN4*, the lethality of *GAL-BFA1* mutants was not suppressed by *rts1*Δ. *GAL-BFA1* and *GAL-KIN4* arrest cells at very similar points in the cell cycle, i.e. just before Tem1 activation. This differential ability of the *rts1*Δ mutation to suppress these two mutant phenotypes suggests that if *RTS1* is downstream of *KIN4*, then it must lie upstream of or parallel to *BFA1*. Our mechanistic understanding of the Kin4-Bfa1 interaction offers few roles for Rts1. Kin4 phosphorylates Bfa1 to protect it from

phosphorylation and downregulation by Cdc5 (Maekawa et al. 2007). It is possible that PP2A-Rts1 dephosphorylates the Cdc5 dependent pool of Bfa1 phosphorylation and thus promotes MEN inhibition. We could detect no differences in Bfa1 phosphorylation by electrophoretic mobility shift. However, it is possible that this assay is not sensitive enough to detect the relevant changes in phosphorylation.

It is further possible that *GAL-BFA1* causes a stronger cell cycle arrest than *GAL-KIN4* or causes this cell cycle arrest by a different mechanism. Indeed, *GAL-KIN4* is suppressed by both *rts1*Δ and *bub2*Δ where as *GAL-BFA1* is suppressed by neither suggesting that *GAL-KIN4* requires an intact GAP complex to mediate MEN inhibition whereas *GAL-BFA1* does not (Lee et al. 1999, Li 1999). It would thus be informative to test if *rts1*Δ can suppress other mutants that arrest in anaphase. Temperature sensitive mutants cannot be employed as *rts1*Δ mutants are themselves temperature sensitive. However, it would be interesting to test if *rts1*Δ could bypass the anaphase arrest caused by Tem1 depletion (*pGAL1-10-UPL-3HA-TEM1)*, Cdc5 depletion (*pMET3-CDC5*) or overexpression of dominant negative forms of Cdc15 (*GAL-cdc15(267-974)*). All of these mutants arrest independently of the GAP complex and thus any suppression of these mutants would suggest a role for *PP2A-RTS1* downstream of *KIN4*.

How is Kin4 localization spatially and temporally controlled?

The zone model underscores the importance of restricting inappropriate Kin4 signaling. This appears to be largely achieved through restriction to the mother cell cortex and to a lesser extent, exclusion from the daughter SPB. We have mapped cis acting domains and sequence determinants that control cortical and asymmetric localization. Identifying trans acting factors that communicate with these regions of Kin4 is an important next step. A more detailed discussion of how such factors might be identified is contained in Appendix II but is summarized below. To identify trans acting factors that promote Kin4 asymmetry at the cortex, a genetic screen for mutations that cause lethality in the *LTE1-deg clb4*Δ background could be conducted. Such a screen would identify trans acting mutations that in effect, produce the same results as symmetrizing Kin4 through the S508A mutation.

To identify trans acting factors that might mediate cortical anchorage, a similar screen could be performed. Due to the strong correlation between Kin4's cortical anchorage and ability to inhibit the MEN, one might expect that a mutant in the cortical anchor of Kin4 would lead to a loss of Kin4 function. If this is the case, then identifying trans acting mutations that suppress the lethality of *KIN4-S508A*, *LTE1-deg*, *clb4*Δ might identify the cortical anchor. Such a screen would also identify any additional factors that Kin4 requires for its function. A biochemical approach is also possible but technically more challenging. Given that we have mapped the domain of Kin4 that mediates cortical anchorage in the mother (kin4(655-800)) and have also identified a mutation that renders this domain non-functional (F793A), we could purify both kin4(655-800) and kin4(655-800)-F793A from yeast extracts and identify the differential interactors. Due to the challenges posed by Kin4 insoluability, such an approach would require a number of modifications that are outlined in Appendix II: Development of Methods to Identify Genetic and Biochemical Interactors of Kin4.

Kin4 also appears to be temporally controlled in that Kin4 only loads onto SPBs in mid-anaphase. The basis for this temporal restriction is unknown. One possibility is that spindle elongation itself is required for Kin4 to load during anaphase. This could be tested by examining Kin4 localization in a *pMET-CDC20 mcd1-1* or in a *pMET-CDC20 ndc10-1* mutant. Both *mcd1-1* and *ndc10-1* mutants decouple spindle elongation from the metaphase to anaphase transition such that cells remain arrested in metaphase due to Cdc20 depletion but still undergo spindle elongation. Another possibility is that the FEAR network, which is responsible for transient release of Cdc14 during early anaphase, is required for Kin4 to load to SPBs. Examination of Kin4 localization in a *pGAL1-10-URL-3HA-CDC14* mutant should reveal any such role for FEAR in Kin4 loading.

How do Kin4 and Lte1 signal to Tem1 and what is the role of the GAP complex?
While the zone model provides a mechanism of how spindle position is sensed and coupled to the cell cycle, it does not account for how the MEN regulators, Lte1 and Kin4,

actually signal to Tem1. This is largely due to the mysterious role of the Bub2-Bfa1 GAP complex in Tem1 regulation and the lack of understanding of the connections between biochemical activity and localization of these proteins.

This signaling is much better understood in the analogous pathway to MEN in fission yeast, the Septation Initiation Network (SIN) (reviewed in (Bardin and Amon 2001)). This pathway has a very similar architecture and is also regulated by a GTPase switch, Spg1p. During anaphase, the Spg1p GAP complex, Bry4p-Cdc16p, only localizes to one of the two SPBs. An antibody that is specific for Spg1p-GDP has shown that Spg1p-GDP is loaded onto the same SPB as the GAP complex whereas Spg1p-GTP is loaded to the opposite SPB. The Spg1p-GTP bound SPB also recruits the Cdc15 homolog, Cdc7p. Moreover, the Lte1 homolog, Etd1p, is localized to bud tips and promotes Spg1p signaling during maximal spindle elongation (Garcia-Cortes and McCollum 2009). Thus, in the case of the SIN, the localization and biochemical activities of the GAP, the GTPase and the downstream kinases are in agreement.

A key difference complicates reasoning by analogy between the SIN and the MEN. Bub2-Bfa1 localization mirrors that of Tem1 whereas in fission yeast, Spg1-GTP and the GAP complex have opposite localization patterns. This difference is difficult to resolve due to our lack of knowledge of the molecular states of MEN components at the SPBs compared to those of the SIN. Tem1 is presumed to be in the GTP bound state at the daughter SPB but this has never been shown. Further complicating the analysis is the fact that while Cdc15 initially associates with the dSPB at anaphase onset suggesting that the daughter SPB is where Tem1-GTP signals from, Cdc15 localization becomes symmetric to both SPBs as anaphase progresses (Molk et al. 2004). Thus it is unclear if Cdc15 SPB loading can be used a surrogate for Tem1 activation.

Biochemical studies of Tem1 signaling have raised an additional set of questions. Tem1 was found to be an unusual GTPase with very appreciable basal rates of both GDP exchange and GTP hydrolysis compared to known rates for other GTPases. Tem1 GTP hydrolysis rates have been reported to be 0.07 (based on visual estimate of data points

and fitting to a single exponential) to 0.12/min at 30°C (Fraschini et al. 2006, Geymonat et al. 2002). For comparison, the rate of GTP hydrolysis for $p21^{ras}$ has been reported to be 0.02/min at 37°C (Neal et al. 1988). GDP exchange for Tem1 was measured to be 0.2/min at 13°C and 1.6/min at 25°C (based on visual estimation of data points and fitting to a single exponential) (extrapolates to 3.3/min at 37°C based on the Arrhenius equation) (Geymonat et al. 2009, Geymonat et al. 2002). The exchange rate for $p21^{ras}$ has been reported to be 0.023/min at 37°C (Huang, Kung and Kamata 1990). Analysis of the GAP complex showed that Bfa1, the non-catalytic subunit, acted as a guanine nucleotide disassociation inhibitor (GDI) for Tem1-GDP and unusually, Tem1-GTP as well (Geymonat et al. 2009, Geymonat et al. 2002). Additionally, GTP hydrolysis by Tem1 was strongly inhibited in the presence of Bfa1 alone (Geymonat et al. 2002). Further addition of Bub2 did not dramatically accelerate the basal rate of GTP hydrolysis by Tem1. GTP hydrolysis rates in a reaction containing Tem1, Bub2 and Bfa1 were only slightly higher than that of Tem1 alone (0.22 - 0.56/min based on visual estimation of data points and fitting to a single exponential – representing a 2-6 fold acceleration) (Fraschini et al. 2006, Geymonat et al. 2002). In contrast, presence of the GAP accelerated GTP hydrolysis of $p21^{ras}$ by 10^5 fold (Goody et al. 1992). This weak acceleration of the Tem1 GTP hydrolysis rate brings into question the importance of GAP activity for the Bub2-Bfa1 complex.

However, biochemical studies of the role of Cdc5 in Tem1 GTPase signaling support a role for GAP activity for Bub2-Bfa1. Phosphorylation of Bfa1 by Cdc5 was found to have no effects on Bfa1's ability to inhibit exchange or hydrolysis in the absence of Bub2 (Geymonat et al. 2003). However, in the presence of Bub2, Cdc5 phosphorylation of Bfa1 was found to have a moderate inhibitory effect on the ability of Bub2-Bfa1 to act as a GAP (Geymonat et al. 2003). In further support of the importance of GAP activity, mutations of the arginine finger in Bub2 rendered the GAP complex biochemically non-functional and also failed to mediate cell cycle arrests in response to defects in both spindle assembly and spindle positioning (Fraschini et al. 2006).

Lte1 contains putative GEF domains and has thus been proposed to act as a GEF for Tem1. Biochemical studies have not supported this hypothesis. Purified Lte1 exhibited no GEF activity for Tem1 (Geymonat et al. 2009). Genetic studies have yielded mixed results. Mutations modeled from other GEFs that reduce GEF activity but not GTPase binding were introduced into Lte1 and found to complement the cold sensitivity of *lte1*Δ mutants suggesting that full GEF activity of Lte1 is not required for its *in vivo* function (Geymonat et al. 2009). However, a deletion in Lte1 that removed nearly all of the protein except for the GEF domains was found to be functional by this cold sensitivity assay (Geymonat et al. 2009). Further phenotypic characterization of this GEF-only mutant in other assays showed that this allele of *LTE1* behaves as a partial loss of function (Geymonat et al. 2009). The homolog of Lte1 in fission yeast has only recently been identified and thus offers little insight into how Lte1 might function (Garcia-Cortes and McCollum 2009).

These data underscore three important questions in Tem1 signaling:

(1) Does Bfa1 ever act on Tem1 in the absence of Bub2? If so, does it act as a GTPase inhibitor, Tem1-GDP disassociation inhibitor and/or Tem1-GTP disassociation inhibitor?

(2) What is the localization of Tem1-GDP versus Tem1-GTP? How do Bub2-Bfa1 regulate this localization?

(3) How does Lte1 promote Tem1 signaling? Does it require Bub2, Bfa1 or even Kin4?

In regards to the first question, if Tem1-GTP is the active form of Tem1 as it is for all other known G-proteins, biochemical characterization of Bfa1 in the absence of Bub2 would suggest that it might have MEN activating activities. Both inhibition of GTP hydrolysis and inhibition of GTP disassociation should promote MEN signaling. However, genetic studies have never shown Bfa1 to act as a promoter of mitotic exit. On the contrary, over-expression of *BFA1* shuts down MEN signaling and deletion of *BFA1* hyper-activates the MEN (Lee et al. 1999, Lee et al. 2001, Li 1999). Moreover, deletion

of *BFA1* mirrors deletion of *BUB2* in all phenotypic assays tested to date suggesting that Bfa1 likely does not act in the absence of Bub2.

To address the second question, development of methods that would allow for microscopic distinction between Tem1-GDP and Tem1-GTP would help to clarify this issue. Attempts to develop a Tem1-GDP specific antibody in the style of the Spg1p-GDP antibody have been unsuccessful (Jeremy Rock, personal communication). However, a discrepancy in the reported localization of Tem1 by differing visualization methods might shed some light on this issue. We and others have observed complete asymmetric Tem1 localization to the daughter SPB and not the mother SPB in anaphase when imaged by indirect immuno-fluoresence (Bardin, Visintin and Amon 2000, Pereira et al. 2000). However, when imaged live by GFP fusion, Tem1 is observed to be brighter on the daughter SPB, but not absent from the mother SPB (Caydasi and Pereira 2009, Molk et al. 2004, Monje-Casas and Amon 2009). This discrepancy is even more striking in cells with mispositioned spindles. When imaged by immuno-fluoresence, C-terminally epitope tagged Tem1 is absent from both poles but when imaged live by GFP fusion, Tem1 is observed to weakly load onto both SPBs (Molk et al. 2004) (L.Y.C unpublished observations). While this discrepancy could simply be an artifact of fixed cell immuno-fluoresence or GFP fusion, it is possible that this discrepancy represents something more functionally relevant. Indeed, when *KIN4* is deleted, Tem1 loads onto both SPBs when the spindle is mispositioned when examined by immuno-fluoresence. This raises the interesting possibility that the immuno-fluorescent signal is actually reflective of activated Tem1, possibly Tem1-GTP and that inactive Tem1 or Tem-GDP is somehow not capable of being imaged by this technique possibly due to epitope masking. The first step to testing this hypothesis would be to tag both the N and C termini with different epitope tags. If the signal associated with the N-terminal tag mirrored Tem1-GFP and a discrepancy still existed between the N and C-terminal tag signals, this would be good evidence that the C-terminal signal represented some functional difference in Tem1 states. The next set of experiments would involve examining the immuno-fluoresent signal of both N and C-terminally tagged Tem1 in cell cycle arrests where Tem1 is

known to be inactive such as SPOC activation, spindle assembly checkpoint activation or overexpression of *KIN4*.

Answering the third question requires a much more thorough understanding of Lte1 function. Further structure-function work as well as careful examination of Kin4, Bub2, Bfa1 and Tem1 localization in the presence and absence of Lte1 are good first steps.

A model that might reconcile the seemingly incongruous biochemical, cell biological and genetic data of Tem1 signaling is as follows. When the SPBs are in the mother cell, both Bub2 and Bfa1 are loaded and function as a GAP. In this form, Bub2-Bfa1 is subject to regulation by both Cdc5 and Kin4. However, when one SPB emerges into the daughter cell, Bub2 is removed, possibly by Lte1 in an unknown fashion. Once Bub2 is removed, Bfa1 can stabalize Tem1-GTP by inhibiting GTP hydrolysis and disassociation. This model might help to explain why symmetrically localized Kin4 can only inhibit mitotic exit in the absence of Lte1. If Kin4 requires Bub2 to be in complex with Bfa1 to inhibit the MEN, then Lte1 removal of Bub2 would trump any effect of Kin4.

Testing such a model would require much more careful time-lapse studies of Bub2, Bfa1 and Tem1. Such a model would also require the isolation of a *BFA1* allele that separated the GAP functions from the presumptive Tem1-GTP stabilization functions as well as a much more mechanistic understanding of Lte1 function.

Concluding Remarks

The work in this thesis has shed light on how spindle position is sensed by the cell and how that information is translated into a cell cycle signal. The two most important questions that remain are: (1) How is the zone of Kin4 inhibition in the mother cell established and maintained? and (2) How does Tem1 receive signals from Lte1 and Kin4?

References

Bardin, A. J. & A. Amon (2001) Men and sin: what's the difference? *Nat Rev Mol Cell Biol,* 2, 815-26.

Bardin, A. J., R. Visintin & A. Amon (2000) A mechanism for coupling exit from mitosis to partitioning of the nucleus. *Cell,* 102, 21-31.

Caydasi, A. K. & G. Pereira (2009) Spindle alignment regulates the dynamic association of checkpoint proteins with yeast spindle pole bodies. *Dev Cell,* 16, 146-56.

Fraschini, R., C. D'Ambrosio, M. Venturetti, G. Lucchini & S. Piatti (2006) Disappearance of the budding yeast Bub2-Bfa1 complex from the mother-bound spindle pole contributes to mitotic exit. *J Cell Biol,* 172, 335-46.

Garcia-Cortes, J. C. & D. McCollum (2009) Proper timing of cytokinesis is regulated by Schizosaccharomyces pombe Etd1. *J Cell Biol,* 186, 739-53.

Geymonat, M., A. Spanos, G. de Bettignies & S. G. Sedgwick (2009) Lte1 contributess to Bfa1 localization rather than stimulating nucleotide exchange by Tem1. *J Cell Biol,* 187, 497-511.

Geymonat, M., A. Spanos, S. J. Smith, E. Wheatley, K. Rittinger, L. H. Johnston & S. G. Sedgwick (2002) Control of mitotic exit in budding yeast. In vitro regulation of Tem1 GTPase by Bub2 and Bfa1. *J Biol Chem,* 277, 28439-45.

Geymonat, M., A. Spanos, P. A. Walker, L. H. Johnston & S. G. Sedgwick (2003) In vitro regulation of budding yeast Bfa1/Bub2 GAP activity by Cdc5. *J Biol Chem,* 278, 14591-4.

Goody, R. S., E. F. Pai, I. Schlichting, H. Rensland, A. Scheidig, S. Franken & A. Wittinghofer (1992) Studies on the structure and mechanism of H-ras p21. *Philos Trans R Soc Lond B Biol Sci,* 336, 3-10; discussion 10-1.

Huang, Y. K., H. F. Kung & T. Kamata (1990) Purification of a factor capable of stimulating the guanine nucleotide exchange reaction of ras proteins and its effect on ras-related small molecular mass G proteins. *Proc Natl Acad Sci U S A,* 87, 8008-12.

Lee, J., H. S. Hwang, J. Kim & K. Song (1999) Ibd1p, a possible spindle pole body associated protein, regulates nuclear division and bud separation in Saccharomyces cerevisiae. *Biochim Biophys Acta,* 1449, 239-53.

Lee, S. E., S. Jensen, L. M. Frenz, A. L. Johnson, D. Fesquet & L. H. Johnston (2001) The Bub2-dependent mitotic pathway in yeast acts every cell cycle and regulates cytokinesis. *J Cell Sci,* 114, 2345-54.

Li, R. (1999) Bifurcation of the mitotic checkpoint pathway in budding yeast. *Proc Natl Acad Sci U S A,* 96, 4989-94.

Maekawa, H., C. Priest, J. Lechner, G. Pereira & E. Schiebel (2007) The yeast centrosome translates the positional information of the anaphase spindle into a cell cycle signal. *J Cell Biol,* 179, 423-36.

Molk, J. N., S. C. Schuyler, J. Y. Liu, J. G. Evans, E. D. Salmon, D. Pellman & K. Bloom (2004) The differential roles of budding yeast Tem1p, Cdc15p, and Bub2p protein dynamics in mitotic exit. *Mol Biol Cell,* 15, 1519-32.

Monje-Casas, F. & A. Amon (2009) Cell polarity determinants establish asymmetry in MEN signaling. *Dev Cell,* 16, 132-45.

Neal, S. E., J. F. Eccleston, A. Hall & M. R. Webb (1988) Kinetic analysis of the hydrolysis of GTP by p21N-ras. The basal GTPase mechanism. *J Biol Chem,* 263, 19718-22.

Pereira, G., T. Hofken, J. Grindlay, C. Manson & E. Schiebel (2000) The Bub2p spindle checkpoint links nuclear migration with mitotic exit. *Mol Cell,* 6, 1-10.

Appendix I: Characterization and Regulation of Kin4 Phosphorylation

Phospho-site mapping was performed by Scott Carlson (Figures 1A and 2A)

All other experiments were performed by Leon Y. Chan

Introduction

In budding yeast, the spindle position checkpoint couples spindle position to mitotic exit and ensures equal partitioning of the genome during cell division. The protein kinase, Kin4, is an essential factor in this checkpoint. Kin4 is phosphorylated and levels of phosphorylation vary during the cell cycle being high in G1 and late anaphase and low in prophase and mitosis. The nature and functional importance of this phosphorylation is unknown. A single trans acting factor has been shown to affect Kin4 phosphorylation, the phosphatase, PP2A-Rts1. Loss of function of this phosphatase leads to hyper-phosphorylation of Kin4 pointing to a role for PP2A-Rts1 in the dephosphorylation of Kin4. Protein kinases that affect Kin4 phosphorylation have not been identified. Moreover, the phosphorylation of Kin4 has not been characterized and phospho-site mutants have not been generated to examine the functional role of Kin4 phosphorylation.

We have mapped phosphorylation sites within the N and C terminal regions of Kin4. The N-terminal 42 amino acids contain two highly similar phosphorylation sites and the activation loop of the kinase domain of Kin4 contains a third site. The C-terminus of Kin4 contains ten phosphorylation sites with no clear similarity. We have generated phospho-mutants of Kin4 based on these sites but have found only subtle defects in Kin4 localization and no defects in Kin4's checkpoint function. In addition, we have found that the kinase Elm1 is required for Kin4 phosphorylation but the functional consequences of this phosphorylation by Elm1 are unclear. Lastly, we show that Kin4 phosphorylation is regulated by cell polarity and we propose the existence of a bud-associated kinase(s) that phosphorylates and possibly inhibits Kin4.

Results and Discussion

Identification and characterization of phosphorylation sites in kin4(1-341)

Kin4 is a phospho-protein whose levels of phosphorylation vary during the cell cycle. Kin4 is maximally phosphorylated in G1, is dephosphorylated upon cell cycle entry and is once again phosphorylated during mitotic exit (Chan and Amon 2009, D'Aquino et al. 2005). To begin to understand the nature and function of Kin4 phosphorylation, we sought to identify the residues that are phosphorylated on Kin4.

Kin4 phosphorylation can only be detected by SDS-PAGE when isolated under denaturing conditions. Phosphorylation of Kin4 is rapidly lost after cells are lysed under native conditions (L. Chan unpublished observations). However, purification of full length Kin4 under transient denaturing conditions is not currently possible due to protein solubility issues (L. Chan unpublished observations). However, we did find that fragments of Kin4 were soluble under denaturing conditions, which allowed us to map the phosphorylation sites of Kin4 in a piecemeal fashion. Development of methods to purify Kin4 under continuous denaturing conditions might circumvent this problem and produce a much more comprehensive map of phosphorylation sites (see Appendix II: development of methods to identify genetic and biochemical interactors of Kin4).

We first purified the kin4(1-341) truncation protein (containing the kinase domain) and mapped phosphorylation sites using LC-MS/MS in collaboration with Scott Carlson in the laboratory of Forest White. This analysis yielded three phosphorylation sites at T9, T42 and a site in the activation loop at either T209, S210 or S213 that could not be unambiguously assigned (Figure 1A). It is important to note that the T9 and T42 sites could only be identified from cells lacking *RTS1* suggesting that these two sites are sensitive to PP2A-Rts1 mediated dephosphorylation. These two sites are similar in sequence in that they both contain a lysine at the -3 position, an aromatic at the +1 position and a glycine at the +2 position (Figure 1A). The third site could not be unambiguously resolved but is likely to be T209 for the following reasons. The most similar kinase to Kin4 in budding yeast is Snf1 (other than the presumed gene duplication

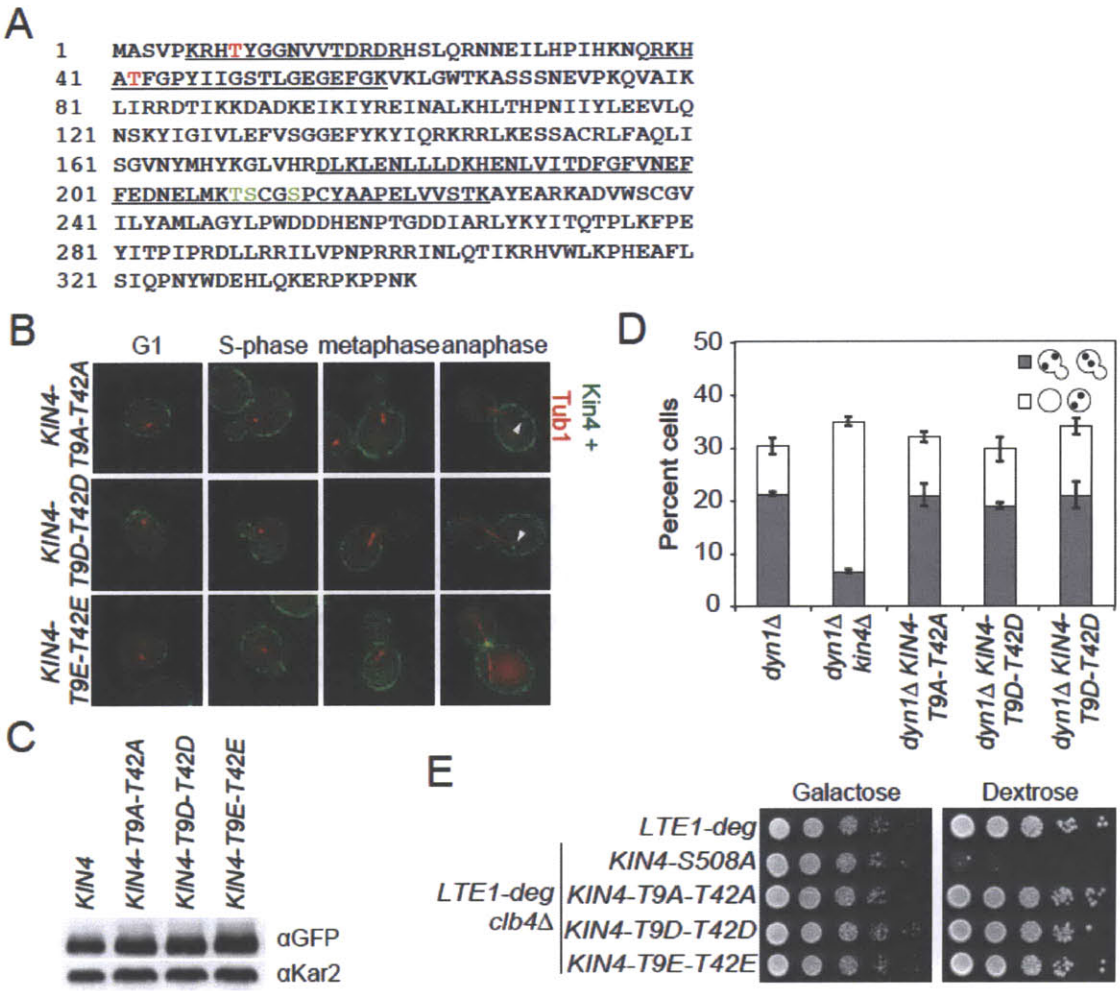

Figure 1. Phospho-mutant analysis of the N-terminus of Kin4

(A) The sequence of amino acids 1-341 of Kin4: phosphorylated residues are in red, ambiguous phosphorylation assignment is in green (T209/S210/S213) and the peptides recovered in the MS analysis are underlined.

(B) Cells expressing an mCherry-Tub1 and Kin4-T9A-T42A-GFP (A24553), Kin4-T9D-T42D-GFP (A24708) or Kin4-T9E-T42E-GFP (A24555) fusion proteins were grown to exponential phase in YePAD and imaged live. The deconvolved GFP signal shown is from 10 serial sections. Kin4-GFP is in green and mCherry-Tub1 is in red. Arrows indicate the mother SPB.

(C) Cells in (B) were analyzed for expression of the Kin4-GFP mutant by western blot. Levels of Kar2 were used as a loading control.

(D) *dyn1*Δ (A17349), *dyn1*Δ *kin4*Δ (A17351), *dyn1*Δ *KIN4-T9A-T42A* (A23868), *dyn1*Δ *KIN4-T9D-T42D* (A24683) and *dyn1*Δ *KIN4-T9E-T42E* (A23873) cells were grown for 24 hours at 14°C. The DNA was visualized by DAPI staining and microtubules were stained by indirect immuno-fluorescence. Gray bars represent the percentage of cells with the arrested morphology and white bars

represent the percentage of cells with the bypassed morphology. $n \geq 100$ and error bars represent SEM.

(E) *LTE1-deg* (A23686), and *LTE1-deg clb4Δ* cells carrying the following *KIN4* alleles: *KIN4-S508A* (A24086), *KIN4-T9A-T42A* (A25292), *KIN4-T9D-T42D* (A25293) or *KIN4-T9E-T42E* (A25294) were spotted on plates containing either dextrose or galactose and raffinose. The first spot represents growth of approximately $3x10^4$ cells and each subsequent spot is a 10 fold serial dilution.

of *KIN4*, *YPL141C*). Snf1 is phosphorylated in the activation loop at the analogous theronine residue to T209 in Kin4. This theronine in Snf1 is required for kinase activity (Estruch et al. 1992). Likewise, mutation of T209 in Kin4 abolishes all kinase activity (Chan and Amon 2009, D'Aquino et al. 2005). Moreover, mutation of T209 to alanine abolished a mobility shift in kin4(1-341) that is likely due to phosphorylation (see Chapter III, Figure 2D).

We focused our attention on the T9 and T42 phospho-sites and generated both phospho-mutant (T to A) and phospho-mimic (T to D/E) mutants of these sites and found that these mutants expressed well (Figure 1C). To begin to characterize these mutants, we examined their localization. Kin4 normally localizes asymmetrically to the mother cell cortex throughout the cell cycle. Both phosho-mutant and phospho-mimic mutants displayed a similar localization pattern (Figure 1B). Kin4 also localizes to the spindle pole body (SPB) in the mother cell during mid-anaphase. The phospho-mutant and phospho-mimics were also capable of SPB loading (Figure 1B). We conclude that both T9 and T42 phospho-sites do not participate in mother cortex nor mother SPB localization.

We next tested if these phospho-sites were important for Kin4's checkpoint function. We took advantage of *dyn1Δ* cells grown at cold temperature (14°C), which induces frequent spindle misposition (Yeh et al. 1995). In the presence of *KIN4*, the SPOC is active and the culture accumulates cells with an anaphase spindle bridging two nuclei contained entirely in the mother cell ("arrested" Figure 1D, gray category). In the absence of *KIN4*, the SPOC is disabled and cells that misposition their spindles prematurely exit mitosis generating cells with no nuclei or too many nuclei ("bypassed" Figure 1D, white category). We found that both the phospho-mutant and the phospho-mimics supported

checkpoint function (Figure 1D). We conclude that phospho-regulation of T9 and T42 is not required for SPOC function.

A major aspect of Kin4 regulation is asymmetric cortical restriction and mutants defective in this regulation hyper-inhibit the MEN. Despite observing no major defects in Kin4 localization in the phospho-mutant and the phospho-mimics, we tested these mutant alleles of *KIN4* for any hyper-activity. The effects of hyperactive *KIN4* are better revealed by disabling the MEN activator, *LTE1*, and the daughter SPB loading inhibitor, *CLB4*. To test if the *KIN4* phospho-mutants and phospho-mimics had any hyperactive effects, we measured the viability of these mutants in the *clb4Δ GAL1-10-URL-3HA-LTE1* (*LTE1-deg*) background. A known hyperactive allele of *KIN4*, *KIN4-S508A*, grew very poorly under conditions of Lte1 depletion (dextrose) (Figure 1E). However, none of the phospho-mimics or the phospho-mutant showed any proliferation defects (Figure 1E). We conclude that phospho-regulation of T9 and T42 of Kin4 likely does not play a role in asymmetric cortical restriction.

Identification and characterization of phosphorylation sites in kin4(655-800)

We next mapped phosphorylation sites on the C-terminal 146 amino acids. This region of Kin4 contains a domain sufficient to localize Kin4 to the cortex of the cell. The LC-MS/MS analysis revealed 10 phosphorylation sites, two of which could not be assigned unambiguously (Figure 2A). We also analyzed kin4(655-800)-F793A based on its lack of cortical localization and the hypo-phosphorylation of kin4-F793A (Figure 2B). This construct was found to only have two phosphorylation sites at S671 and S682 (Figure 2A). This suggests that phosphorylation of the C-terminus of Kin4 either requires cortical localization or that cortical localization is required for phosphorylation.

We generated phospho-mutants with varying numbers of phospho-sites mutated to alanine (*KIN4-7A, KIN4-9A, KIN4-10A-1, KIN4-10A-2, KIN4-12A* – see Table 1) and found that they expressed well (Figure 2D). We examined the localization of these mutants and found that Kin4-7A, Kin4-9A and Kin4-10A-2 all localized as wild-type (Figure 2C). Kin4-10A-1 displayed a symmetric cortical localization pattern that was

Table 1: Phospho-mutants of the C-terminus of Kin4

mutant	S671A	S682A	S684A	T685A	S699A	S700A	S704A	S707A	S744A	S748A	S770A	S773A
7A					X	X	X		X	X	X	X
9A			X	X	X	X	X	X	X		X	X
10A-1	X		X	X	X	X	X	X	X		X	X
10A-2			X	X	X	X	X	X	X	X	X	X
12A	X	X	X	X	X	X	X	X	X	X	X	X

weaker than that previously described for the Kin4-S508A symmetric mutant (Figure 2C, Chapter III). Kin4-10A-1 did load onto the mother SPB but did not load onto the daughter SPB in the ~50 anaphase cells inspected (data not shown). Kin4-12A also displayed this weak symmetric localization but also displayed a weaker cortical localization pattern than wild-type suggesting that phosphorylation is a prerequisite for efficient cortical localization (Figure 2C).

We next examined if these phospho-mutants behaved as gain or loss of function alleles of *KIN4*. We found that all phospho-mutants supported SPOC function suggesting that these phospho-mutants are not hypomorphic (Figure 2E). We also found that these phospho-mutants did not hyper-inhibit the MEN in the absence of *LTE1* and *CLB4* suggesting that these mutants are not hypermorphic (Figure 2F). This was particularly surprising for the *KIN4-10A-1* mutant that localizes more symmetrically than wild-type. Perhaps the level of symmetric localization required to hyper-inhibit the MEN is only provided by the *KIN4-S508A* mutation and the 10A-1 mutation is not sufficient. It is also possible that the sites mutated in the 10A-1 mutant represent two functional pools, one that is involved in asymmetric cortical localization of Kin4 and one that might be involved in exclusion from the daughter SPB. Indeed, we did not observe daughter SPB loading of the Kin4-10A-1 mutant while we did observe low levels of this loading in the S508A mutant. It would be informative to characterize SPB loading in the *KIN4-10A-1 clb4*Δ double mutant. We conclude that phosphorylation of the C-terminus does not play a major functional role in either activating or inhibiting Kin4.

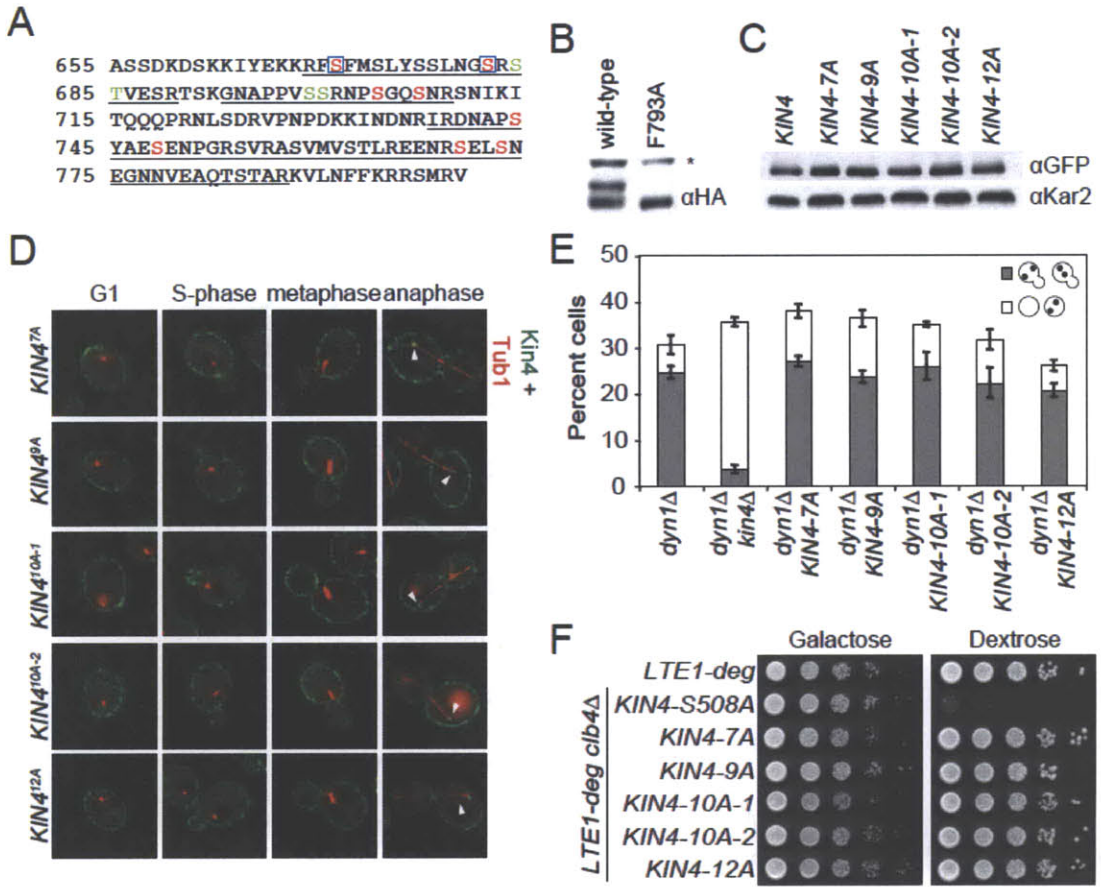

Figure 2. Phospho-mutant analysis of the C-terminus of Kin4

(A) The sequence of amino acids 655-800 of Kin4: phosphorylated residues are in red, ambiguous phosphorylation assignment is in green (S684/T685 and S699/S700), residues found to also be phosphorylated in the F793A sample are boxed in blue and the peptides recovered in the MS analysis are underlined.

(B) Cells expressing Kin4-3HA (A11779) or kin4-F793A-3HA (A20606) were lysed and analyzed as in Figure 1C. The asterisk indicates a cross reacting band with the HA antibody.

(C) expressing an mCherry-Tub1 and GFP fused Kin4 with the following mutations: *KIN4-7A* (A21644), *KIN4-9A* (A21645), *KIN4-10A-1* (A21641), *KIN4-10A-2* (A21647) and *KIN4-12A* (A21651) were imaged as in Figure 1B.

(D) Cells in (C) were analyzed as in Figure 1B.

(E) *dyn1Δ* (A17349), *dyn1Δ kin4Δ* (A17351), *dyn1Δ KIN4-7A* (A21328), *dyn1Δ KIN4-9A* (A21334), *dyn1Δ KIN4-10A-1* (A21311), *dyn1Δ KIN4-10A-2* (A21347) and *dyn1Δ KIN4-12A* (A21313) were analyzed as in Figure 1D.

(F) *LTE1-deg* (A23686), and *LTE1-deg clb4Δ* cells carrying the following *KIN4* alleles: *KIN4-S508A* (A24086), *KIN4-7A* (A25296), *KIN4-9A* (A25297), *KIN4-10A-1* (A25295), *KIN4-10A-2* (A25299) or *KIN4-12A* (A25298) were analyzed as in Figure 1E.

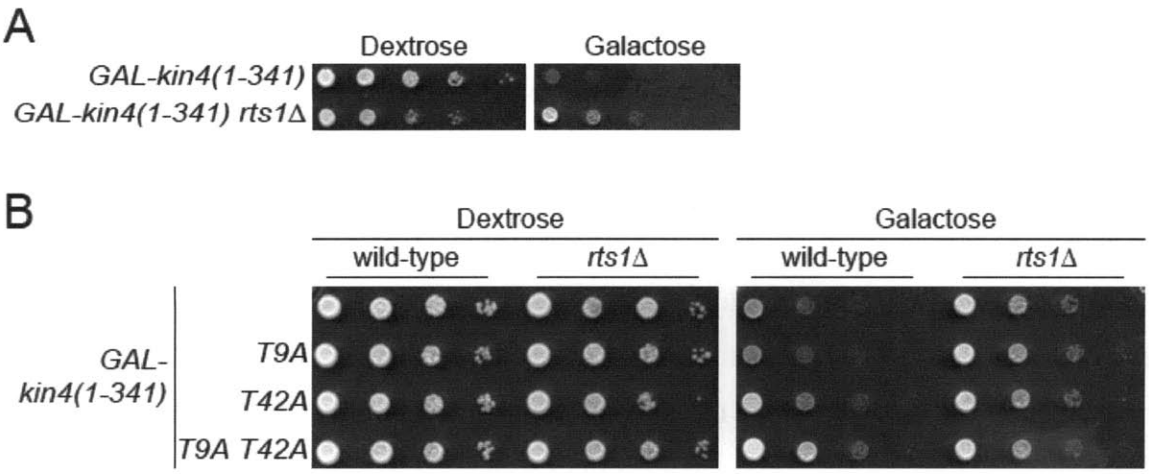

Figure 3. Genetic interaction between the kinase domain of Kin4 and PP2A-Rts1

(A) *GAL1-10-GFP-kin4(1-341)* (A14570) and *GAL1-10-GFP-kin4(1-341) rts1Δ* (A21580) cells were analyzed as in Figure 1E.
(B) *rts1Δ* or wild-type cells carrying *GAL1-10-kin4(1-341)* (A22879 or A22886), *GAL1-10-kin4(1-341)-T9A* (A22880 or A22887), *GAL1-10-kin4(1-341)-T42A* (A22881 or A22888) or *GAL1-10-kin4(1-341)-T9A-T42A* (A22882 or A22889) were analyzed as in Figure 1E.

Interaction of *KIN4* phospho-mutants with *RTS1*

We previously found that the phosphatase, PP2A-Rts1, dephosphorylates Kin4 and is required for SPB loading which is critical for Kin4's SPOC function. If Kin4 dephosphorylation is required for the loss of SPB loading and SPOC function, then one might except that a phospho-mutant would behave as a PP2A-Rts1 insensitive allele of Kin4. We tested this hypothesis by making use of the suppression of *GAL1-10-KIN4* by *rts1Δ*. We have previously shown that overexpression of the kinase domain alone of Kin4 is sufficient to arrest cells in anaphase prior to exit from mitosis (Chapter II). We found that this lethality was suppressed by *rts1Δ* as well (Figure 3A). We reasoned that the only sites relevant for Rts1 regulation of Kin4 must lie in the N-terminal domain. Over-expression of kin4(1-314)-T9A lead to a proliferation defect comparable to overxpression of kin4(1-341) whereas over-expression of kin4(1-341)-T42A displayed a weaker defect (Figure 3B). Overexpression of the kin4(1-341)-T9A-T42A double mutant led to little or no decrease in proliferation (Figure 3B). Deletion of *RTS1* suppressed all of the proliferation defects of the phospho-mutants as well as the wild-type (Figure 3B). The apparent loss of function in the *GAL1-10-kin4(1-341)-T9A-T42A* is particularly surprising

given that full length *KIN4-T9A-T42A* supports full checkpoint function (Figure 1D). This may indicate that other determinants C-terminal to the kinase domain of Kin4 may be involved in Rts1 mediated regulation of Kin4 and as such, using the over-expression phenotype of the kinase domain of Kin4 alone could be a misleading assay. Perhaps measuring the function of Kin4 phospho-mutants in the *rts1*Δ background should be performed in the context of the full length protein perhaps by the same over-expression associated lethality, localization to SPBs or checkpoint function. Indeed we have observed that the electrophoretic mobility shift associated with Kin4 in *rts1*Δ cells is likely due to hyper-phosphorylation of residues contained within the C-terminus of the protein.

ELM1 is required for Kin4 phosphorylation

To identify regulators of Kin4 phosphorylation, we searched the list of annotated protein kinases and phosphatases that based on localization, function or timing, could be potential regulators of Kin4. This method identified the phosphatase Rts1, and the kinases Elm1 and Cdc28 (Figure 4A). The analysis of the interaction of Rts1 and Kin4 is discussed in chapter II and the analysis of Cdc28 is discussed below. Cells lacking the bud neck associated kinase, Elm1, failed to phosphorylate Kin4 (Figure 4B). As noted in chapter II, dephosphorylation of Kin4 correlates with presumptive time of Kin4 function. If this is the case, then one might expect over-expression of Elm1 to result in hyper-phosphorylation of Kin4 and inactivation of its function. The only previously described mutant phenotype of *ELM1* over-expression is an elongated bud morphology (Moriya and Isono 1999). We over-expressed *ELM1* by driving its expression from the *GAL* promoter on a high copy 2μ plasmid. Despite this massive over-expression, we did not observe a SPOC defect in such cells nor did we observe strong hyper-phosphorylation of Kin4 (Figures 4C and 4D). We conclude that Elm1 is necessary but not sufficient for Kin4 phosphorylation.

A

	gene	phosphorylation shift	strain
Kinases	*ALK2*	none detected	A23356
	BUD32	none detected	A19801
	CBK1	none detected	A19241
	CDC15	none detected	A18280
	CDC28	increased	A19509
	CDC5	none detected	A19182
	CLA4	none detected	A19107
	ELM1	decreased	A20170
	GIN4	none detected	A19540
	HOG1	none detected	A19527
	HSL1	none detected	A19222
	KCC4	none detected	A19544
	KIC1	none detected	A24652
	KIN4	none detected	A22119
	MOB2	none detected	A19240
	PKH1	none detected	A19554
	RCK1 RCK2	none detected	A19669
	SAK1	none detected	A20809
	STE20	none detected	A19517
	YCK1 YCK2	none detected	A19515
	YPL141C	none detected	A19384
Phosphatases	*CDC14*	none detected	A19111
	CDC55	none detected	A19804
	GLC7	none detected	A19808
	PPH21 PPH22	increased	A20126
	RTS1	increased	A20187
	SIT4	increased	A20176

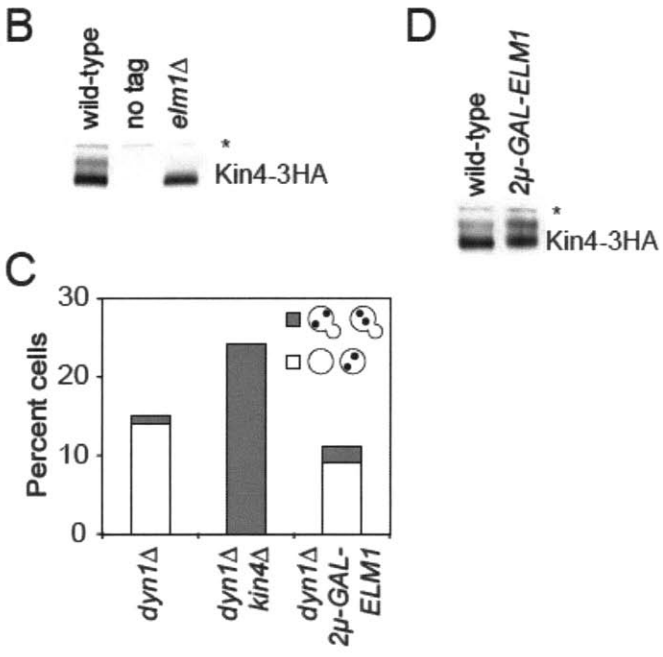

Figure 4. *ELM1* is required for phosphorylation of Kin4

(A) Cells expressing a Kin4-3HA fusion with the indicated mutations were harvested at room temperature for deletion mutations, at half hour intervals for 3 hours after shift to the non-permissive temperature for temperature sensitive mutations or at half hour intervals for 2 hours for analog sensitive mutations and analyzed for Kin4 phosphorylation state by western blot. The results are summarized in the table.

(B) Wild-type (A11779) or *elm1*Δ (A20170) cells expressing a Kin4-3HA fusion were analyzed as in Figure 1C. The asterisk indicates a cross reacting band with the HA antibody.

(C) *dyn1*Δ (A17349), *dyn1*Δ *kin4*Δ (A17351) and *dyn1*Δ *2μ-pGAL1-10-ELM1* (A20965) were grown to log phase in S-LEU + 2% raffinose, shifted to YePA + 2% each raffinose and galactose for 2 hours prior to shift to low temperature.

(D) Wild-type (A11779) and *2μ-pGAL1-10-ELM1* (A20865) cells expressing Kin4-3HA were analyzed as in Figure 1C. The asterisk indicates a cross reacting band with the HA antibody.

Maintenance of cell polarity is required for regulation of Kin4 phosphorylation

A number of chance observations led to the notion that cell polarity may regulate Kin4 phosphorylation. In generating the symmetric mutants of *KIN4*, *kin4(Δ503-511)* and *KIN4-S508A*, we observed that their phosphorylation was subtly increased (Figure 5A). We had also previously observed that Kin4 was transiently hyper-phosphorylated upon

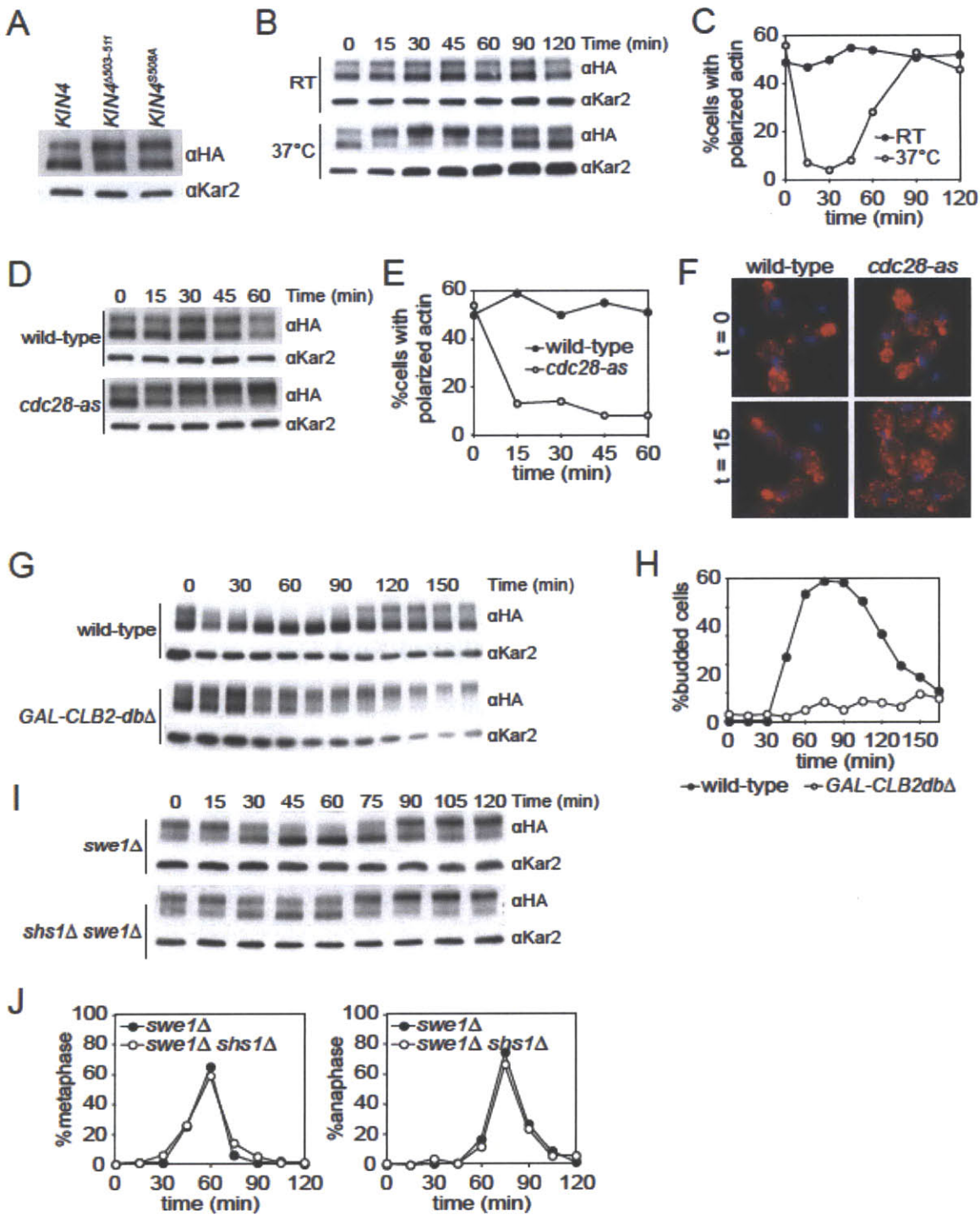

Figure 5. Cell polarity regulates phosphorylation of Kin4.

(A) Cell expressing Kin4-3HA (A11779), Kin4$^{\Delta 503\text{-}511}$-3HA (A20603) or Kin4^{S508A}-3HA (A20608) were lysed and analyzed for Kin4-3HA expression by western blot. Levels of Kar2 were used as a loading control.

(B-C) Cells expressing Kin4-3HA (A11779) were grown to exponential phase in YePAD at room temperature and either shifted to 37°C or maintained at room temperature. Samples were collected for western blot analysis and phalloidin staining. Levels of Kar2 were used as a loading control. Cells were fixed and the actin cytoskeleton was stained with phalloidin and the DNA was stained with DAPI. Cells were counted as polarized when there was clear asymmetric distribution of actin patches in the bud and actin cables in the mother cell. $n \geq 100$.

(D-F) Wild-type (A11779) or *cdc28-as* (A19509) cells expressing a Kin4-3HA fusion protein were grown to exponential phase in YePAD and 5 μM NM-PP1 was added to both cultures at t = 0. Samples were collected for western blot analysis and phalloidin staining and analyzed as in (B) and (C). $n \geq 100$.

(G-H) Wild-type (A11779) or *GAL1-10-CLB2db*Δ (A19510) cells expressing a Kin4-3HA fusion protein were grown in YePA + 2% raffinose and arrested with the addition of 5 μg/mL of α factor. 30 minutes prior to release of the cells from the G1 block, 2% galactose was added to the cultures. Cells were released from the G1 arrest into YePA +2% raffinose + 2% galactose and samples for western blot analysis and bud morphology were collected. Levels of Kar2 were used as a loading control. Cells were fixed and bud morphology was counted.

(I-J) *swe1*Δ (A24023) or *swe1*Δ *shs1*Δ (A24022) cells expressing a Kin4-3HA fusion protein were grown in YePAD and arrested with the addition of 5 μg/mL of α factor. Cells were released from the G1 arrest and samples for western blot and indirect immuno-fluorescence were collected. Levels of Kar2 were used as a loading control. Cells were fixed and stained as in Figure 1D. Metaphase and anaphase cells were determined by spindle and nuclear morphology. $n \geq 100$.

temperature shift from room temperature to 37°C for about 30-45 minutes (Figure 5B and Chapter II Figures 1B and 1C). We had also observed that loss of *CDC28* function led to hyper-phosphorylation of Kin4 (Figure 5D). It has been previously reported that cells shifted to 37°C transiently depolarize their actin cytoskeletons for about 30-45 minutes (Palmer et al. 1992). We also found this to be the case and to also correlated well with Kin4 hyper-phosphorylation (Figures 5B and 5C). We also examined actin polarization in cells lacking Cdc28 activity and observed rapid depolarization of the actin cytoskeleton upon inhibition of Cdc28 (Figure 5E an 5F). This suggests that while Cln-CDK activity is required for establishment of cell polarity, Clb-CDK activity may be required to maintain this polarized state. Moreover, we again observe a strong correlation between loss of cell polarization and Kin4 hyper-phosphorylation. To further test this notion, we examined Kin4 phosphorylation in cells that are unable to establish a polarized actin cytoskeleton.

Clb-CDK activity inhibits Cln transcription and cells that overexpress a non-degradable form of Clb2 (*GAL1-10-CLB2db*Δ) enter the cell cycle without CLN activity and thus do not bud or polarize the cell (Amon, Irniger and Nasmyth 1994). If generation of a polarized cytoskeleton is required to dephosphorylate Kin4, then cells that cannot polarize their cytoskeleton should have hyper-phosphorylated Kin4. Indeed, we found this to be the case (Figures 5G and 5H).

How might cell polarity regulate Kin4 phosphorylation? One possibility is that a kinase exists that is partitioned away from Kin4 in the bud. Such a kinase would be able to phosphorylate Kin4 in G1 when there are no mother and bud compartments but would be unable to access Kin4 during the cell cycle when Kin4 is localized to the mother cell. Given the correlation between time of Kin4 function and Kin4 phosphorylation, such a kinase would likely act as an inhibitor of Kin4 function and possibly serve as a layer of Kin4 regulation in the bud in addition to Lte1 and Clb4. To test this hypothesis, we took advantage of the fact that the septin ring serves as a diffusion barrier preventing daughter specific components from leaking back into the mother (Barral et al. 2000, Takizawa et al. 2000). Impairment of the septin ring leads to a low level of leakiness in daughter specific factors. To bypass the cell cycle delay observed in septin mutants due to activation of the morphogenesis checkpoint, we performed our analysis in the *swe1*Δ mutant background (reviewed in (Keaton and Lew 2006)). Consistent with the existence of a bud-localized kinase for Kin4, we observed mild hyper-phosphorylation of Kin4 in the septin mutant (Figures 5I and 5J). Identification of this kinase would be important to the further study of the phospho-regulation of Kin4.

Experimental Procedures

Yeast Strains and Growth Conditions

All strains are derivatives of W303 (A2587) and are listed in Table 2. *mob2Δ::His3Mx6, cbk1Δ::His3Mx6, ste20Δ::TRP1, elm1Δ::TRP1, sak1Δ::NatMx6, swe1Δ::NatMx6, alk2Δ::TRP1* and *kic1Δ::His3Mx6* were constructed by standard PCR based methods (Goldstein and McCusker 1999, Longtine et al. 1998). *kin4(Δ503-511)-3HA, kin4-F793A-3HA, kin4-S508A-3HA, KIN4(S671A, S684A, T685A, S699A, S700A, S704A, S707A, S744A, S770A, S773A), KIN4(S671A, S682A, S684A, T685A, S699A, S700A, S704A, S707A, S744A, S748A, S770A, S773A), KIN4(S699A, S700A, S704A, S744A, S748A, S770A, S773A), KIN4(S684A, T685A, S699A, S700A, S704A, S707A, S744A, S770A, S773A), KIN4(S684A, T685A, S699A, S700A, S704A, S707A, S744A, S748A, S770A, S773A), KIN4-T9A-T42A* and *KIN4-T9E-T42E, KIN4-T9D-T42D* were constructed by two-step gene replacement using the *URA3* gene from *Kluyveromyces lactis* and PCR products derived from plasmids pA1607, pA1608 and pA1609 respectively pA1607, pA1609, pA1608, pA1646, pA1648, pA1685, pA1687, pA1688, pA1741, pA1774 and pA1768 respectively. *ura3:pGAL1-10-kin4(1-341)-3HA:URA3, ura3:pGAL1-10-kin4(1-341)-T9A-3HA:URA3, ura3:pGAL1-10-kin4(1-341)-T42A-3HA:URA3* and *ura3:pGAL1-10-kin4(1-341)-T9A-T42A-3HA:URA3* were generated by digesting plasmids pA1725, pA1739, pA1740 and pA1741 with EcoRV and integrated at the *URA3* locus. Growth conditions are described in the figure legends.

Plasmid Construction

All plasmids used in this study are listed in Table 3. pA1607 was constructed by digesting pA1207 (D'Aquino et al. 2005) and a PCR fragment containing the Δ503-511 deletion (constructed by PCR mediated ligation of two overlapping fragments spanning the deletion) with BsrGI and MscI and ligating the two fragments together. pA1608, pA1609, pA1646, pA1648, pA1685, pA1687 and pA1688 were generated by site directed mutagenesis of pA1207. pA1725 was constructed by digesting YIplac211-*pGAL1-10* (pA55) and a PCR product containing *kin4(1-341)-3HA* with XbaI and HindIII and ligating the two fragments together. pA1739, pA1740, pA1741, pA1768 and pA1774 were generated by site directed mutagenesis of pA1725.

Immunoblot Analysis

Immunoblot analysis to determine total amount of Kin4-GFP and Kin4-3HA were as previously described (Chan and Amon 2009). For immunoblot analysis of Kar2, cell lysates were prepared as previously described (Chan and Amon 2009). Kar2 was detected using a rabbit anti-Kar2 anti-serum (Rose, Misra and Vogel 1989) at 1:200,000.

Fluorescence Microscopy

Indirect *in situ* immunofluorescence methods for Tub1 were as previously described (Kilmartin and Adams 1984). Visualization of F-actin is as previously described (Monje-Casas and Amon 2009). Live cell imaging techniques are as previously described (Chan and Amon 2009).

Identification of phosphorylation sites

Denaturing immuno-precipitation to purify Kin4 fragments is as described in (Brar et al. 2006) with the following modification: Kin4-3HA fragments were pulled down using an anti-HA affinity matrix [Roche]. LC-MS/MS to identify phosphorylated residues is as previously described (Brar et al. 2006).

Table 2: Yeast Strains

A2587	*MATa ade2-1, leu2-3, ura3, trp1-1, his3-11,15, can1-100, GAL, psi+* (wild-type W303)
A11779	*MATa KIN4-3HA:KanMx6*
A14570	*MATa His3Mx6:pGAL1-10-GFP-kin4(1-341)-3HA:KanMx6*
A17349	*MATa dyn1Δ::URA3*
A17351	*MATa kin4Δ::KanMx6 dyn1Δ::URA3*
A18280	*MATa cdc15::CDC15-as1(L99G)::URA3 KIN4-3HA:KanMX6*
A19107	*MATa KIN4-3HA:KanMx6, cla4Δ::His3Mx6*
A19111	*MATa KIN4-3HA:KanMx6 cdc14-3*
A19182	*MATa KIN4-3HA:KanMx6 cdc5-1*
A19222	*MATa KIN4-3HA:KanMx6 hsl1Δ::KanMx6*
A19240	*MATa KIN4-3HA:KanMx6 mob2Δ::His3Mx6*
A19241	*MATa KIN4-3HA:KanMx6 cbk1Δ::His3Mx6*
A19384	*MATa ypl141cΔ::His3Mx6 ura3:kin4-T209A-3HA:URA3*
A19509	*MATa KIN4-3HA:KanMx6 cdc28-as1*
A19510	*MATa GAL-CLB2dbΔ:URA3 KIN4-3HA:KanMx6*
A19515	*MATalpha, yck1Δ yck2-1ts Kin4-3HA:KanMx6* (S288C derivative)
A19517	*MATa KIN4-3HA:KanMx6 ste20Δ::TRP1*
A19527	*MATa hog1Δ::KanMx6 KIN4-3HA:KanMx6*
A19540	*MATa KIN4-3HA:TRP1 gin4Δ::KanMx6* (BY4741/W303 hybrid)
A19544	*MATa KIN4-3HA:TRP1 kcc4Δ::KanMx6* (BY4741/W303 hybrid)
A19554	*MATa KIN4-3HA:TRP1 pkh1Δ::KanMx6* (BY4741/W303 hybrid)
A19669	*MATa KIN4-3HA:TRP1 rck1Δ::KanMx6 rck2Δ::KanMx6* (BY4741/W303 hybrid)
A19801	*MATa KIN4-3HA:HISMx6, bud32Δ::KanMx6* (BY4741)
A19804	*MATa KIN4-3HA:TRP1 cdc55Δ::KanMx6*
A19808	*MATa trp1:glc7-12:TRP1 glc7Δ::LEU2 KIN4-3HA:KanMx6*
A20126	*MATa pph21Δ1::HIS3 pph22-12 pph3Δ1::LYS2 ssd1-d2 KIN4-3HA:KanMx6*
A20170	*MATa KIN4-3HA:KanMx6 elm1Δ::TRP1*
A20176	*MATa sit4Δ::HIS3 ssd1-d1 KIN4-3HA:KanMx6 Ycp50-sit4-102 (URA/CEN)*
A20187	*MATa KIN4-3HA:KanMx6 rts1Δ::NatMx6*
A20603	*MATa kin4(Δ503-511)-3HA:KanMx6*
A20606	*MATa Kin4-F793A-3HA:KanMx6*
A20608	*MATa Kin4-S508A-3HA:KanMx6*
A20809	*MATa KIN4-3HA:KanMx6 sak1Δ::NatMx6*
A20865	*MATa KIN4-3HA:KanMX6 yep13-pGAL1-10-ELM1*
A20965	*MATa KIN4-3HA:KanMX6 yep13-pGAL1-10-ELM1 dyn1Δ::URA3*
A21311	*MATa KIN4(S671A, S684A, T685A, S699A, S700A, S704A, S707A, S744A, S770A, S773A):Kin4'3'UTR:KanMx6 dyn1Δ::URA3*
A21313	*MATa KIN4(S671A, S682A, S684A, T685A, S699A, S700A, S704A, S707A, S744A, S748A, S770A, S773A):Kin4'3'UTR:KanMx6 dyn1Δ::URA3*
A21328	*MATa KIN4(S699A, S700A, S704A, S744A, S748A, S770A, S773A):Kin4'3'UTR:KanMx6 dyn1Δ::URA3*
A21334	*MATa KIN4(S684A, T685A, S699A, S700A, S704A, S707A, S744A, S770A,*

S773A):Kin4'3'UTR:KanMx6 dyn1Δ::URA3

A21347 *MATa KIN4(S684A, T685A, S699A, S700A, S704A, S707A, S744A, S748A, S770A, S773A):Kin4'3'UTR:KanMx6 dyn1Δ::URA3*

A21580 *MATa His3Mx6:pGal1-10-GFP-kin4(1-341)-3HA::KanMx6 rts1Δ::NatMx6*

A21641 *MATa ura3:pRS306-mCherry-TUB1:URA3 KIN4(S671A, S684A, T685A, S699A, S700A, S704A, S707A, S744A, S770A, S773A)-GFP:HisMx6:Kin4'3'UTR:KanMx6*

A21644 *MATa ura3:pRS306-mCherry-TUB1:URA3 KIN4(S699A, S700A, S704A, S744A, S748A, S770A, S773A)-GFP:HisMx6:Kin4'3'UTR:KanMx6*

A21645 *MATa ura3:pRS306-mCherry-TUB1:URA3 KIN4(S684A, T685A, S699A, S700A, S704A, S707A, S744A, S770A, S773A)-GFP:HisMx6:Kin4'3'UTR:KanMx6*

A21647 *MATa ura3:pRS306-mCherry-TUB1:URA3 KIN4(S684A, T685A, S699A, S700A, S704A, S707A, S744A, S748A, S770A, S773A)-GFP:HisMx6:Kin4'3'UTR:KanMx6*

A21651 *MATa ura3:pRS306-mCherry-TUB1:URA3 KIN4(S671A, S682A, S684A, T685A, S699A, S700A, S704A, S707A, S744A, S748A, S770A, S773A)-GFP:HisMx6*

A22119 *MATa kin4-T209A-3HA:KanMx6*

A22879 *MATa ura3:pGAL1-10-kin4(1-341)-3HA:URA3*

A22880 *MATa ura3:pGAL1-10-kin4(1-341)-T9A-3HA:URA3*

A22881 *MATa ura3:pGAL1-10-kin4(1-341)-T42A-3HA:URA3*

A22882 *MATa ura3:pGAL1-10-kin4(1-341)-T9A-T42A-3HA:URA3*

A22886 *MATa rts1Δ::NatMx6 ura3:pGAL1-10-kin4(1-341)-3HA:URA3*

A22887 *MATa rts1Δ::NatMx6, ura3:pGAL1-10-kin4(1-341)-T9A-3HA:URA3*

A22888 *MATa rts1Δ::NatMx6 ura3:pGAL1-10-kin4(1-341)-T42A-3HA:URA3*

A22889 *MATa rts1Δ::NatMx6 ura3:pGAL1-10-kin4(1-341)-T9A-T42A-3HA:URA3*

A23356 *MATa alk2Δ::TRP1 KIN4-3HA:KanMx6*

A23686 *MATa KanMx6:pGAL1-10-URL-3HA-LTE1*

A23868 *MATα KIN4-T9A-T42A:Kin4'3'UTR:KanMx6 dyn1Δ::URA3*

A23873 *MATa KIN4-T9E-T42E:Kin4'3'UTR:KanMx6 dyn1Δ::URA3*

A24022 *MATa shs1Δ::His3Mx6 KIN4-3HA:KanMx6 swe1Δ::NatMx6*

A24023 *MATa KIN4-3HA:KanMx6 swe1Δ::NatMx6*

A24086 *MATa KanMx6:pGAL1-10-URL-3HA-LTE1 KIN4-S508A:Kin4'3'UTR:KanMx6 clb4Δ::HIS3*

A24553 *MATa KIN4-T9A-T42A-GFP:His3Mx6:Kin4'3'UTR:KanMx6 ura3:pRS306-mCherry-TUB1:URA3*

A24555 *MATa KIN4-T9E-T42E-GFP:His3Mx6:Kin4'3'UTR:KanMx6 ura3:pRS306-mCherry-TUB1:URA3*

A24652 *MATa kic1Δ::NatMx6 KIN4-3HA:KanMx6*

A24683 *MATa KIN4-T9D-T42D:Kin4'3'UTR:KanMx6 dyn1Δ::URA3*

A24708 *MATa KIN4-T9D-T42D-GFP:His3Mx6:Kin4'3'UTR:KanMx6 ura3:pRS306-mCherry-TUB1:URA3*

A25292 *MATa KanMx6:pGAL1-10-URL-3HA-LTE1 KIN4-T9A-T42A:Kin4'3'UTR:KanMx6 clb4Δ::HIS3*

A25293 *MATa KanMx6:pGAL1-10 -URL-3HA-LTE1 KIN4-T9E-*

T42E:Kin4'3'UTR:KanMx6 clb4Δ::HIS3

A25294 *MATa KanMx6:pGAL1-10 -URL-3HA-LTE1 KIN4(T9D, T42D):Kin4'3'UTR:KanMx6 clb4Δ::HIS3*

A25295 *MATa KanMx6:pGAL1-10 -URL-3HA-LTE1 clb4Δ::HIS3 Kin4(S671A, S684A, T685A, S699A, S700A, S704A, S707A, S744A, S770A, S773A):Kin4'3'UTR:KanMx6*

A25296 *MATa KanMx6:pGAL1-10 -URL-3HA-LTE1 clb4Δ::HIS3 Kin4(S699A, S700A, S704A, S744A, S748A, S770A, S773A):Kin4'3'UTR:KanMx6*

A25297 *MATa KanMx6:pGAL1-10 -URL-3HA-LTE1 clb4Δ::HIS3 Kin4(S684A, T685A, S699A, S700A, S704A, S707A, S744A, S770A, S773A):Kin4'3'UTR:KanMx6*

A25298 *MATa KanMx6:pGAL1-10 -URL-3HA-LTE1 clb4Δ::HIS3 Kin4(S671A, S682A, S684A, T685A, S699A, S700A, S704A, S707A, S744A, S748A, S770A, S773A):Kin4'3'UTR:KanMx6*

A25299 *MATa KanMx6:pGAL1-10 -URL-3HA-LTE1 clb4Δ::HIS3 Kin4(S682A, S684A, T685A, S699A, S700A, S704A, S744A, S748A, S770A, S773A):Kin4'3'UTR:KanMx6*

A25293 *MATa KanMx6:pGAL1-10 -URL-3HA-LTE1 KIN4(T9E, T42E):Kin4'3'UTR:KanMx6 clb4Δ::HIS3*

A25294 *MATa KanMx6:pGAL1-10 -URL-3HA-LTE1 KIN4(T9D, T42D):Kin4'3'UTR:KanMx6 clb4Δ::HIS3*

A25295 *MATa KanMx6:pGAL1-10 -URL-3HA-LTE1 clb4Δ::HIS3 Kin4(S671A, S684A, T685A, S699A, S700A, S704A, S707A, S744A, S770A, S773A):Kin4'3'UTR:KanMx6*

A25296 *MATa KanMx6:pGAL1-10 -URL-3HA-LTE1 clb4Δ::HIS3 Kin4(S699A, S700A, S704A, S744A, S748A, S770A, S773A):Kin4'3'UTR:KanMx6*

Table 3: Plasmids

pA1607	YIplac211-*kin4(Δ503-511)-3HA*
pA1608	YIplac211-*kin4-F793A-3HA*
pA1609	YIplac211-*KIN4-S508A-3HA*
pA1646	YIplac211-*KIN4(S671A, S684A, T685A, S699A, S700A, S704A, S707A, S744A, S770A, S773A)-3HA*
pA1648	YIplac211-*KIN4(671A, S682A, S684A, T685A, S699A, S700A, S704A, S707A, S744A, S748A, S770A, S773A)-3HA*
pA1685	YIplac211-*KIN4(S699A, S700A, S704A, S744A, S748A, S770A, S773A)-3HA*
pA1687	YIplac211-*KIN4(S684A, T685A, S699A, S700A, S704A, S707A, S744A, S770A, S773A)-3HA*
pA1688	YIplac211-*KIN4(S682A, S684A, T685A, S699A, S700A, S704A, S744A, S748A, S770A, S773A)-3HA*
pA1725	YIplac211-*pGAL1-10-kin4(1-341)-3HA-tADH1*
pA1739	YIplac211-*pGAL1-10-kin4(1-341)-T9A-3HA-tADH1*
pA1740	YIplac211-*pGAL1-10-kin4(1-341)-T42A-3HA-tADH1*
pA1741	YIplac211-*pGAL1-10-kin4(1-341)-T9A-T42A-3HA-tADH1*
pA1768	YIplac211-*pGAL1-10-kin4(1-341)-T9D-T42D-3HA-tADH1*
pA1774	YIplac211-*pGAL1-10-kin4(1-341)-T9E-T42E-3HA-tADH1*

References

Amon, A., S. Irniger & K. Nasmyth (1994) Closing the cell cycle circle in yeast: G2 cyclin proteolysis initiated at mitosis persists until the activation of G1 cyclins in the next cycle. *Cell,* 77, 1037-50.

Barral, Y., V. Mermall, M. S. Mooseker & M. Snyder (2000) Compartmentalization of the cell cortex by septins is required for maintenance of cell polarity in yeast. *Mol Cell,* 5, 841-51.

Brar, G. A., B. M. Kiburz, Y. Zhang, J. E. Kim, F. White & A. Amon (2006) Rec8 phosphorylation and recombination promote the step-wise loss of cohesins in meiosis. *Nature,* 441, 532-6.

Chan, L. Y. & A. Amon (2009) The protein phosphatase 2A functions in the spindle position checkpoint by regulating the checkpoint kinase Kin4. *Genes Dev,* 23, 1639-49.

D'Aquino, K. E., F. Monje-Casas, J. Paulson, V. Reiser, G. M. Charles, L. Lai, K. M. Shokat & A. Amon (2005) The protein kinase Kin4 inhibits exit from mitosis in response to spindle position defects. *Mol Cell,* 19, 223-34.

Estruch, F., M. A. Treitel, X. Yang & M. Carlson (1992) N-terminal mutations modulate yeast SNF1 protein kinase function. *Genetics,* 132, 639-50.

Goldstein, A. L. & J. H. McCusker (1999) Three new dominant drug resistance cassettes for gene disruption in Saccharomyces cerevisiae. *Yeast,* 15, 1541-53.

Keaton, M. A. & D. J. Lew (2006) Eavesdropping on the cytoskeleton: progress and controversy in the yeast morphogenesis checkpoint. *Curr Opin Microbiol,* 9, 540-6.

Kilmartin, J. V. & A. E. Adams (1984) Structural rearrangements of tubulin and actin during the cell cycle of the yeast Saccharomyces. *J Cell Biol,* 98, 922-33.

Longtine, M. S., A. McKenzie, 3rd, D. J. Demarini, N. G. Shah, A. Wach, A. Brachat, P. Philippsen & J. R. Pringle (1998) Additional modules for versatile and economical PCR-based gene deletion and modification in Saccharomyces cerevisiae. *Yeast,* 14, 953-61.

Monje-Casas, F. & A. Amon (2009) Cell polarity determinants establish asymmetry in MEN signaling. *Dev Cell,* 16, 132-45.

Moriya, H. & K. Isono (1999) Analysis of genetic interactions between DHH1, SSD1 and ELM1 indicates their involvement in cellular morphology determination in Saccharomyces cerevisiae. *Yeast,* 15, 481-96.

Palmer, R. E., D. S. Sullivan, T. Huffaker & D. Koshland (1992) Role of astral microtubules and actin in spindle orientation and migration in the budding yeast, Saccharomyces cerevisiae. *J Cell Biol,* 119, 583-93.

Rose, M. D., L. M. Misra & J. P. Vogel (1989) KAR2, a karyogamy gene, is the yeast homolog of the mammalian BiP/GRP78 gene. *Cell,* 57, 1211-21.

Takizawa, P. A., J. L. DeRisi, J. E. Wilhelm & R. D. Vale (2000) Plasma membrane compartmentalization in yeast by messenger RNA transport and a septin diffusion barrier. *Science,* 290, 341-4.

Yeh, E., R. V. Skibbens, J. W. Cheng, E. D. Salmon & K. Bloom (1995) Spindle dynamics and cell cycle regulation of dynein in the budding yeast, Saccharomyces cerevisiae. *J Cell Biol,* 130, 687-700.

Appendix II: Development of Methods to Identify Genetic and Biochemical Interactors of Kin4

Leon Y. Chan performed all experiments.

Introduction

The spindle position checkpoint (SPOC) couples spindle position to cell cycle progression. Kin4 delays mitotic exit by inhibiting the mitotic exit network (MEN) when the spindle has not elongated into the daughter. This inhibition appears to be controlled by restricting Kin4 to specific cellular locations and not by regulating its activity (See Chapter III). How this restricted localization is controlled is unknown. Only one potential binding partner of Kin4 has been identified and only one potential regulator of Kin4 has been identified.

Spc72 appears to directly or indirectly anchor Kin4 to the spindle pole body (SPB). While this is critical for Kin4 function, it also appears that anchoring Kin4 to the mother cell cortex is key for its function and likely restriction as mutants defective in cortical anchorage fail to as SPOC components and do not asymmetrically localize (see Chapter III). PP2A-Rts1 appears to regulate Kin4 function, likely by promoting its proper localization to the cortex and SPB. However, how Kin4 is localized to the mother cell but not the daughter cell is unknown.

By screening a multi-copy plasmid library of genomic fragments for genes that can suppress Kin4 over-expression associated lethality, we have identified two previously known regulators of mitotic exit and potentially one novel regulator, possibly of Kin4 itself. In light of what has been learned about Kin4 regulation during my thesis project, we propose improved and more focused screens to identify cortical anchors and asymmetry factors. As a natural extension of these screens, we propose an additional screen for factors that control SPB asymmetry and determination. Lastly, we discuss the limitations associated with biochemical methods in the analysis of Kin4 and propose a purification scheme that might aid in identifying Kin4 interactors.

Results and Discussion

A genetic screen identifies *YHR127W* as a potential regulator of Kin4

To identify potential interactors of *KIN4*, we designed a screen based on the most "screen-able" phenotype associated with *KIN4* known at the time, lethality upon over-expression of Kin4. We reasoned that potential negative regulators of Kin4 might be identified by focusing our mutant hunt on hypermoprhic mutants that suppress the lethality associated with Kin4 over-expression. To identify genes that when over-produced suppress Kin4 over-expression associated lethality, we transformed *pGAL1-10-KIN4* cells with a high copy plasmid library of yeast genomic DNA and isolated mutants that could grow upon induction of the *GAL* promoter. We screened ~28,000 colonies and identified six genomic fragments that in high copy could suppress the lethality of *pGAL1-10-KIN4* (Figure 1A). We identified three genes involved in regulation of the *GAL* promoter, *MIG1* – the transcription factor involved in glucose repression of the *GAL* promoter, *GAL80* – the inhibitor of the *GAL* transcriptional activator, Gal4 and *GAL10* – which likely down regulates expression of *pGAL1-10-KIN4* by providing extra copies of the *GAL1-10* promoter to titrate away factors like Gal4 which are necessary for galactose mediated transcription. We also identified two known activators of mitotic exit, *SPO12* and *TEM1*. *SPO12* is a member of the Cdc14 Early Anaphase Release (FEAR) network, which promotes timely mitotic exit. Over-expression of Spo12 has previously been shown to bypass the anaphase arrest of other mitotic exit mutants such as *cdc15-2* (Jaspersen et al. 1998). *TEM1* is the central GTPase switch of the MEN and over-expression of Tem1 has been shown to hyperactivate the MEN and bypass some MEN mutants (Alexandru et al. 1999, Ro, Song and Lee 2002).

A third gene was identified from two independent genomic fragments and the genes contained in the overlap of the two fragments are *FUR1*, a gene involved in uridine mono-phosphate synthesis, and *YHR127W*, a gene of unknown function. To identify the relevant suppressor gene, we cloned each gene into the same high copy plasmid and tested their abilities to suppress *pGAL1-10-KIN4*. We found that over-expressed *FUR1* was not able to suppress *pGAL1-10-KIN4* while *YHR127W* suppressed as well as the

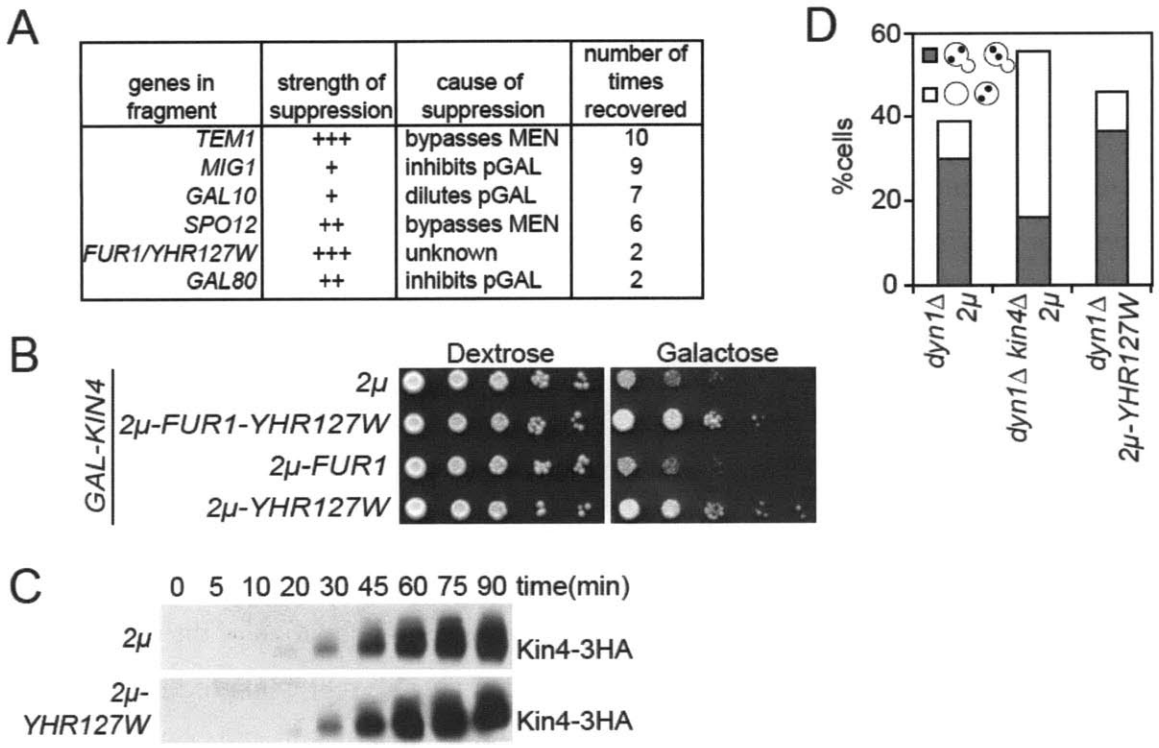

genes in fragment	strength of suppression	cause of suppression	number of times recovered
TEM1	+++	bypasses MEN	10
MIG1	+	inhibits pGAL	9
GAL10	+	dilutes pGAL	7
SPO12	++	bypasses MEN	6
FUR1/YHR127W	+++	unknown	2
GAL80	++	inhibits pGAL	2

Figure 1. Identification of hypermorphic suppressors of Kin4 over-expression

(A) A strain conditionally over-expressing Kin4 (*pGAL1-10-KIN4*, A9249) was transformed with a high copy plasmid library containing random yeast genomic DNA. Mutants were isolated based on their ability to proliferate in the presence of galactose. The genes isolated, the strength of suppression, the likely cause of suppression and the number of times each gene was recovered is summarized in the table.

(B) *pGAL1-10-KIN4* cells carrying 2μ (Yep13, A16798), 2μ-*FUR1-YHR127W* (A16799), 2μ-*FUR1* (A16800) and 2μ-*YHR127W* (A16801) plasmids were spotted on S-LEU plates containing either dextrose or galactose and raffinose. The first spot represents growth of approximately $3x10^4$ cells and each subsequent spot is a 10 fold serial dilution.

(C) *pGAL1-10-3HA-KIN4* cells carrying 2μ (A17084) or 2μ-*YHR127W* (A17085) were grown in YeP + 2% raffinose. At time 0, 2%galactose was added to the medium and samples for western blot analysis were collected and analyzed for expression of 3HA-Kin4.

(D) *dyn1*Δ 2μ (A16624), *dyn1*Δ *kin4*Δ 2μ (A16625) and *dyn1*Δ 2μ-*YHR127W* (A16627) cells were grown for 24 hours at 14°C. The DNA was visualized by DAPI staining and microtubules were stained by indirect immuno-fluorescence. Gray bars represent the percentage of cells with the arrested morphology and white bars represent the percentage of cells with the bypassed morphology. $n \geq 100$.

original plasmid isolate (Figure 1B). To test if *YHR127W* is involved in regulation of the *GAL* promoter, we analyzed the expression of 3HA-Kin4 expressed from the *GAL* promoter in the presence and absence of high copy *YHR127W*. Like *TEM1* and unlike *GAL80*, 2μ-*YHR127W* did not inhibit induction of the *GAL* promoter (data not shown and Figure 1C). If hypermorphic *YHR127W* antagonizes *KIN4* function, we might expect 2μ-*YHR127W* to behave as a *kin4*Δ mutant. Using the *dyn1*Δ mutant grown at low temperature which induces spindle misposition to analyze SPOC function, we observed that the *dyn1*Δ 2μ-*YHR127W* mutant supported checkpoint function (Yeh et al. 1995) (Figure 1D). It is possible that high copy *YHR127W* is not able to sufficiently suppress *KIN4* function when the spindle is mispositioned or perhaps, *YHR127W* may promote mitotic exit for reasons unrelated to *KIN4* antagonism. A more detailed examination of Kin4 localization in both gain and loss of function *YHR127W* mutants would be helpful in dissecting the function of this gene.

What little is known about *YHR127W* might offer some hypotheses as to how *YHR127W* might mediate suppression of *pGAL1-10-KIN4*. This gene was previously isolated as a high copy suppressor of a dominant negative mutation in the GTPase, Sec4. Perhaps *YHR127W* plays a similar role here for the GTPase, Tem1. *YHR127W* has also recently been shown to be required for efficient asymmetric SPB localization of the cytoskeletal adapter protein, Kar9 (Schoner et al. 2008). This is of particular interest in that SPB asymmetry also plays a role in Kin4 restriction. Examination of Kin4-S508A-GFP in both *yhr127w*Δ and 2μ-*YHR127W* mutants should uncover what if any role this gene plays in Kin4 SPB localization.

A proposed genetic screen to identify cortical anchors and asymmetry factors for Kin4

As shown in Chapter III, a major mode of restricting Kin4 activity is its asymmetric localization to the mother cell cortex. We have no current insights into the machinery that establishes or maintains this unusual localization pattern. We know that cortical anchorage is important for Kin4 function and suspect that it participates in the maintenance of asymmetric localization. To identify factors that control asymmetric

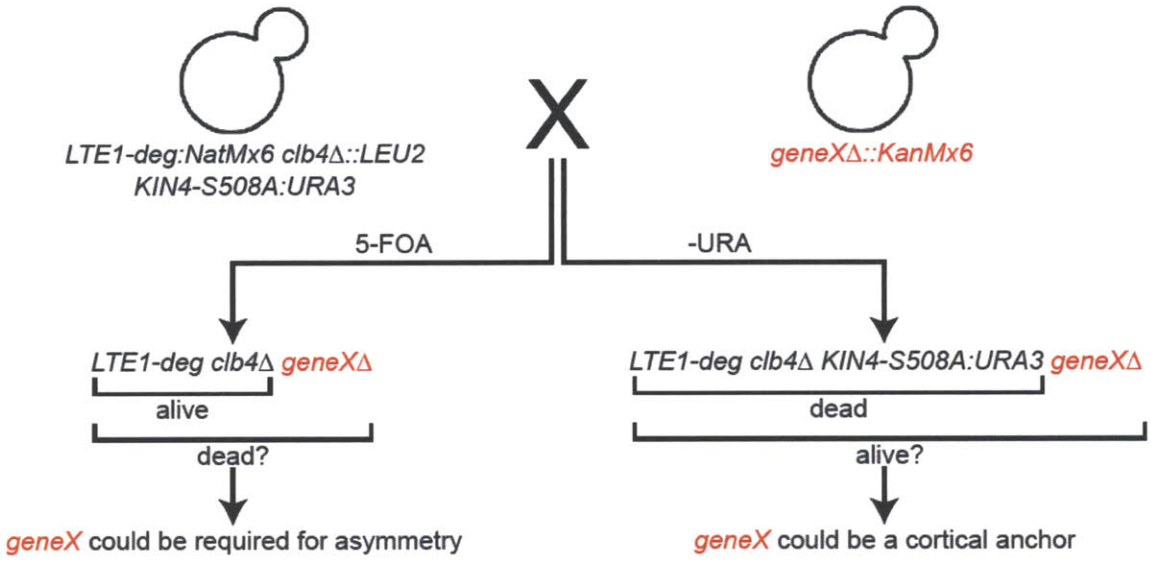

Figure 2. Proposed screens to identify cortical anchors and asymmetry factors for Kin4

localization and cortical anchorage, we propose a screen based on the conditional lethality of the *pGAL1-10-URL-3HA-LTE1* (*LTE1-deg*) *clb4Δ KIN4-S508A* mutant. The screen is described in Figure 2 and utilizes a *URA3* marked *KIN4-S508A* allele. The initial cross of the triple mutant is made against the collection of non-essential gene deletions (Tong and Boone 2006). The screen on the left of the diagram negatively selects against *KIN4-S508A* and screens for gene deletions that cause lethality in the *LTE1-deg clb4Δ* double mutant. Loss of function in such *trans* acting genes mimics the S508A *cis* mutation and thus might lead to symmetric localization of Kin4. The screen on the right hand side of the diagram starts from the same cross but positively selects for *KIN4-S508A* and screens for gene deletions that cause suppression of the lethality of *LTE1-deg clb4Δ KIN4-S508A*. Such a screen should identify trans acting factors that *KIN4* requires for its function. *BUB2* and *BFA1* are two such genes and should serve as strong positive controls. Other such genes might include factors required for Kin4 cortical anchorage and activity.

A proposed screen to identify SPB asymmetry factors

Centrosome asymmetry has been shown to be required for spindle positioning and thus proper cell fate determination in stem cell division (reviewed in (Cabernard and Doe

2007)). This asymmetry is also required for proper spindle movement in yeast and as demonstrated in Chapter III, contributes to the restriction of Kin4 activity to only the mother SPB. How spindle asymmetry is generated is unknown. We propose a screen, similar to the ones described above, to identify genes required for SPB asymmetry (Figure 3). To search the collection of non-essential gene deletions for such factors, we cross the *LTE1-deg KIN4-S508A* mutant to the collection and screen for enhancers of the slow growth phenotype of *LTE1-deg KIN4-S508A* double mutants. *KAR9* and *CLB4* are two known factors that behave in this manner and can be used as positive controls. A potential downside to this screen is the dynamic range of the phenotypes being scored. *LTE1-deg KIN4-S508A* is already quite sick and additional deletion of *CLB4* only enhances the sickness by ~10 fold (see Chapter III).

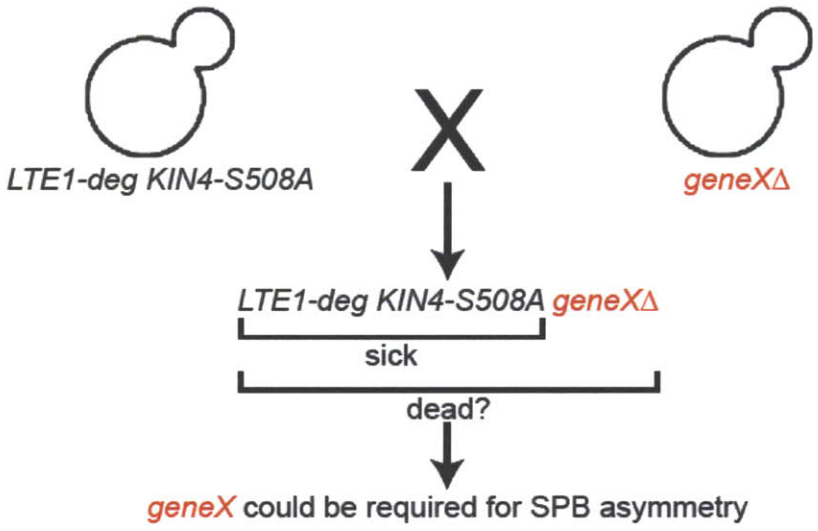

Figure 3. A proposed screen to identify SPB asymmetry factors

Analysis of Kin4 solubility

In an attempt to characterize Kin4's mode of cortical association, we embarked on an analysis of Kin4's differential fractionation and solubility. We first tested its ability to partition in 13,000 and 100,000 g fractions. We found that Kin4 partitions equally between the supernatant and pellet fractions in a 13,000 g centrifugation and only

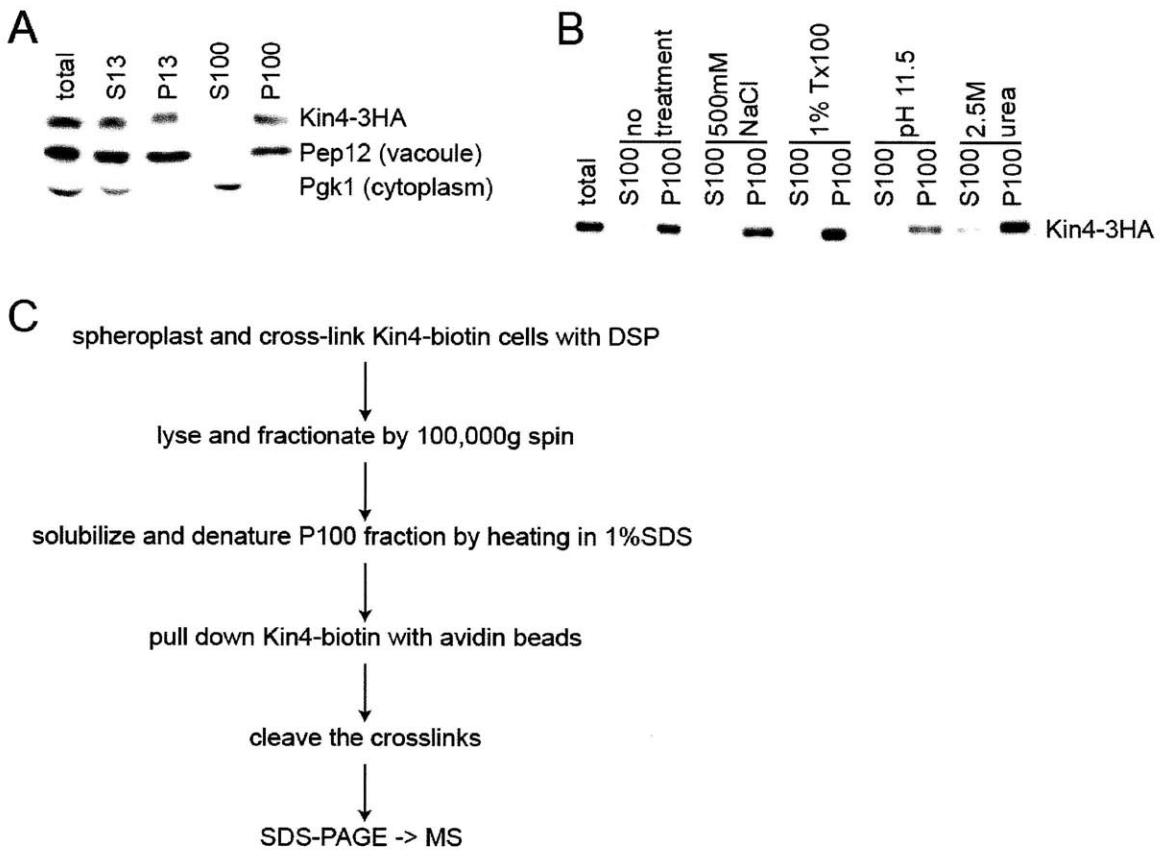

Figure 4. Solubility properties of Kin4 and a proposed scheme to identify Kin4 interactors.

(A) Cells expressing a Kin4-3HA fusion (A11779) were lysed under native conditions and split into three pools. The first was untreated, the second was fractionated by a 13,000 g centrifugation and the third by a 100,000 g centrifugation. Fractions were analyzed for differential partitioning by western blot for Kin4-3HA and the control proteins, Pep12 and Pgk1.

(B) Cells expressing a Kin4-3HA fusion (A11779) were lysed under native conditions and split into six pools. The first pool was untreated and unfractionated. The second through sixth pools were subjected to a 100,000 g fractionation after a one hour incubation under the following conditions: (2) untreated, (3) 500mM NaCl, (4) 1% Triton X-100 (5) pH 11.5 by addition of 100mM sodium carbonate (6) 2.5M urea. The differential solubility was analyzed by western blot.

(C) A schematic describing a proposed method to purify Kin4 interactors. See text for details.

partitions with the pellet in a 100,000 g centrifugation (Figure 4A). This pattern is similar to those of membrane associated proteins such as the vacuolar membrane protein, Pep12 (Figure 4A). We then attempted to examine the mode of cortex association by treating the

cell lysate with various conditions that destabilize protein structure, association or membrane anchorage prior to 100,000 g centrifugation. We found that Kin4 was not solubilized by high salt, high detergent, high pH and only weakly solubilized by high denaturant (Figure 4B). We conclude that Kin4 is a highly insoluble protein.

A proposed method to identify Kin4 binding partners

2-hybrid approaches to identify Kin4 binding partners have proven fruitless (L.Y.C personal observation, Elmar Schiebel personal communication). Biochemical methods to identify interactors are largely defeated by Kin4's solubility profile. A cross-linking/denaturing approach would work if Kin4 remained soluble after transient denaturation but it does not (Appendix I). We propose a method to purify Kin4 under continuous denaturing conditions (Figure 4C). This method takes advantage of the fact that the biotin-avidin interaction is resistant to up to 3% SDS which has been used for chromatin immunoprecipitation (van Werven and Timmers 2006). The scheme is briefly as follows: Cells carrying biotinylated Kin4 are spheroplasted to allow access to the proteins by a cross-linking agent such as Dithio-bis(Succinimidyl Propionate) (DSP). The cells are then lysed and fractionated by a 100,000 g centrifugation. This allows for removal of the supernatant which contains many of the endogenously biotinylated yeast proteins. The P100 fraction is then boiled in 1% SDS to solubilize Kin4-biotin which is then purified using an avidin bead matrix. After purification, the cross-links can be cleaved and the interacting proteins can be identified by SDS-PAGE/MS. A similar protocol sans cross-linking might be employed to purify full length Kin4 under denaturing conditions to provide better starting material for a more comprehensive map of Kin4 phosphorylation sites.

Experimental Procedures

Yeast Strains and Growth Conditions

All strains are derivatives of W303 (A2587) and are listed in Table 1. Growth conditions are described in the figure legends.

Plasmid Construction

All plasmids used in this study are listed in Table 2. p8.6.3 was isolated from the high copy suppression of *pGAL1-10-KIN4* screen. pA1363 and pA1364 were generated by gap repair cloning with YEp13 (pA43) digested with BamHI and PCR products spanning the *FUR1* and *YHR127W* genes respectively.

Immunoblot Analysis

Immunoblot analysis to determine total amount of Kin4-3HA or 3HA-Kin4 were as previously described (Chan and Amon 2009). Detection of Pep12 was performed using a mouse anti-Pep12 antibody [2C3 Invitrogen] at 0.5 μg/mL. Detection of Pgk1 was performed using a mouse anti-Pgk1 antibody [Molecular Probes] at 1:10,000.

Differential centrifugation and solubility

Cells were analyzed as previously described (Kaiser, Chen and Losko 2002).

Table 1: Yeast Strains

A9249	*MATa trp1:pGAL1-10-KIN4:TRP1 3HA-CDC14*
A11779	*MATa KIN4-3HA:KanMx6*
A16624	*MATa 3HA-CDC14 dyn1Δ::URA3 YEp13*
A16625	*MATa kin4::KanMx6 dyn1Δ::URA3 3HA-CDC14 YEp13*
A16627	*MATa 3HA-CDC14 dyn1Δ::URA3YEp13-FUR1-YHR127W*
A16798	*MATa trp1:pGAL1-10-KIN4:TRP1 3HA-CDC14 YEp13*
A16799	*MATa trp1:pGAL1-10-KIN4:TRP1 3HA-CDC14 YEp13-FUR1-YHR127W*
A16800	*MATa trp1:pGAL1-10-KIN4:TRP1 3HA-CDC14 YEp13-FUR1*
A16801	*MATa trp1:pGAL1-10-KIN4:TRP1 3HA-CDC14 YEp13-YHR127W*
A17084	*MATa KanMx6:pGAL1-10-3HA-KIN4 YEp13*
A17085	*MATa KanMx6:pGAL1-10-3HA-KIN4 YEp13-YHR127W*

Table 2: Plasmids

pA43	*YEp13*
p8.6.3	*YEp13-FUR1-YHR127W*
pA1363	*YEp13-FUR1*
pA1364	*YEp13-YHR127W*

References

Alexandru, G., W. Zachariae, A. Schleiffer & K. Nasmyth (1999) Sister chromatid separation and chromosome re-duplication are regulated by different mechanisms in response to spindle damage. *EMBO J,* 18, 2707-21.

Cabernard, C. & C. Q. Doe (2007) Stem cell self-renewal: centrosomes on the move. *Curr Biol,* 17, R465-7.

Chan, L. Y. & A. Amon (2009) The protein phosphatase 2A functions in the spindle position checkpoint by regulating the checkpoint kinase Kin4. *Genes Dev,* 23, 1639-49.

Jaspersen, S. L., J. F. Charles, R. L. Tinker-Kulberg & D. O. Morgan (1998) A late mitotic regulatory network controlling cyclin destruction in Saccharomyces cerevisiae. *Mol Biol Cell,* 9, 2803-17.

Kaiser, C. A., E. J. Chen & S. Losko (2002) Subcellular fractionation of secretory organelles. *Methods Enzymol,* 351, 325-38.

Ro, H. S., S. Song & K. S. Lee (2002) Bfa1 can regulate Tem1 function independently of Bub2 in the mitotic exit network of Saccharomyces cerevisiae. *Proc Natl Acad Sci U S A,* 99, 5436-41.

Schoner, D., M. Kalisch, C. Leisner, L. Meier, M. Sohrmann, M. Faty, Y. Barral, M. Peter, W. Gruissem & P. Buhlmann (2008) Annotating novel genes by integrating synthetic lethals and genomic information. *BMC Syst Biol,* 2, 3.

Tong, A. H. & C. Boone (2006) Synthetic genetic array analysis in Saccharomyces cerevisiae. *Methods Mol Biol,* 313, 171-92.

van Werven, F. J. & H. T. Timmers (2006) The use of biotin tagging in Saccharomyces cerevisiae improves the sensitivity of chromatin immunoprecipitation. *Nucleic Acids Res,* 34, e33.

Yeh, E., R. V. Skibbens, J. W. Cheng, E. D. Salmon & K. Bloom (1995) Spindle dynamics and cell cycle regulation of dynein in the budding yeast, Saccharomyces cerevisiae. *J Cell Biol,* 130, 687-700.

Appendix III: Development of methods to identify inhibitors of sporulation

Introduction

Sporulation is a developmental program that diploid yeast cells undergo in response to nutrient starvation. This developmental program generates four haploid spores from a diploid progenitor cell and is studied as a model of meiosis. Many genes have been identified which promote proper sporulation (*SPO* genes) but comparatively few have been identified that inhibit sporulation. There are many multi-step processes required for proper sporulation that might be subject to negative regulation such as sporulation entry, homolog pairing, recombination, synaptonemal complex assembly, chromosome segregation and spore maturation. To identify such regulators, we screened a multi-copy plasmid library of genomic fragments that could inhibit sporulation. Due to technical issues, the candidate mutants from this screen were not further analyzed. We discuss potential improvements to the screening methodology and the development of reporter constructs for rapid secondary screening of potential mutants.

Results and Discussion

Design of a screen to identify inhibitors of sporulation

To capture the largest set of mutants defective in sporulation, we analyzed the most terminal outcome of sporulation, the generation of viable spores. We took advantage of the sensitivity of vegetative cells and resistance of spores to ether (Rockmill, Lambie and Roeder 1991). As a control for this methodology, we tested wild-type haploid, wild-type diploid and *spo11*Δ homozygous diploid cells for ether sensitivity post sporulation. As expected, none of the haploid cells grew, the wild-type diploid grew very robustly and consistent with the ~1% spore viability of *spo11*Δ mutants, very few cells grew from the *spo11*Δ diploid strain (Klapholz, Waddell and Esposito 1985) (Figure 1A). Using this methodology, we screened ~7000 transformants and isolated ~200 candidate mutants. Initial sequencing of these candidate plasmids showed suspiciously high enrichment for certain plasmids potentially indicating that the initial plasmid library was poorly representative of the genome. Indeed, independent analyses of this library reached this same conclusion (Ashwini Jambhekar, personal communication). Due to this poor library quality, candidate plasmids were not further analyzed.

Proposed improvements to the screen

The poor library quality resulted from high levels of amplification of an initially high quality library, which was deemed necessary due to the poor transformability of the SK1 strain which is the standard model in the sporulation field. SK1 transforms about one thousand fold more poorly compared to W303 (personal observation). To circumvent this problem, we propose first transforming haploid W303, which transforms with high efficiency, and then subsequently mating the resulting colonies to a lawn of an SK1 haploid strain of the opposite mating type. These diploid cells can then be analyzed for sporulation efficiency. Because the efficient sporualtion phenotype of SK1 is dominant to the less efficient sporualtion phenotype of W303, we can utilize such a screening strategy without excessive amplification of the plasmid library (Figure 1B). One potential downside to this methodology is that the SK1/W303 hybrid, while forming tetrads at SK1/SK1 levels, does display a minor spore viability reduction of 5-10% (pure diploids sporulate with over 95% viability). This may lead to a loss in sensitivity of the screen.

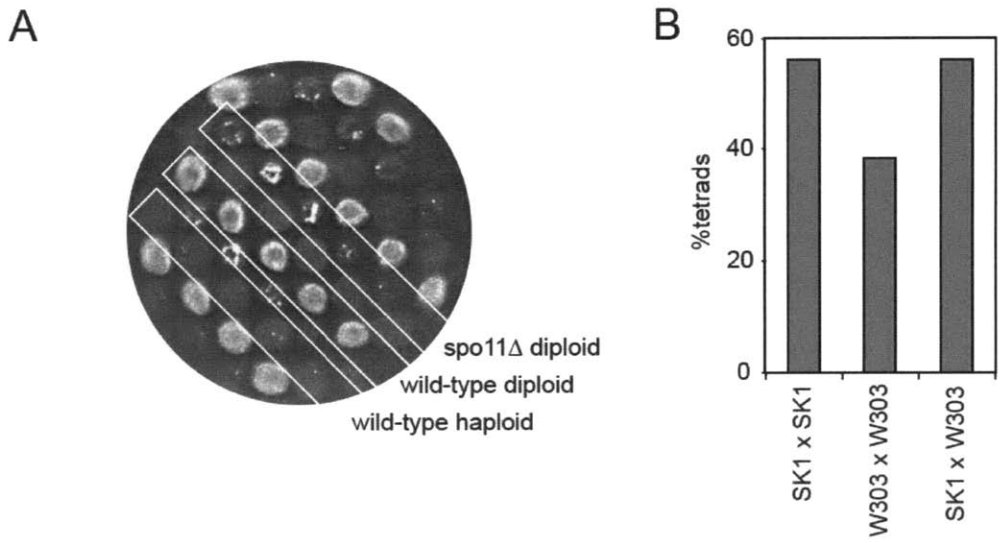

Figure 1. Ether resistance of spores and sporulation of SK1 and W303.

(A) Wild-type haploid (A4841), wild-type diploid (A4962) and *spo11*Δ diploid (A2983) cells were replica plated from sporulation media to rich media and exposed to ether for 45 minutes. Surviving spores were allowed to germinate and grow for 20 hours and scored for spore viability.
(B) SK1 diploid (A4962), W303 diploid (A16629) and W303/SK1 hybrid diploid (A2587 x A4842) cells were sporulated on solid media and the number of tetrads were counted after three days. $n \geq 200$ cells.

A second improvement that would aid in the implementation of this screen is a less labor intensive method to measure spore viability. Ether exposure, while very informative can only reasonably be processed for about 4 plates at a time which translates to about 12 plates per day. An alternative method has been previously employed to select for viable haploids from a cross based on the recessive drug resistance alleles, *cyh2* and *can1* (Klapholz and Esposito 1982). The advantage of this method is the ability to screen more colonies at once. The potential downside is that this method reduces the total number of viable spores by four fold potentially leading to a loss in sensitivity.

Development of secondary screens

Based on the general phenotype being screened for, the expectation is that such a screen would isolate a large number of candidate plasmids. Rapid secondary screens are thus necessary to grossly characterize the sporulation defect of candidate colonies. In this

vein, we have built two constructs that express enzymatic reporters at defined stages of sporulation. The first construct is a fusion of the promoter of *IME1* to the *E. coli* *lacZ*$^{+}$coding sequence, which expresses the β-galactosidase enzyme (Jambhekar and Amon 2008) (Figure 2B). *IME1* is the master regulator of entry into meiosis and is weakly expressed in stationary phase even in rich media (Figures 2A and 2B). Mutants defective in respiration do not induce *IME1* expression such as the *pet100*Δ mutant, which is unable to properly fold cytochrome C. Indeed, no β-galactosidase activity was detected in a *pet100*Δ mutant carrying the *pIME1-lacZ* reporter construct (Figure 2B). The *pIME1-lacZ* construct should help to identify colonies that fail to enter the sporulation program.

The second construct is a fusion of the promoter of *SPS1* to the *E. coli gusA*$^{+}$ coding sequence, which expresses the β-glucuronidase enzyme (Figure 2B). Sps1, a kinase involved in spore wall formation, is expressed at the pachytene to meiosis I transition and depends on the master transcription factor of middle sporualtion genes, Ndt80. Mutants that activate the pachytene checkpoint such as *dmc1*Δ do not express Ndt80 and thus do not express Sps1 (Figure 2B). In combination, these reporters should help to narrow down which stage of sporulation is defective in these candidate colonies. Two other methods should also help in the initial characterization of these colonies. Growth on a non-fermentable carbon source such as glycerol should identify those colonies that cannot sporulate due to defects in respiration and assaying for di-tyrosine fluorescence, which is associated with spore wall formation, should identify colonies defective in stages prior to spore wall formation (Figure 2A).

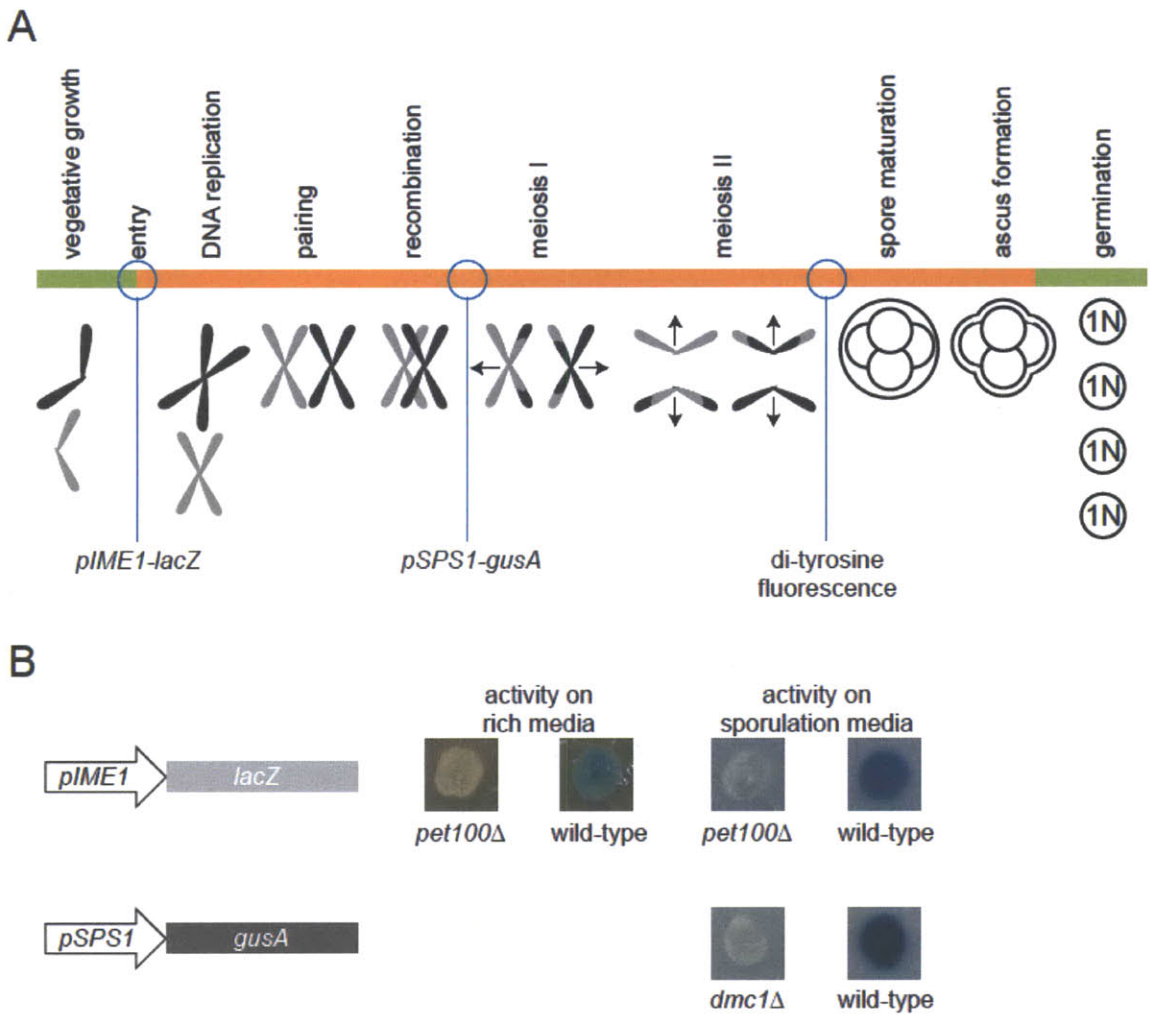

Figure 2. Sporulation progression and proposed secondary readouts.

(A) Schematic of the sporulation program.
(B) Wild-type (A16880) and *pet100*Δ (A17109) diploid cells carrying the *pIME1-lacZ* reporter were patched on rich media and sporulation media and allowed to grow/sporulate for 24 hours. Cells were then assayed for β-galactosidase activity by plate overlay. Wild-type (A16692) and *dmc1*Δ (A16690) diploid cells carrying the *pSPS1-gusA* reporter were patched on sporulation media and allowed to sporulate for 24 hours. β-glucuronidase activity was determined by plate overlay.

Experimental Procedures

Yeast Strains and Growth Conditions

All strains are derivatives of SK1 or W303 (A4841 or A2587) and are listed in Table 1. Growth conditions are described in the figure legends.

Plasmid Construction

Plasmid pA1351 (YIplac204-*pSPS1-gusA-tADH1*) was generated by first constructing the *pSPS1-gusA-tADH1* fragment by three way PCR mediated ligation. The template for *pSPS1* was SK1 genomic DNA, for *gusA*, *E. coli* MG1655 (gift from Drew Endy's lab) genomic DNA and for *tADH1*, plasmid pFA6a-*KanMx6-pGAL1-10-3HA-tADH1* (Longtine et al. 1998). This fragment and YIplac204 were digested with HindIII and PstI and ligated together. Integration into the *TRP1* locus was performed by digestion with Bsu36I.

Ether spore selection

Ether spore selection was adapted from (Rockmill et al. 1991). Cells were patched to YePAD media and allowed to grow for 24 hours. Plates were then replica plated to sporulation media (1% potassium phosphate, 100 mg/L adenine, 100mg/L histidine, 100 mg/L lysine, 200 mg/L leucine, 5.6 mg/L uracil and 20 mg/L tryptophan) and allowed to sporulate for 2-3 days. Cells were then replica plated to YePAD media in glass plates and exposed to ether face down in a enclosed cabinet suspended above a pool of ether for 45 minutes. Excess ether was vented off in a fume hood for 20 minutes and plates were incubated at 30°C for 24 hours and then scored for spore viability.

Detection of β-galactosidase and β-glucuronidase activity

Detection of β-galactosidase and β-glucuronidase activity was adapted from (Duttweiler 1996). Cells were patched to YePAD or sporulation media and allowed to grow/sporulate for 24 hours. Cells were then over-layed with chloroform for 5 minutes in a fume hood. The chloroform was poured off and the plates were vented in the fume hood for 5 minutes. Plates were then over-layed with 15 mL of soft agarose indicator (0.7% agarose, 100mM potassium phosphate pH 7.0, 1 mg/mL 5-bromo-4-chloro-3-indolyl-β-D-

galactopyranoside (X-gal) or 5-bromo-4-chloro-3-indolyl-β-D-glucuronic acid (X-gluc)) and allowed to solidify. X-gal or X-gluc staining was assayed 8-24 hours later.

Table 1: Yeast Strains

A2587	*MATa ade2-1 leu2-3 ura3 trp1-1 his3-1115 can1-100 GAL phi+* (wild-type W303)
A2983	SK1 - *MATa spo11Δ::URA3 MATalpha spo11::URA3*
A4841	*MATa ho::LYS2 lys2 ura3 leu2::hisG his3::hisG trp1::hisG* (wild-type SK1)
A4842	*MATalpha ho::LYS2 lys2 ura3 leu2::hisG his3::hisG trp1::hisG* (wild-type SK1)
A4962	SK1 - *MATa MATalpha*
A16629	W303 - *MATa MATalpha*
A16692	SK1 - *MATa trp1:pSPS1-gusA:TRP1 MATalpha*
A16690	SK1 - *MATa dmc1Δ::HIS3 MATalpha dmc1Δ::HIS3 trp1:pSPS1-gusA:TRP1*
A16880	SK1 – *MATa MATalpha IME1:pIME1-lacZ:URA3*
A17109	SK1 - *MATa pet100Δ::KanMx6 IME1:pIME1-lacZ:URA3 MATalpha pet100Δ::KanMx6*

References

Duttweiler, H. M. (1996) A highly sensitive and non-lethal beta-galactosidase plate assay for yeast. *Trends Genet,* 12, 340-1.

Jambhekar, A. & A. Amon (2008) Control of meiosis by respiration. *Curr Biol,* 18, 969-75.

Klapholz, S. & R. E. Esposito (1982) A new mapping method employing a meiotic rec-mutant of yeast. *Genetics,* 100, 387-412.

Klapholz, S., C. S. Waddell & R. E. Esposito (1985) The role of the SPO11 gene in meiotic recombination in yeast. *Genetics,* 110, 187-216.

Longtine, M. S., A. McKenzie, 3rd, D. J. Demarini, N. G. Shah, A. Wach, A. Brachat, P. Philippsen & J. R. Pringle (1998) Additional modules for versatile and economical PCR-based gene deletion and modification in Saccharomyces cerevisiae. *Yeast,* 14, 953-61.

Rockmill, B., E. J. Lambie & G. S. Roeder (1991) Spore enrichment. *Methods Enzymol,* 194, 146-9.